R-04-31

Flow of groundwater from great depths into the near surface deposits – modelling of a local domain in northeast Uppland

Johan G Holmén, Jonas Forsman
Golder Associates

January 2005

Svensk Kärnbränslehantering AB
Swedish Nuclear Fuel
and Waste Management Co
Box 5864
SE-102 40 Stockholm Sweden
Tel 08-459 84 00
+46 8 459 84 00
Fax 08-661 57 19
+46 8 661 57 19

ISSN 1402-3091
SKB Rapport R-04-31

Flow of groundwater from great depths into the near surface deposits – modelling of a local domain in northeast Uppland

Johan G Holmén, Jonas Forsman
Golder Associates

January 2005

Abstract

Purpose: To study the flow of groundwater from rock masses at great depths and into the surface near deposits by use of mathematical models; and to estimate the spatial and temporal distribution of groundwater from great depths in the surface near deposits (quaternary deposits). The study is about the hydraulic interaction between the geosphere and the biosphere.

Methodology: The system studied is represented by time dependent three dimensional mathematical models. The models include groundwater flows in the rock mass and in the quaternary deposits as well as surface water flows. The established groundwater models have such a resolution (degree of detail) that both rock masses at great depth and near surface deposits are included in the flow system studied. The modelling includes simulations under both steady state conditions and transient conditions The transient simulations represents the varying state of the groundwater system studied, caused by the variation in hydro-meteorological conditions during a normal year, a wet-year and a dry-year. The boundary condition along the topography of the model is a non-linear boundary condition, representing the ground surface above the sea and the varying actual groundwater recharge.

Area studied: The area studied is located in Sweden, in the Northeast of the Uppland province, close to the Forsmark nuclear power plant.

Water balance modelling: To obtain three significantly different groundwater recharge periods for the transient groundwater flow simulations a water balance modelling was carried out based on a statistical analysis of available hydro-meteorological data. To obtain a temporal distribution of the runoff (i.e. potential groundwater recharge), we have conducted a numerical time dependent water balance modelling.

General conclusions of groundwater modelling: The discharge areas for the flow paths from great depth are given by the topography and located along valleys and lakes; the spatial and temporal extension of these areas do not vary much for different values of the permeability of the uppermost part of the flow medium or for the applied different values of groundwater recharge.

Flow paths were released on-shore inside of the shore line (no paths were released below the sea) and at an approximate repository depth (i.e. 420 m), the flow paths will either discharge into the sea (i.e. 34%) or above the sea (i.e. 66%). Considering the discharge areas above the sea, nearly all of the flow paths from repository depth will discharge into lakes, and especially where a fracture zones intersects a lake.

Considering a lake with a thick layer of low–permeable sediments at the base of the lake (a large flow-resistance), for such a situation nearly all flow paths discharges along the lake perimeter where no sediments occur. And for a situation in which a lake has sediments of small resistance along its base, for such a situation most flow paths discharge at the base of the lake through the lake sediments.

Most flow routes from repository depths demonstrate short path lengths in the quaternary deposits. Only a small percentage (< 5%) of the flow paths demonstrate path lengths in the surface near material (in the uppermost 1.5 m of quaternary deposits) that are longer than

about 50 m. This is because most flow paths from great depth flow towards lakes and other strong sinks, and reaches these areas from deep below and hence the surface near part of the flow paths will be short.

Nevertheless, a small amount of flow paths (less than approximately 5% of all paths) demonstrate lengths between 50 m and 250 m in the quaternary deposits below lakes, that is however for a situation in which the resistances of the lake sediments are large. Outside of the lakes, the lengths of the studied flow paths in the quaternary deposits tend to be shorter and are not much influenced by the resistance of the lake sediments.

For most flow paths from great depth, the total break through times depend very strongly on the time spent in the rock mass between fracture zones. In comparison, the time spent in fracture zones and in the quaternary deposits is not very important. It should be noted that these conclusions corresponds to flow paths released at repository depth; and that the analyses do not include times spent in lake sediments.

The groundwater flow situation in the quaternary deposits varies significantly during a year, because the groundwater recharge varies during a year. This variation is however not very important for the flow paths from great depth. The simulations of transient flow paths from a depth of 420 m produced results (length, breakthrough time and discharge areas) that were almost the same as the results produced by a steady state situation and a normal year. Even a steady state simulation of a dry-year produced the same discharge areas as a simulation of a normal year; also a model without quaternary deposits produced the same discharge areas.

Executive summary

General purpose of study and area studied

The purpose is to study the flow of groundwater from rock masses at great depths and into the surface near deposits by use of mathematical models and to estimate the spatial and temporal distribution of groundwater from great depths in the surface near deposits (quaternary deposits). This study will look at the following question: How is groundwater from great depth distributed in the surface near deposits? This is an interesting aspect of groundwater flow from great depths, as many biological processes takes place in the surface near deposits, processes that may be of importance when analysing contaminant transport from a repository located at great depth. Hence, this study is about the hydraulic interaction between the geosphere and the biosphere. We will of course not provide the reader with a complete answer to the above given question, but we will present some results of a numerical modelling focused on the given question.

The system studied is represented by time dependent three dimensional mathematical models. The models will include groundwater flows in the rock mass and in the surface near deposits (quaternary deposits) as well as surface water flows.

It is a purpose of this study to: (i) Establish groundwater models having such a resolution (degree of detail) that both rock masses at great depth and near surface deposits are included in the flow system studied. (ii) Analyse both steady state conditions and transient conditions (time dependent conditions). The transient simulations will represent the varying state of the groundwater system studied, caused by the variation in hydro-meteorological conditions during a normal year, a wet-year and a dry-year. (iii) Analyse and follow the simulated groundwater flow, from great depths via rock masses and fracture zones, to the quaternary deposits, and through the quaternary deposits to the final discharge areas.

The area studied is located in Sweden, in the Northeast of the Uppland province, close to the Forsmark nuclear power plant. The studied area has been selected as a candidate area for a deep repository for nuclear waste. This study is about analysing the general behaviour of a groundwater flow system; the results of this study are not to be interpreted as results of a site specific modelling analysing the suitability of the studied area as a host domain for a deep repository. This study is not based on data gathered during the site investigation programme.

Hydrometeorology and water balance modelling

To obtain three significantly different groundwater recharge periods for the transient groundwater flow simulations we have derived a normal, a dry and a wet precipitation period based on a statistical analysis of available hydro-meteorological data. The statistical analysis is based on time series of precipitation and potential evapotranspiration. The analysed data covers the period 1961–2000, i.e. a total of 40 years. The data originates from SMHI's monitoring station Lövsta, in the Forsmark area. The statistical analysis has produced precipitation for a normal year, as well as a wet-year and a dry-year with return periods of 1,000 years.

To obtain a temporal distribution of the runoff (i.e. potential groundwater recharge), we have conducted a time dependent water balance calculation. We have used a numerical method and derived the run-off for the normal year, as well as for a wet-year and a dry-year

with return periods of 1,000 years. The potential recharge is a result of the water balance modelling; the potential recharge as an input to the groundwater modelling, the actual recharge is calculated by the groundwater model.

Properties of established groundwater model

Size and boundary conditions of groundwater model

The outer vertical boundaries of the model coincide with regional fracture zones, large surface water bodies or water divides. These boundaries give the model a length in a north-south direction that is close to 8 km, and in the west-east direction the maximum length of the model is close to 10 km. The upper boundary of the groundwater model follows the topography. The model is defined with a no-flow boundary condition at the lateral sides and at the base of the model. The top boundary condition used for the model is either: (i) the specified head condition, representing the seawater table or (ii) a non-linear boundary condition, representing the ground surface above the sea and the varying actual groundwater recharge.

Conceptual model of the hydraulic properties of the rock mass

In the established groundwater model, the rock mass extends from a depth of 3 m down to a depth of 600 m. The rock mass is intersected by vertical fracture zones. The permeability of the fracture zones is much larger than that of the rock mass between the zones. For both the rock mass and the zones the permeability is defined as constant with depth. In the models of this study, the conductivity of the rock mass between the regional fracture zones is set to 5×10^{-9} m/s; the regional fracture zones are defined with a theoretical width of 30 m and a conductivity of 8.0×10^{-7} m/s.

Conceptual model of the hydraulic properties of the quaternary deposits

We have established a groundwater model with such resolution that the model is capable of reproducing the flow of groundwater in the quaternary deposits, and at the same time include groundwater flow at great depth. The hydraulic properties of the quaternary deposits of the established model are based on a conceptual model of the near surface groundwater flow system in which a very permeable material takes place close to the ground surface, having a thickness of a few decimetres. Accordingly, we have in our model defined the uppermost 0.5 m with a very large permeability, for the Base case the conductivity is 1×10^{-4} m/s (except for areas covered with clay which are defined with a much smaller conductivity). The permeability of the quaternary deposits decreases with depth. The thickness of the quaternary deposits is set to 3 m.

Computer code

The groundwater model was established by use of the computer code GEOAN.

Results of modelling: Recharge and discharge

Amount of recharge areas and discharge areas and thickness of unsaturated zone

The amount of recharge areas and discharge areas, as well as the thickness of the unsaturated zone, depend on the permeability of the uppermost part of the flow medium. We have carried out a sensitivity analysis with the purpose of calculating:

- Size of discharge areas and recharge areas, as well as size of unsaturated zone and comparing these sizes to the corresponding different values of the hydraulic conductivity of the uppermost 0.5 m of the model.

It was demonstrated by the sensitivity analysis that:

- If the conductivity is large, a large amount of the precipitation and surface waters will infiltrate and create groundwater in the quaternary deposits. For such a situation, the amount of recharge areas will be large (but it cannot be 100%, as there must always be discharge areas). For such a situation the discharge areas will be few, but the outflow of groundwater is large at these areas.
- If the conductivity is small, only a small amount of the precipitation will be able to infiltrate; it follows that most of the areas will be saturated up to the ground surface. Consequently most areas will be discharge areas, even if the discharge is small.

For the Base case the amount of discharge areas above the sea (not including the lakes) is approximately 40% when considering steady state conditions and a normal year. For the same situation, the thickness of the unsaturated zone varies from a few decimetres up to a few metres; for 40% of the area the thickness of the unsaturated zone is zero, for 99% of the area the unsaturated thickness is less than 0.9 m. The thickness of the unsaturated zone depends, to a large extent, on the thickness and permeability of the uppermost highly permeable part of the quaternary deposits (and on amount of recharge).

A balanced normal year occurs when the state of the system studied is the same at the beginning of the year and at the end of the year. We have calculated the temporal variation in amount of discharge areas, considering the Base case. For the balanced normal year, the spatial extension of the discharge areas varies as follows: The discharge areas are the largest during the spring, at the end of April, 76% of the areas above the shoreline are discharge areas (not including the lakes). During the summer, the amount decreases and at the end of September the discharge areas make up 24% of all areas. After summer follows the autumn with increasing amounts of discharge areas; at the end of November the amount of discharge areas is 47%. The smallest amount of discharge areas occurs at the end of March (23%). The thickness of the unsaturated zone will also vary. The largest unsaturated zone takes place when the amount of discharge areas is the smallest.

We have carried out the same calculations for a wet-year and a dry-year. Considering the wet-year, the discharge areas are the largest during the spring, at the end of April all of the areas above the shoreline are saturated with groundwater. Also for the dry-year, the discharge areas are the largest during the spring; at the end of April 43% of the areas above the shoreline are saturated with groundwater. During the dry-year, the amount of discharge areas decreases steadily during the summer and the autumn since no groundwater recharge takes place during the autumn of the dry-year. At the end of the dry-year, the amount of discharge areas is 18%.

Groundwater recharge to quaternary deposits

The potential recharge is a result of the water balance modelling; the potential recharge is given as an input to the groundwater modelling while the actual recharge is calculated by the groundwater model. The actual groundwater recharge to the quaternary deposits (and to the rock mass) has been calculated for different values of permeability of the uppermost part of the quaternary deposits. The size of the recharge depends on the conductivity of the uppermost part of the flow medium; the larger the conductivity, the larger the amount of the precipitation and surface waters will infiltrate and create groundwater.

Considering the Base case, a normal year and a steady state solution, the actual recharge to the quaternary deposits is equal to 122 mm/year.

For the Base case, we have calculated the temporal variation in size of groundwater recharge to the quaternary deposits. For the balanced normal year, the water balance calculations indicate that potential recharge is only available during the spring (April) and during the autumn (October and November). It follows that nearly all of the actual recharge will take place during those periods. However, as the model includes surface water flows, actual recharge will also take place during months with zero potential recharge. This recharge comes from surface water flow; it is water that has been transported as a surface flow that infiltrates into the groundwater system of the model (e.g. along hill sides and streams). The size of this 'extra' recharge is however small and always less than one millimetre per month (when averaged out over the whole of the model). Both the intensity and the total volume of recharge are the largest during the spring. During the month of April the potential recharge is 160 mm, and out of this 64 mm will infiltrate into the quaternary deposits and produce groundwater recharge. During October and November, the potential recharge is 79 mm, and out of this 39 mm will infiltrate and produce groundwater recharge. For the whole year (normal year), the transient simulations indicate an actual recharge of 103 mm/year.

For the wet-year, the water balance modelling predicts a potential recharge for all months, except the winter months (temperature below zero). A very large potential recharge takes place during April when the snow melts, and during the whole summer there will be a potential recharge (especially in August). For the normal year, the potential recharge is large during the autumn. For all months with a potential recharge, there will be an actual recharge calculated by the groundwater model. In total, the potential recharge is 1,036 mm/year for the wet-year, and the corresponding actual recharge is 207 mm/year.

For the dry-year, the water balance modelling produces a potential recharge for the month of April, only. It follows that actual recharge will take place during April, only. In total the potential recharge is 61 mm/year for the dry-year, and the corresponding actual recharge is 29.8 mm/year.

Groundwater recharge to rock mass

Groundwater recharge to the rock mass is made up of the groundwater that flows from the quaternary deposits to the rock mass. When we discuss groundwater recharge to the rock mass we mean recharge to the fracture zones and the rock between these zones.

The permeability of the rock mass is (on the average) much smaller than that of the quaternary deposits, accordingly the recharge to the rock mass is much smaller than the recharge to the quaternary deposits.

The size of the recharge to the rock mass depends not directly on the potential recharge (and the precipitation etc), but on the size of groundwater head in the quaternary deposits in relation to the head in the rock mass, i.e. the hydraulic gradient between the rock mass and the quaternary deposits. Hence, the recharge to the rock mass is indirectly coupled to the potential recharge, via the groundwater heads of the quaternary deposits that depend on the potential recharge.

Since the variation in hydraulic gradient between the rock masses and quaternary deposits is small, compared to the variation in potential recharge; it follows that the recharge to the rock mass varies much less during a year than the recharge to the quaternary deposits. The

recharge to the rock mass is the largest during the spring, when the groundwater heads are the highest, and smallest at the end of the winter and at the end of the summer, as the groundwater heads are the lowest at these times of the year.

Considering a normal year, the potential recharge is 240 mm/year. The groundwater recharge to the quaternary deposits is equal to 103 mm/year, which is about 45% of the potential recharge. The groundwater recharge to the rock mass is 2.5 mm/year; this is close to 1% of the potential recharge, and close to 2% of the recharge to the quaternary deposits. Hence only a small fraction of the groundwater of the quaternary deposits will recharge into the rock mass.

The temporal variation of recharge to the rock mass is small (as discussed above), it follows that the difference is small between: (i) recharge to the rock mass calculated by use of a steady state solution and (ii) recharge to the rock mass calculated by use of a transient solution.

As the recharge to the rock mass is not directly coupled to the potential recharge, the recharge to the rock mass will not vary much even if the potential recharge varies a lot. For a wet-year, with a potential recharge that is two times that of a normal year, the recharge to the rock mass will be only 15% larger than the recharge of a normal year. For a dry-year, with a potential recharge that is less than one third of the recharge of a normal year, the recharge to the rock mass will be only 13% smaller than the recharge of a normal year. As long as there is groundwater in the quaternary deposits, there will be recharge to the rock mass. A single dry-year, with a very small potential recharge, will not influence the recharge to the rock mass in a dramatic way.

We have established models without any quaternary deposits, but with surface water flows. The quaternary deposits were changed into rock mass and fracture zones. These models have been established for the purpose of comparisons to the Base case. Considering recharge to the rock mass we conclude that it is not always necessary to include the quaternary deposits in a groundwater model. If the purpose of the model is to study the flow in the rock mass, an acceptable approximation may be derived without the quaternary deposits. This is valid for a flow situation in which the groundwater levels in the quaternary deposits are close the ground surface and the thickness of the quaternary deposits is small compared to thickness of the rock masses. The flow situation in the rock mass below the depth of the quaternary deposits is approximately the same for situations with: (i) a large groundwater flow in the upper part of the quaternary deposits or (ii) a large surface water flow above the quaternary deposits (or directly above the rock mass). The important property is the size and distribution of the recharge to the rock mass, which may be approximately the same for both situations.

Results of modelling: Analyses of flow paths

Methodology: Analyses of flow field by use of flow paths

In this study the flow pattern of the groundwater is analysed by use of flow paths. The applied model (GEOAN) creates flow paths by use of simulated particles that follow the flow of groundwater through the model (i.e. particle tracking).

The particles were released at a depth close to an estimated depth of a repository, i.e. 420 m below ground surface. Particles (flow paths) were released in a regular pattern, one path in each volume (cell or element) studied, regardless of the flow through the volume studied.

Particles were released on-shore, inside of the shore line; no particles were released below the sea. All parts of the model inside of the shore line were covered by release positions (at a depth of 420 m).

In the models, the flow paths will develop inside a flow field that controls the movements of the paths. For a time-independent flow path (steady state paths), the path will develop inside a flow field that will not change with time. For a time-dependent flow path (a transient path), the flow field will change with time during the movement of the simulated particle that produces the flow path. In this study we have generated both time independent and time dependent flow paths.

The flow paths were analysed considering different parameters: length, breakthrough time, average velocity etc, in different materials along the flow route; but also for the overall spatial distribution in the different materials and for points of discharge.

We have studied the uppermost 1.5 m of quaternary deposits separately, because this zone is important considering biological activity (roots, unsaturated zone etc). We would like to stress that the results derived for the surface near part of the flow paths consider flow paths from great depth only. If all the flow in the quaternary deposits had been studied, the results would have been different.

In this study we have examined advective flow paths only; diffusion, mechanical mixing and retardation were not included in the models studied.

Flow paths – Spatial distribution and type of discharge areas

The spatial distribution of discharge areas of the flow paths from great depth is not the same as the spatial distribution of discharge areas for all flow paths from all depths. Flow paths from great depth tend to flow towards the strongest sinks of the flow system. The strongest sinks occur at areas with a low groundwater potential (groundwater head). Such areas are: (i) the sea floor, (ii) lakes and (iii) other strong discharge areas such as swamps and streams. The flow towards these strong sink will partly take place along fracture zones. The spatial distribution of the discharge areas for flow paths from a depth of 420 m is given in Figure 9-2 and in Figure 9-5 The figures demonstrates that the discharge areas of the paths from a depth of 420 m are concentrated to a few different types of hydrogeological structures:

34% discharges below the sea, the discharge will take place along fracture zones, or if no fracture zones occur in the local area, along the deepest parts of the sea floor.

66% discharges above the sea. Nearly all of the flow paths (with very few exceptions) discharges into the lakes (including Bolundsfjärden as one of the lakes), and in the lakes the discharge areas are often concentrated to where fracture zones intersect a lake.

We may conclude as follows: Flow paths released on-shore (no paths released below the sea) and at repository depth (i.e. 420 m) will either discharge into the sea (i.e. 34%) or above the sea (i.e. 66%). Considering the discharge areas above the sea, nearly all of the flow paths from repository depth will discharge into lakes, and especially where fracture zones intersect a lake. Groundwater from great depth flows towards the strongest sinks and the deeper the release points, the more the flow will be concentrated to a few strong discharge areas (sinks).

Flow paths – Discharge into lakes

In the groundwater model, the contact between the lake and the groundwater system is defined as follows.

(i) Along the lake perimeter, the groundwater system is in direct contact with the lake via a highly permeable material (a wave eroded material).

(ii) Along the base of the lake, the contact between the groundwater system and the lake takes place through a material having a low permeability; this material represents sediments at the base of the lake.

In our model there are three different flow routes of water into a lake: (i) as a surface flow directly into the lake, (ii) as a groundwater flow via the lake perimeter, or (iii) as a groundwater flow via sediments at the base of the lake (lake-floor sediments).

We have estimated the percentage of the groundwater flow paths (released at a depth of 420 m) that uses the two different groundwater flow routes. It is important to note the difference between the percentage of all released flow paths, and the percentage of all paths that reaches a lake studied. For example, for the Base case of lake Fiskarfjärden, 20% of all the released flow paths will discharge into this lake. For the lake Fiskarfjärden, the balance of the number of groundwater flow paths at each flow rout is 59% via sediments at base of lake and 41% via the lake perimeter.

If the lake sediments are impermeable, 100% of the groundwater flow will discharge at the lake perimeter. For situations with more permeable sediments, more and more of the groundwater will use the flow route via the sediments. The amount of flow that will discharge via sediments at the base of a lake depends on the flow-resistance of the sediments (the concept of flow-resistance includes both the thickness of the sediments and the permeability of the sediments).

The actual resistance of the sediments of the lakes studied is not known in detail. The thickness of the sediments may vary a lot, and it is not unlikely that a layer of sediments will demonstrate a thickness of several metres along the lake-floor. The conductivity of the sediment is probably very low – in line with that of clay or perhaps smaller. For the Base case, the resistance of the lake sediments is set to $1\times10^{+10}$ s, which for example corresponds to 1 m of a material with a conductivity equal to 1×10^{-10} m/s, or 5 m of a material with a conductivity equal to 5×10^{-10} m/s.

We have established a number of sensitivity cases for the purpose of investigating the importance of the flow-resistance of the sediments. The only difference between the sensitivity cases and the Base case is the value of resistance at the base of the lakes. The results of the calculations demonstrated that the balance of the number of flow paths at each flow rout depends strongly on the resistance of the lake sediments.

Flow paths – Lengths

Considering the complete paths from release position to position of discharge, there are flow paths that demonstrate a movement that is more or less straight upward from the start point to the discharge point. Such paths are released in fracture zones; the lengths of these paths are close to the depth of the start point. It follows that 5% of the paths are shorter than 490 m. There are also paths that take a much more complicated route to the point of discharge, through rock mass, fracture zones and quaternary deposits; such a path may have a large length and 5% of the paths are longer than 2 km. The median length of the flow paths is 920 m.

Considering the lengths of the simulated flow paths in the quaternary deposits (uppermost 3 m of model), most paths have a length between 3.5 m (1st percentile) to 75 m (99th percentile); the median is 18 m. These results indicate that flow paths from great depth tend to flow through the quaternary deposits by use of rather short flow routs. Only a small percentage (< 5%) of the flow paths demonstrate path lengths in the surface near material (in the uppermost 1.5 m of quaternary deposits) that is longer than 50 m. This is because most flow paths from great depth flow towards lakes and other strong sinks, and reaches these areas from deep below (see Figure 9-2 and Figure 9-5), and hence the surface near part of the flow paths will be short. Nevertheless, a small amount of flow paths (less than approximately 5% of all paths) demonstrates lengths between 50 m and 250 m in the quaternary deposits below lakes. This is however for a situation in which the resistances of the lake sediments are large. Outside of the lakes, the lengths of the flow paths (the studied flow paths in the quaternary deposits) tend to be short and are not much influenced by the resistance of the lake sediments.

Flow paths – Breakthrough time

The breakthrough times of the flow paths (released at depth of 420 m) have also been analysed. As for the previously presented results (lengths), we have studied the results (time) for: (i) The complete paths, with rock mass, fracture zones and quaternary deposits. These distributions represent the breakthrough time, from release positions to points of discharge. (ii) The time spent in the quaternary deposits. (The results refer to the same flow paths, released at a depth of 420 m).

Because of the uncertainty in the properties of the lake sediments, we have not included time spent in lake sediments in the calculation of breakthrough times or time spent in quaternary deposits.

Considering the complete paths, there are flow paths that flow more or less straight upward, in a fracture zone, from the start point to the discharge point; such paths will produce short breakthrough times – the 1st percentile is equal to 16 years. There are also paths that spend a very long time in the flow media, often by use of a long flow route between fracture zones. For such paths the breakthrough times are large – the 99th percentile is equal to 6,000 years. The median is 680 years.

Considering the flow in the quaternary deposits (vertical extension 3 m), some flow paths spend only a few months in this zone – the 5th percentile is equal to 0.9 years, the median is however 12.5 years, and some flow paths stay in the quaternary deposits for hundreds of years, flowing slowly under the lakes – the 99th percentile is equal to 867 years. For the uppermost 1.5 m of quaternary deposits we get the following results: the 10th percentile is equal to 0.9 years, the median is 4.5 years, and the 99th percentile is equal to 376 years.

Regarding the flow in the quaternary deposits, but only the flow below lakes, we note that the time spent below lakes can be considerable: the 10th percentile is equal to 2 years, the median is 66 years, and the 99th percentile is equal to 983 years. (Note that the time spent in lake sediments is not included.)

It should however be kept in mind that the transport process of diffusion was not included in these simulations, and that the calculated breakthrough times are directly proportional to the effective porosity. The value of the effective porosity is uncertain, and we have not included time spent in lake sediments in these analyses.

Flow paths – Comparison of breakthrough time, advective velocity and path lengths in different domains along the flow routes

By studying the advective movement of the virtual particles (flow paths) through the model, and by comparing length of paths, velocities and times spent in different domains along the flow paths, we are able to derive some general conclusions regarding the advective flow from great depth to the discharge areas at ground surface.

The simulated flow paths have demonstrated that in general the longest flow path lengths are within the fracture zones. In the rock mass between fracture zones, the flow path lengths tend to be shorter. The median flow path length, in the rock mass between the fracture zones, is 441 m and the median flow path length in the fracture zones is 537 m. These results are of course strongly dependent on the distance between fracture zones. The path lengths are the shortest in the quaternary deposits (uppermost 3 m); the median is only 13 m.

The advective velocities in the rock mass, the fracture zones and the quaternary deposits are very different. The velocities in the fracture zones are between 40 and 50 times faster than in the rock mass between the zones. (It should however be noted that the effective porosity assigned to the fracture zones is probably on the small side of a likely range of values, which will result in high velocities in the zones.) The velocities in the quaternary deposits are in general low; this follows from either the relatively large porosity (moraine, gravel etc), or from the small conductivity (clay), or from a combination of these properties. The lowest velocities of all the different domains studied are within the clay of the quaternary deposits. There exists however also flow routes which demonstrate larger velocities within the quaternary deposits than within the rock mass between fracture zones. It should also be mentioned that the average velocity of the groundwater inside the lower moraine of the quaternary deposits is much smaller than the velocity of the groundwater of the fracture zones. Hence the advective flow velocity of the groundwater may be dramatically reduced when the groundwater leaves the fracture zones and enters the quaternary deposits.

The advective breakthrough time is the quota between length and velocity. It follows that even if the velocities are low in the quaternary deposits, the quaternary deposits are not very important for the total breakthrough times of the complete paths, as the flow length in the quaternary deposits are very short. In a similar way the fracture zones are not very important for the total breakthrough times of the complete paths, as the velocity in the fracture zones are so high.

For most flow paths, the total break through times depend very strongly on the time spent in the rock mass between fracture zones; in comparison, the time spent in fracture zones and in the quaternary deposits is not very important. This conclusion is based on two of the curves in Figure 9-19: the curve representing: (i) time spent in rock mass between fracture zones, and the curve representing (ii) breakthrough time of complete paths. As these two curves are very similar it is demonstrated that it is the time spent in rock mass that is the most important contributor to the total breakthrough time.

It should be noted that the conclusions correspond to flow paths released at a depth of 420 m and that the time spent in lake sediments are not included in these analyses. All calculations were carried out for a normal year and a steady state solution. Flow paths were released in a uniform pattern and only flow paths that discharged above the sea were included in the analyses.

Flow paths – Results for a model without quaternary deposits

We have established models without any quaternary deposits. The quaternary deposits were changed into rock mass and fracture zones; hence the rock mass and the zones were extended all the way up to the ground surface. These models have been established for the purpose of comparisons to the Base case.

Flow paths – Distribution and type of discharge areas. The spatial distribution of the discharge areas for flow paths from a depth of 420 m is nearly identical when comparing the models with and without quaternary deposits.

Flow paths – Length. The length-distribution of flow paths, from a depth of 420 m, produced by a model without quaternary deposits is very much the same as the length-distribution produced by a model with quaternary deposits (considering complete paths).

Flow paths – Breakthrough time. The breakthrough time-distribution of flow paths, from a depth of 420 m, produced by a model without quaternary deposits is rather similar to the breakthrough time-distribution produced by a model with quaternary deposits (considering complete paths). The difference is that for the model without quaternary deposits, the breakthrough times are somewhat shorter. The largest differences, in percent, take place for the shortest breakthrough times. The main reason for the differences is that in a model without quaternary deposits, the fracture zones extend all the way up to the surface, and the zone will be fast routes to the discharge areas. In the model with quaternary deposits, the fracture zones will not extend up to the ground surface. Above the zones there is a layer of "lower moraine", and this layer will delay the flow in the zones and increase the breakthrough times.

Flow paths – Type of discharge areas considering a steady state situation with a potential recharge according to a dry-year

The results presented below were derived by use of a steady state solution. The potential recharge in the model was set to that of a dry-year. This is much smaller than the potential recharge of a normal year. The studied case is not a realistic case, because by modelling steady state conditions we model an average situation assuming that the average recharge is that of a dry-year (and not that of a normal year). Hence, the studied case will produce lower groundwater levels than the case representing a normal year, but also lower levels than a transient case representing a dry-year that follows after a normal year. The flow paths will develop inside a head field that will not change with time. The presented case, which combines a steady state solution and the potential recharge of a dry-year, was introduced for the purpose of comparing the discharge areas produced by this case to the discharge areas produced by the normal year. Considering a steady state solution and a dry-year; flow paths from a depth of 420 m will discharge at the same discharge areas as the steady state paths of the normal year. Hence, the discharge areas for flow paths from great depth are very stable and will not change much, even if the groundwater situation in the quaternary deposits changes dramatically.

Flow paths – Transient simulations with time dependent flow paths

Methodology: We have derived results by use of transient simulations and time dependent flow paths (transient paths). The simulated situation represents the changing flow conditions during a normal year. Simulated virtual particles produce advective flow paths that will develop inside a changing flow field. The particles may stay in the studied flow domain during a simulated period of many years; it follows that the simulated normal year is repeated many times as the studied flow path develops in the model. From a numerical

viewpoint the calculations are somewhat more complicated than for the steady state flow paths. For the transient paths the particles develop within 12 different flow fields, each flow field represents a single month of the normal year. Each particle is studied separately. Hence, the result of this section represents time dependent flow paths that develop inside a transient flow field, representing the different flow conditions during the different months of a series of normal years.

Distribution and type of discharge areas: Transient flow paths from a depth of 420 m will discharge at the same discharge areas as the steady state paths.

Lengths: The lengths of the transient flow paths (released at depth of 420 m) have been analysed. The length-distribution of the transient paths is very much the same as the length-distribution of the steady state paths.

Breakthrough time: The break through time-distributions of the transient paths is very much the same as that of the steady state paths.

General conclusions

The purpose is to study the flow of groundwater from rock masses at great depths and into the surface near deposits, and to estimate the spatial and temporal distribution of groundwater from great depths in the surface near deposits (quaternary deposits).

The discharge areas for the flow paths from great depth are given by the topography and located along valleys and lakes; the spatial and temporal extension of these areas do not vary much for different values of the permeability of the uppermost part of the flow medium or for the applied different values of groundwater recharge.

In this study flow paths were released on-shore inside of the shore line (no paths were released below the sea) and at an approximate repository depth (i.e. 420 m). The flow paths will either discharge into the sea (i.e. 34%) or above the sea (i.e. 66%). Considering the discharge areas above the sea, nearly all of the flow paths from repository depth will discharge into lakes, and especially where a fracture zone intersects a lake. The flow routes (from great depth) to the discharge areas are influenced by the fracture zones, which tend to be directed along valleys and therefore lead the flow paths to the lakes which are also located along valleys.

Considering a lake with a thick layer of low-permeable sediments at the base of the lake (a large flow-resistance), nearly all flow paths discharge along the lake perimeter where no sediments occur. For a situation in which a lake has sediments of small resistance along its base, most flow paths discharge at the base of the lake through the lake sediments.

Most flow routes from repository depths demonstrate short path lengths in the quaternary deposits. Only a small percentage (< 5%) of the flow paths demonstrate path lengths in the surface near material (in the uppermost 1.5 m of quaternary deposits) that are longer than about 50 m. This is because most flow paths from great depth flow towards lakes and other strong sinks and reach these areas from deep below. Hence the surface near part of the flow paths will be short.

Nevertheless, a small amount of flow paths (less than approximately 5% of all paths) demonstrate lengths between 50 m and 250 m in the quaternary deposits below lakes. This is however for a situation in which the resistances of the lake sediments are large. Outside of the lakes, the lengths of the studied flow paths in the quaternary deposits tend to be shorter and are not much influenced by the resistance of the lake sediments.

For most flow paths from great depth, the total break through times depend very strongly on the time spent in the rock mass between fracture zones. In comparison, the time spent in fracture zones and in the quaternary deposits is not very important. It should be noted that these conclusions correspond to flow paths released at repository depth, and that the analyses do not include time spent in lake sediments.

The groundwater flow situation in the quaternary deposits varies significantly during a year because the groundwater recharge varies. This variation is however not very important for the flow paths from great depth. The simulations of transient flow paths from a depth of 420 m produced results (length, breakthrough time and discharge areas) that were almost the same as the results produced by a steady state situation and a normal year. Even a steady state simulation of a dry-year produced the same discharge areas as a simulation of a normal year; also a model without quaternary deposits produced the same discharge areas.

Contents

1	**Introduction and purpose**	21
1.1	General purpose of study	21
1.2	Method	22
1.3	Detailed objectives	22
2	**Hydrological cycle and some important hydrogeological definitions**	23
2.1	Hydrological cycle	23
2.2	Catchment area, watershed and drainage basin	23
2.3	The concept of run-off and groundwater recharge	23
2.4	The concept of recharge areas and discharge areas	24
	2.4.1 False discharge areas or saturated recharge areas	25
2.5	Evapotranspiration and potential evapotranspiration	26
2.6	Conceptual model of the hydraulic properties of the quaternary deposits	26
3	**Methodology**	29
3.1	The system analysis approach	29
3.2	Original flow equation	29
3.3	Numerical and analytical approach, computer codes	30
3.4	Mathematical approach to the flow media – the heterogeneity of the flow media and the models	30
	3.4.1 Fractured rock	30
	3.4.2 Near surface deposits – quaternary deposits	31
3.5	Salt water and the importance of variable density flow	31
3.6	The shore level displacement – the land uplift	33
3.7	Calibration	33
3.8	Methodology for calculation of flow paths	33
3.9	Dispersion and retardation	34
4	**Hydrogeological properties of the domain studied**	35
4.1	Location of area studied	35
4.2	Topography	36
4.3	Topographic water divides	38
4.4	Fracture zones	38
4.5	Lakes	39
4.6	Clays	39
5	**Hydrometeorology and water balance modelling**	41
5.1	Average run-off	41
5.2	Statistical analysis of precipitation	42
5.3	Water balance modelling	45
6	**Properties of the groundwater model**	49
6.1	Size of model and boundary conditions	49
	6.1.1 Size of model	49
	6.1.2 Outer vertical boundary – Lateral boundaries	49
	6.1.3 Boundary at base of model	49
	6.1.4 Boundary condition along the top of the model	49
	6.1.5 Surface water flows	50
	6.1.6 Boundary at lakes	51
	6.1.7 Boundary condition at surface areas with clay	52

6.2 Discretization of domain studied 52
6.2.1 The Grid 52
6.2.2 Discretization of the lakes 52
6.2.3 Discretization of the areas that carries a surface clay layer 52
6.2.4 Discretization of the fracture zones 54
6.2.5 Representation of the topography 55
6.3 Permeability and porosity of flow domain 56
6.3.1 Introduction 56
6.3.2 Permeability and depth of quaternary deposits 56
6.3.3 Permeability of rock mass 56
6.3.4 Permeability of regional fracture zones 57
6.3.5 Porosity, yield and storativity 57
6.4 Principle lay-out of model 60

7 Calculation of recharge areas and discharge areas, thickness of unsaturated zone 61
7.1 Introduction 61
7.2 Amount of recharge areas and discharge areas, and thickness of unsaturated zone; versus conductivity of the uppermost 0.5 m – Steady state solution 61
7.3 Amount of recharge areas and discharge areas, and thickness of unsaturated zone; versus time – Normal year 66
7.3.1 Methodology of transient simulation 66
7.3.2 Results 66
7.4 Selection of Base case 69
7.5 Simulation of wet-year 70
7.5.1 Methodology of transient simulation – Wet-year 70
7.5.2 Results 70
7.6 Simulation of dry-year 71
7.6.1 Methodology of transient simulation – Wet-year 71
7.6.2 Results 71

8 Calculated groundwater recharge 75
8.1 Introduction 75
8.2 Size of recharge (flow); versus conductivity of the uppermost 0.5 m – Steady state solution 75
8.3 Size of recharge with alternative top boundary condition 77
8.4 Size of recharge and amount of discharge areas versus conductivity of flow medium, steady state solution 78
8.5 Size of recharge versus time 79
8.5.1 Normal year 79
8.5.2 Wet-year 80
8.5.3 Dry-year 81
8.6 Recharge to the rock mass 82
8.6.1 Introduction 82
8.6.2 General behaviour of the system 83
8.6.3 Normal year 83
8.6.4 Wet-year 84
8.6.5 Dry-year 85
8.6.6 Recharge to rock mass without quaternary deposits 86
8.6.7 Recharge to rock mass – Concluding remarks 87

9 Analyses of flow paths from great depth 89
9.1 Introduction and methodology 89
9.1.1 Introduction 89
9.1.2 Method for calculation of flow paths 89
9.1.3 Method for release of particles 89
9.1.4 Time dependency of flow paths 90
9.1.5 Dispersion and retardation 90
9.1.6 The not included heterogeneity of the local domain 90
9.1.7 Percentiles 90
9.1.8 Separation of results from flow paths analyses into results for complete paths and results for surface near part of paths 90
9.2 Steady state and time-independent flow paths 92
9.2.1 Methodology 92
9.2.2 Visualisation of discharge areas and flow paths 92
9.2.3 Flow paths – distribution within different materials 95
9.2.4 Flow paths – distribution and type of discharge areas 95
9.2.5 Flow paths – Amount of discharge into lakes 96
9.2.6 Flow paths – Discharge via lake sediments or via lake perimeter 97
9.2.7 Flow paths – Length 100
9.2.8 Flow paths – Breakthrough time 105
9.2.9 Comparison of breakthrough time, advective velocity and path lengths, in different domains along the flow paths 108
9.2.10 Flow paths – Results for a model without quaternary deposits 110
9.2.11 Flow paths – Type of discharge areas considering a steady state situation, with a potential recharge according to a dry-year 112
9.3 Transient simulations with time dependent flow paths 113
9.3.1 Methodology 113
9.3.2 Transient flow paths – distribution within different materials 114
9.3.3 Transient flow paths – distribution and type of discharge areas 114
9.3.4 Transient flow paths – Length 114
9.3.5 Transient flow paths – Breakthrough time 116

10 Conclusions 119

11 References 121

1 Introduction and purpose

1.1 General purpose of study

The purpose of the presented work is to study the flow of groundwater from rock masses at great depths and into the surface near deposits by use of mathematical models; and to estimate the spatial and temporal distribution of groundwater from great depths in the surface near deposits (quaternary deposits).

This study will look at the following question: Groundwater from great depth how is it distributed in the surface near deposits? This is an interesting aspect of groundwater flow from great depths, as many biological processes takes place in the surface near deposits, processes that may be of importance when analysing contaminant transport from a repository located at great depth. Hence, this study is about the interaction between the geosphere and the biosphere. We will of course not provide the reader with a complete answer to the above given question, but we will present some results of a numerical modelling focused on the given question.

The presented work is a theoretical study. The system studied is represented by a time dependent three dimensional mathematical model. The model will include groundwater flows in the rock mass and in the surface near deposits (quaternary deposits) as well as surface water flows.

It is a purpose of this study to:

- Established groundwater models having such a resolution (degree of detail) that both rock masses at great depth and near surface deposits are included in the flow system studied and represented in the established models.
- Analyse both steady state conditions and transient conditions (time dependent conditions). The transient simulations will represent the varying state of the groundwater system studied, caused by the variation in hydro-meteorological conditions (variation in run-off) during a normal year, a wet-year and a dry-year. The shore-level displacement (or shore level progress) is not included in this study.
- Analyse and follow the simulated groundwater flow, from great depths via rock masses and fracture zones, to the quaternary deposits, and through the quaternary deposits to the final discharge areas.

The area studied is located in Sweden, in the Northeast of the Uppland province, close to the Forsmark nuclear power plant. The studied area has been selected as a candidate area for a deep repository for nuclear waste. This study is about analysing the general behaviour of a groundwater flow system; the results of this study are not to be interpreted as results of a site specific modelling, that analyses the suitability of the studied area as a host domain for a deep repository. This study is not based on data gathered during the site investigation programme.

1.2 Method

The study is based on a system analysis approach, and the studied system is the groundwater flow in rock mass and in quaternary deposits at a domain located in Northeast Uppland. To reach the objectives of the study, mathematical models are devised of the studied domain; these models will, in an idealised and simplified way, reproduce the groundwater movements at the area studied. The formal models (the mathematical models) used for simulation of the groundwater flow are three-dimensional mathematical descriptions of the studied hydraulic system. To set up the formal models we used the numerical code GEOAN /Holmén, 1992/, which is based on the finite difference method

1.3 Detailed objectives

The results of the study include:

- Water balance modelling for the purpose of deriving temporal distribution of the run-off (monthly values) for a normal year, a wet-year and a dry-year.
- Magnitude and direction of groundwater flow.
- Amount of recharge areas and discharge areas; and thickness of unsaturated zone, for steady state and transient conditions.
- Groundwater recharge to quaternary deposits, groundwater recharge to rock mass; for steady state and transient conditions. Groundwater recharge, considering a model without quaternary deposits.
- Length and breakthrough time of flow paths from great depth (a depth of 420 m). Total lengths and breakthrough times, as well as length, velocity and time spent in different domains and structures along the paths, for example length and time in the near surface quaternary deposits. Comparison of breakthrough time, advective velocity and path lengths, in different domains along the flow paths.
- Distribution of discharge areas for the flow paths from great depth. Importance of lake sediments.
- Flow paths – Results for a model without quaternary deposits
- The importance of the changes in the head field caused by monthly changes in groundwater recharge; considering flow paths from great depths

2 Hydrological cycle and some important hydrogeological definitions

2.1 Hydrological cycle

The circulation of water between ocean, atmosphere and land is called the hydrologic cycle. Inflow to the hydrologic system arrives as precipitation (rain or snow). Outflow takes place as streamflow and as evapotranspiration. Evapotranspiration is a combination of evaporation from open bodies of water, evaporation from soil surfaces and transpiration from the soil by plants. Streamflow water is made up by: (i) direct precipitation on the stream, (ii) surface flows that reaches the stream and (iii) groundwater flows that reaches the stream.

An estimate of the total water balance of the world is given below in Table 2-1 /based on Nace, 1971/:

Table 2-1. Estimate of the water balance of the world /Based on Nace, 1971/.

Parameter	Surface area (km^2)×10^6	Volume (km^3)×10^6	Volume (%)	Residence time
Oceans and seas	361	1,370	94	~ 4,000 years
Lakes and reservoirs	1.55	0.13	0.01	~ 10 years
River channels	< 0.1	< 0.01	< 0.01	A few weeks
Groundwater	130	60	4	Weeks to ten thousands of years
Icecaps and glaciers	17.8	30	2	A few years to thousands of years
Atmospheric water	504	0.01	< 0.01	~ 10 days

2.2 Catchment area, watershed and drainage basin

A catchment area, or a drainage basin, or a watershed, is often defined as: “The whole area having a common outlet for its surface runoff” /Nordic Glossary of Hydrology, 1984/. However, when studying the flows of water within such an area it is often necessary to study both surface flows and groundwater flows; and the catchment area for the groundwater flow may not be exactly the same as that for the surface flows.

2.3 The concept of run-off and groundwater recharge

As precipitation falls on an area, a certain amount of the precipitation evaporates directly from leaves or from the ground surface. Some of the water infiltrates into the pores of the soil, percolates through the unsaturated zone, and reaches finally the saturated zone, where the pores are fully saturated with groundwater. Plants consume a substantial part of the water as it moves through the flow medium towards the groundwater surface. The amount of water that makes it all the way down to the groundwater surface, and adds water to the groundwater system, is called the groundwater recharge.

Recharge is often defined as: “A process, natural or artificial by which water is added from outside to the zone of saturation, either directly into a formation or indirectly by way of another formation” /Nordic Glossary of Hydrology, 1984/.

The amount of water that during a studied period is theoretically available to create groundwater is called the run-off, or the potential groundwater recharge (or the potential recharge). All of this water will normally not create groundwater; a certain amount may directly create surface water flows.

The run-off is equal to the precipitation minus the actual evapotranspiration. The evapotranspiration is the amount of water transferred from soil and plants to the atmosphere by evaporation and transpiration, respectively.

Run-off is often defined as “That part of the precipitation that flows towards the stream on the ground surface (surface run-off) or within the soil and rock (subsurface run-off)” /Nordic Glossary of Hydrology, 1984/.

Hence, the run-off is equal to the surface run-off (surface flows) plus the subsurface run-off (groundwater flow), and often described as the difference between the precipitation and the evapotranspiration.

Considering a steady state situation and a catchment area, the groundwater flow is equal to the subsurface run-off, which is given by the actual groundwater recharge.

We have calculated the temporal distribution of the potential groundwater recharge, by use of a mathematical model. This is discussed in Section 5.

2.4 The concept of recharge areas and discharge areas

A recharge area can be defined as “that portion of the drainage basin in which the net saturated flow of groundwater is directed away from the water table”; and a discharge area can be defined as “that portion of the drainage basin in which the net saturated flow of groundwater is directed from the water table”, definitions according to /Freeze and Cherry, 1979/. Hence, we may say that recharge areas are the areas were surface water (e.g. precipitation) enters the groundwater system; and discharge areas are the areas were groundwater leaves the groundwater system and form surface water. At a recharge area, the water table (groundwater table) usually lies at some depth; at a discharge area the groundwater table is usually at or very near the ground surface.

Some soils, especially those near the ground surface, are not necessarily saturated with groundwater. Their voids may only partially be filled with water, the rest of the pore space being occupied by air. If a zone of partially saturated pores exists, such a zone is called the unsaturated zone. An unsaturated zone can only exist at recharge areas. According to our definition above, at discharge areas the groundwater flows out of the soil/rock and consequently there is no unsaturated zone at discharge areas. The unsaturated zone occurs above the groundwater table (and above the capillary fringe).

In general, precipitation may occur everywhere, hence groundwater recharge may take place everywhere. However, the actual amount of the precipitation that infiltrates and where it infiltrates depends (among other things) on the permeability of the soil/rock upon which the precipitation falls. It is the total transport capacity of the groundwater flow medium that determines the size of the groundwater flow and thereby the size of the groundwater recharge. The topography is another important parameter of the total transport capacity

of the studied system, because the groundwater gradient is very much influenced by the topography. Nevertheless, when considering the infiltration of surface water and creation of groundwater, the uppermost part of the flow medium (the part closest to the ground surface) becomes very important. The amount of recharge areas depends on the permeability of the uppermost part of the flow medium (assuming everything else being equal). If the permeability is large, a large amount of the precipitation and surface waters will infiltrate and create groundwater. The amount of recharge areas will be large for such a situation (but it cannot be 100%, as there must always be discharge areas). If the permeability is small, only a small amount of the precipitation will be able to infiltrate, it follows that most of the areas will be saturated up to the ground surface, consequently for such a situation most areas will be discharge areas, even if the discharge is small.

In addition, the actual distribution of recharge and discharge areas, and the amount of recharge and discharge areas, vary during a year, dependent of the spatial and temporal distribution of precipitation (e.g. rainy seasons) and temperature (e.g. freezing of ground or not).

In the models of this study and at a local area (a cell), the locally produced surface water flow is given by the part of the potential groundwater recharge that has not infiltrated in the model, as well as by groundwater discharge, if such discharge takes place at the area studied. A surface water flow coming to the area studied from uphill areas is not locally produced surface water. We define the locally produced surface water as the local discharge.

In this study we have defined a discharge area, as an area at which the locally produced surface water flow (the discharge) is larger than the potential groundwater recharge. The groundwater head is equal to the topographic elevation at such areas. It also follows from the definition of discharge areas used in this study, that local streams and swamps may be defined as discharge areas. We have however not included areas defined as lakes in the analyses of recharge and discharge areas.

2.4.1 False discharge areas or saturated recharge areas

Precipitation falls over both recharge and discharge areas, it follows that the surface water flow at a discharge area is not only given by groundwater discharge, but also by the precipitation that falls directly on a discharge area. There are two different types of discharge areas, partly related to the intensity of the precipitation, the conductivity of the flow media and the length of the time period studied.

False discharge areas are areas were the amount of locally produced surface water flow is smaller than the potential recharge. At such areas there is actually no outflow of groundwater. At such areas, the potential recharge itself will saturate the flow system; the saturation of the flow system is not a result of an outflow of groundwater, but by a large inflow of recharge. A certain amount of the potential recharge will be added to the ground-water system and the rest will form a surface water flow. It is important to note that the groundwater head will be bounded by the topography at these areas (as at true discharge areas), and there is no unsaturated zone at these areas (as at true discharge areas), but at false discharge areas the locally produced discharge is smaller than the potential recharge of the area.

At a true discharge area the amount of locally produced surface water flow is larger than the potential recharge. At such areas groundwater leaves its flow medium and creates surface water flows.

The amount of false discharge areas is given by the intensity of the precipitation (length/time) and the conductivity (length/time) of the flow medium into which the precipitation tries to infiltrate. If a recharge area is studied during a period of precipitation and the intensity of the precipitation increases and becomes larger than the transport capacity (conductivity) of the flow medium, the area studied will be a false discharge area during the period of precipitation.

It follows that the length of the time period studied is important when performing transient modelling of groundwater recharge. In this study we have used annual or monthly values of precipitation and potential recharge. Hence in our model the precipitation and recharge is equally spread of the length of a year or a month. The actual precipitation is however not equally spread over a year or a month, periods of varying intensity takes place (days of rainy weather and days of sunny weather). Our results are to be looked upon as average results representing the length of the period studied.

Some authors use the term "saturated recharge areas" for the type of areas that we have called false discharge areas.

In this study when we discuss discharge areas, we have not included false discharge areas in the analyses.

2.5 Evapotranspiration and potential evapotranspiration

The evapotranspiration is defined as: "The amount of water transferred from soil and plants to the atmosphere by evaporation and transpiration, respectively." /Nordic Glossary of Hydrology, 1984/.

The potential evapotranspiration is defined as: "The theoretical evapotranspiration from a surface completely covered by a homogeneous surface of green vegetation (crop) experiencing no lack of soil water. Usually estimated from climatological data alone." /Nordic Glossary of Hydrology, 1984/.

2.6 Conceptual model of the hydraulic properties of the quaternary deposits

We have establish a model with such resolution that the model is capable of reproducing the flow of groundwater in the quaternary deposits, and at the same time include some aspects of the groundwater flow at great depth. The hydraulic properties of the quaternary deposits of the established model are based on a conceptual model of the near surface groundwater flow system in which a very permeable material takes place close to the ground surface, having a thickness of a few decimetres. Accordingly, we have in our model defined the uppermost 0.5 m with a very large permeability (except for areas covered with clay or lakes). This conceptual model is based on /Grip and Rodhe, 1985/ and /Rodhe, 1987/ in these studies the authors present and argues for a conceptual model with a very permeable layer close to the ground surface.

There are several reasons for a large permeability close to the ground surface:

(i) Near the ground surface the deposits are less consolidated, because the do not carry the large weight of overlaying materials.

(ii) Biological activity (roots, worms, insects etc).

(iii) Downward transport of fine-grained materials.

(iv) Temperature changes during the year, in combination with soil water, i.e. freezing and melting of the soil water, etc.

It is in the highly permeable layer, close to the ground surface, that a very large amount of the precipitation infiltrates and flows towards the local streams. Considering typical Swedish climate, geology and vegetation, for such circumstances an overland flow of surface water takes place very rarely; this is also discussed in /Grip and Rodhe, 1985/ and /Rodhe, 1987/. Most of the water that reaches a local stream is groundwater, even if it may be a very surface near groundwater. During a rainfall, the flow in local streams may increase – a precipitation induced flow peek. Investigations have demonstrated that such a flow peek is primarily created by groundwater that discharges into the stream, and not by surface water, about 60–85 percent of the flow is made up by discharging groundwater /Grip and Rohde, 1985; Rodhe, 1987/.

3 Methodology

3.1 The system analysis approach

In this study the limited part of the reality that we are investigating is called the system. The model is an idealised and simplified description of the studied system. This study is based on the system analysis approach. This is a method for solving complicated problems by: (i) establishing a model of the studied system, (ii) using the model for simulations which imitate the behaviour of the studied system and (iii) based on the results of the simulations, gain insight into the behaviour of the studied system.

Based on the objectives, and on available information of the system studied, a conceptual model is established. The conceptual model includes information of the studied media (rock mass, quaternary deposits etc) and the physical processes governing the surface and groundwater flow, but it includes only information relevant as regards the objectives of the study. Based on the conceptual model a formal model is established. The formal model is a mathematical description of the conceptual model; it is established by the use of a computer code. The formal model is used for simulations.

3.2 Original flow equation

The formal model is a three-dimensional, time-dependent mathematical description of the studied hydraulic system. Groundwater flow will be calculated with by use of different formulations of Darcy's law /Darcy, 1856/, and the continuity equation. Darcy's law assumes a non-deformable flow medium and that the inertial effects and the internal friction inside the fluid are negligible; these generalisations are applicable, considering the flow system studied. The governing equation for groundwater flow in a continuous medium is the following differential equation (presuming constant fluid density, the X-direction and the Y-direction is in the horizontal plane, the Z direction is in the vertical plane).

$$\frac{\partial}{\partial x}\left(K_x \frac{\partial \phi}{\partial x}\right)+\frac{\partial}{\partial y}\left(K_y \frac{\partial \phi}{\partial y}\right)+\frac{\partial}{\partial z}\left(K_z \frac{\partial \phi}{\partial z}\right)-VF = Ss \frac{\partial \phi}{\partial t} \qquad \text{Equation 2.1}$$

Where

K_x, K_y, K_z = Hydraulic conductivity along axes (L t^{-1})

ϕ = Hydraulic head (Piezometric head, Groundwater head) (L)

VF = Volumetric flow (flow per unit volume, inflow and outflow of water) (T^{-1})

Ss = Specific storage of medium (L^{-1})

t = Time (T)

The head (hydraulic head) is defined as the sum of pressure and elevation. The development of Equation 2.1 from Darcy's law and from the continuity equation is well known, see for example /Bear and Verruit, 1987/.

Equation 2.1 constitutes, together with initial conditions and boundary conditions, a mathematical representation of a flow system. Analytical solutions to the equation normally exist only for very idealised and simplified cases. Consequently, we need to use numerical models.

3.3 Numerical and analytical approach, computer codes

The formal models are mathematical descriptions of the studied hydraulic system. The formal models are based on a numerical approach and established by use of the GEOAN computer code. GEOAN is a computer code based on the finite difference numerical method. The finite difference method and the GEOAN code are briefly presented in /Holmén, 1997/; the code was first presented by /Holmén, 1992/.

3.4 Mathematical approach to the flow media – the heterogeneity of the flow media and the models

The established model represents fractured crystalline rock masses and porous quaternary deposits.

3.4.1 Fractured rock

Groundwater flow in a fractured rock occurs in fractures and in fracture zones of different size and significance. These fractures and fracture zones determine the heterogeneous and anisotropical hydraulic properties of the rock mass. There are different approaches available when establishing a mathematical description of a fractured medium. In this study we will use the continuum approach, which replaces the fractured medium by a representative continuum in which spatially defined values of hydraulic properties can be assigned to blocks of a given size. A large number of blocks represent the studied media. We will in this study not discuss in detail the concept of the continuum method; for a detailed presentation of the continuum method we refer to /Bear and Verruit, 1987/ and /Bear and Bachmat, 1990/.

Properties may be assigned to the blocks in a deterministic way, i.e. a deterministic continuum model. If we replace a heterogeneous property (e.g. the conductivity) with an average value and assign that value to the blocks of a model, we will get a model that we will call a uniform continuum model. If detailed information of the hydraulic properties are unknown and we want to include the heterogeneity into the model, we can use a stochastic continuum model. In a stochastic continuum model the hydraulic properties of the blocks are described by probability distributions, selected to fit the size of the studied blocks. The different methods should be regarded as different ways of idealising and simplifying the system studied, when establishing a mathematical model representing the system.

For the system that we will study, it is possible to identify two different types of flow media in the fractured rock: the rock mass between large fracture zones and the large fracture zones. We will use the following approach considering the continuity and the conductivity of these two flow media:

- The rock mass between large fracture zones will be defined as continuous, having a homogeneous conductivity by use of representative averages values of conductivity.

- Large fracture zones will be defined as separate continuous structures, by use of an implicit formulation as regards the conductivity of the different volumes defining the geometry of the models (the cells). The conductivity of the zones is defined as being homogeneous, by use of representative average values of conductivity.

Our specific knowledge of the local heterogeneity of the fractured crystalline rock mass between the regional fracture zones is limited. However, we can assume that in principle it will be similar to the heterogeneity of the fractured crystalline rock mass at Äspö Hard Rock Laboratory, which has been investigated in several studies, see e.g. /Gustafson et al. 1989/ and /Wikberg et al. 1991/. Investigations at Äspö HRL have demonstrated that the heterogeneity of a fractured rock mass is scale dependent. At small scales the heterogeneity is large and at large scales the heterogeneity is small.

In a numeric model, the properties of the model are defined at the cells (elements) of the model grid (model mesh). Heterogeneity in the properties of a domain studied is included in a numerical model by assigning different properties to different cells of the model grid. However, as the heterogeneity of a fractured rock is scale dependent, the variation in properties assigned to the cells of the grid should depend on the size of the cells. In this study we have not included any heterogeneity within the rock mass, except for the large fracture zones.

For some of the objectives of this study, the unknown and not included heterogeneity of the rock mass (the heterogeneity that is not represented by the regional fracture zones), is of less importance – these objectives are the predictions of the average flow directions. For other objectives, the unknown and not included heterogeneity might be of more importance. For example the estimated distribution of lengths of flow paths from the repository to the discharge areas and the estimated distribution of breakthrough times will demonstrate a larger variation if the local heterogeneity is included in the model.

Considering the results of the flow path analysis, the calculated variation in length of flow paths and breakthrough times are probably smaller than the actual variation. This is because the local heterogeneity of the rock mass and especially the heterogeneity inside the fracture zones are not included in the models of this study.

3.4.2 Near surface deposits – quaternary deposits

The near surface deposits, also called the quaternary deposits, are explicitly included in this model. The quaternary deposits consist primarily of (glacial till) moraine, clay and gravel. These materials are examples of porous media and are therefore well represented by the continuum approach. The continuum approach replaces the porous medium by a representative continuum in which spatially defined values of hydraulic properties can be assigned to blocks of a given size. A large number of blocks represent the studied media. For a detailed presentation of the continuum method we refer to /Bear and Verruit, 1987/ and /Bear and Bachmat, 1990/.

3.5 Salt water and the importance of variable density flow

The groundwater at the domain studied is of different origin, and partly dependent on its position in the flow system it is of different age. It is possible to distinguish four different types of groundwater: (i) Fresh water, (ii) Relict glacial meltwater with low levels of salinity, (iii) Relict seawater with a salinity close to that of the present Baltic Sea, and (iv) Shield brine with large levels of salinity (larger than the levels of the sea).

The fresh water is generally found at shallow depths, but may occur at great depth at some distance from the shoreline. The distribution of the relict glacial water is not well known. Relict seawater is likely to be found anywhere in the domain studied; as the whole of the domain studied was below the sea at about 8,000 years before present /Påsse, 1996/, because of the shore level progress.

Shield brine is generally found at great depth, below the fluids described above. The processes that create the shield brine are not very well understood.

The groundwater models of this study include the area that surrounds the SFR repository. SFR is a repository located about 50 m below the sea floor and about one kilometre off the shoreline, outside of the Forsmark nuclear power plant. /Stigson et al. 1998/ investigated the importance of variable density flow at SFR, by use of two-dimensional models (SUTRA), representing a large vertical cross-section. A large number of different cases were studied. The changed parameters were:

- Permeability.
- Porosity.
- Change in long term evolution of the salinity in the seawater.
- Presence of vertical and/or horizontal structures.

The most important conclusions were:

- The porosity has a large impact on the results since higher porosity means that the transport time is longer and that more saline water has to be flushed out.
- As the model becomes more complex (i.e. incorporating heterogeneity structures, etc) the spatial differences in salinity and the difference in flow through the SFR, between variable-density and uniform-density flow, becomes less significant.
- Differences between modelling groundwater as a variable-density flow or a uniform-density flow with salt (chloride) as a tracer at the SFR is negligible.

It should however be noted that the SFR is a repository located at depth of only 50 m below the sea floor. At greater depths, where heavy shield brine may occurs, the salinity of the groundwater is more important for the flow of the groundwater.

The following is stated in /Voss and Andersson, 1993/: “Because of the large density contrast between fresh water and shield brine, circulation of shield brine is likely driven by both fluid density differences and topographic forces, whereas flow of the more dilute fluids, including relict seawater, is driven primarily by topographic forces”.

For a flow system that includes variable-density flow and carries shield brine at great depth, the shield brine will limit the vertical extension of the flow of the less heavy groundwater above the shield brine, including the flow of relict seawater. The heavy shield brine will to a large extent act as a confining layer, which creates an upper flow system with less saline groundwater and a lower system with heavy saline water (shield brine). Because of the density difference between the shield brine and the groundwater above it, the less heavy groundwater (above the shield brine) will not penetrate into the domain of the shield brine.

In this study we have not included density dependent flow, consequently the models of this study do not include the shield brine, and instead these models are defined with a limited depth (600 m). The limited depth of the models is a simplified method of representing the confining effects of the shield brine. Such an approach could be motivated by the study of /Stigson et al. 1998/, which demonstrates that the flow in the domain above the shield

brine can be simplified to a non-density dependent flow system; and as it is primarily not an objective of this study to simulate the very deep and slow groundwater flow at very large depths inside the shield brine domain, but the flow of groundwater in the near surface quaternary deposits.

3.6 The shore level displacement – the land uplift

During the latest glacial period large amounts of water were tied to the ice mass, which had a maximum thickness of about 3 km. When the ice began to melt both the levels of the land and the water levels of the seas became higher. The interplay between land, ice and the water has resulted in different water levels and different types of water in the Baltic Sea as well as in the Baltic shield rock. In some periods the Baltic Sea was a freshwater lake while in others it was a saline sea. The sum of the ground level changes and the sea level changes is called shore level displacement (or shore level progress). The shore level displacement is not considered in the models of this study, as this study is not about the effects of the shore level displacement.

3.7 Calibration

The models are not calibrated, as no applicable data is available for calibration at the scale of the models. However, the properties of the models are according to observed and measured values and the calculated actual recharge and size of recharge areas of the models are in line with empirical estimations. The properties of the models are given in Chapter 3 and Chapter 4.

3.8 Methodology for calculation of flow paths

In this study the flow pattern of the groundwater is analysed by the use of flow paths. The GEOAN model create flow paths by use of simulated particles, particles that follow the flow of groundwater through the model (i.e. particle tracking). For calculation of flow paths the GEOAN model provides the user with both a semi-analytical method /Pollock, 1989/ and an iterative method; in this study we have used the semi-analytical method.

The flow fields of the models were analysed by use of flow paths released at a depth close to an estimated depth of a repository, i.e. 420 m below ground surface. In this study the flow paths are not released based on the size of the groundwater flow through a given volume. Paths are released in a regular pattern, one or several paths in each volume (cell or element) studied, regardless of the flow through the volume studied.

In the models, the virtual particles will move and the flow paths will develop inside a flow field that controls the movements of the paths. For a time-independent flow path, the path will develop inside a flow field that will not change with time. Hence, the flow field is constant during the movement of the simulated particle that gives the flow path. For a time-dependent flow path, the flow field will change with time during the movement of the simulated particle that gives the flow path. In this study we have generated both time independent and time dependent flow paths. Time-independent flow paths represent the flow field of a studied moment. Time dependent flow paths represent the changing flow field during a studied period.

The flow paths were analysed considering length, breakthrough time, average velocity etc, in different materials along the flow route (e.g. rock mass, fracture zones, quaternary deposits); but also as regards the overall distribution in the different materials.

3.9 Dispersion and retardation

Dispersion is the tendency for a solute, dissolved in the groundwater, to spread out from the path that it would be expected to follow according to the advective hydraulics of the flow system. Dispersion is caused by diffusion and mechanical mixing during fluid advection. Additionally, in a mathematical model an unwanted numerical dispersion may also take place, due to the method used for representation of the transport process.

- Diffusion, is not included in the established model.
- The mechanical mixing, called mechanical dispersion, is caused by the heterogeneous properties of the flow medium. Mechanical dispersion is scale dependent and will occur both at a microscopic scale and at a macroscopic scale. In the models we have not included mechanical dispersion as a tendency for the flow paths to spread out from the advective path.
- Numerical dispersion. If the model uses a fixed mesh and the solution of the advection-dispersion equation for representation of the transport process, numerical dispersion will influence the results. However, the model of this study (GEOAN) uses the approach of tracking of virtual particles and for this approach there is no numerical dispersion. Hence, the established model will not be influenced by unwanted numerical dispersion.
- Retardation. No retardation is included in this model.

Thus, in this study we have examined advective transport only.

4 Hydrogeological properties of the domain studied

4.1 Location of area studied

The area studied is located in Sweden, in the Northeast of the Uppland province, approximately 50 km North of Stockholm and close to the Forsmark nuclear power plant. The location o f the area studied is given in Figure 4-1 and Figure 4-2.

Figure 4-1 presents the regional position of the area studied (red dot); Figure 4-2 presents the extension of the area studied (purple line) in a local scale.

The horizontal extension of the area studied is approximately 10×8 km.

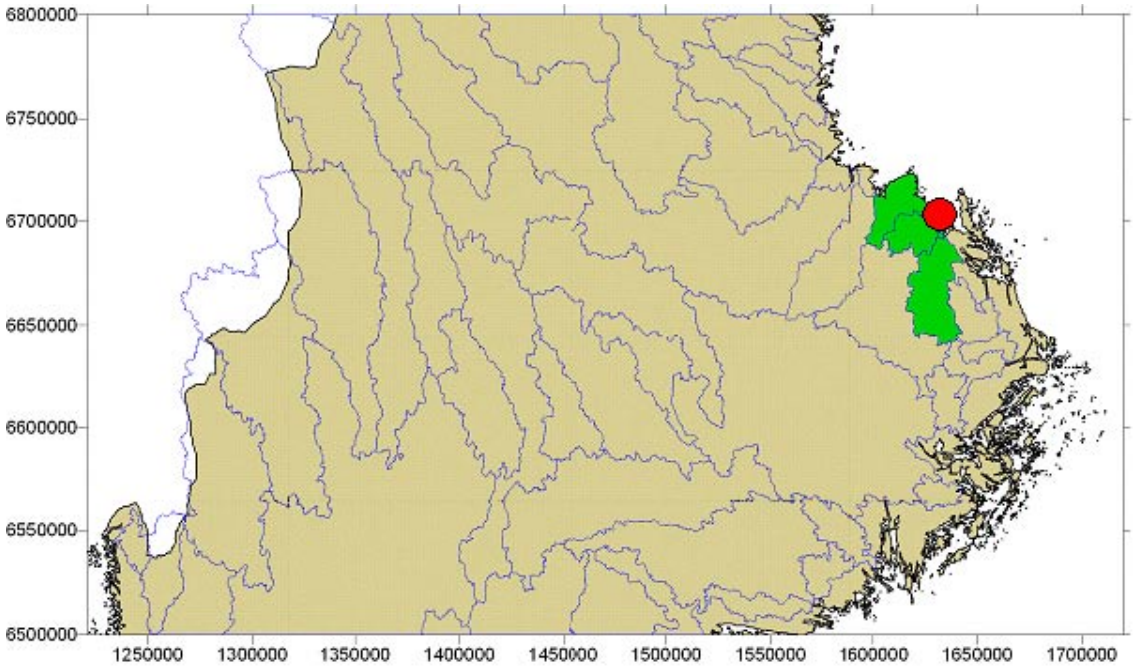

Figure 4-1. *Location of area studied – Super regional scale. The red dot denotes the area studied. It is located in Sweden, in the North East of the Uppland province, approximately 50 km North of Stockholm. The green areas in the figure above denote the extension of the three regional catchment areas surrounding the studied area. The regional topographic water divides are denoted by blue lines and the shore line is denoted by black lines.*

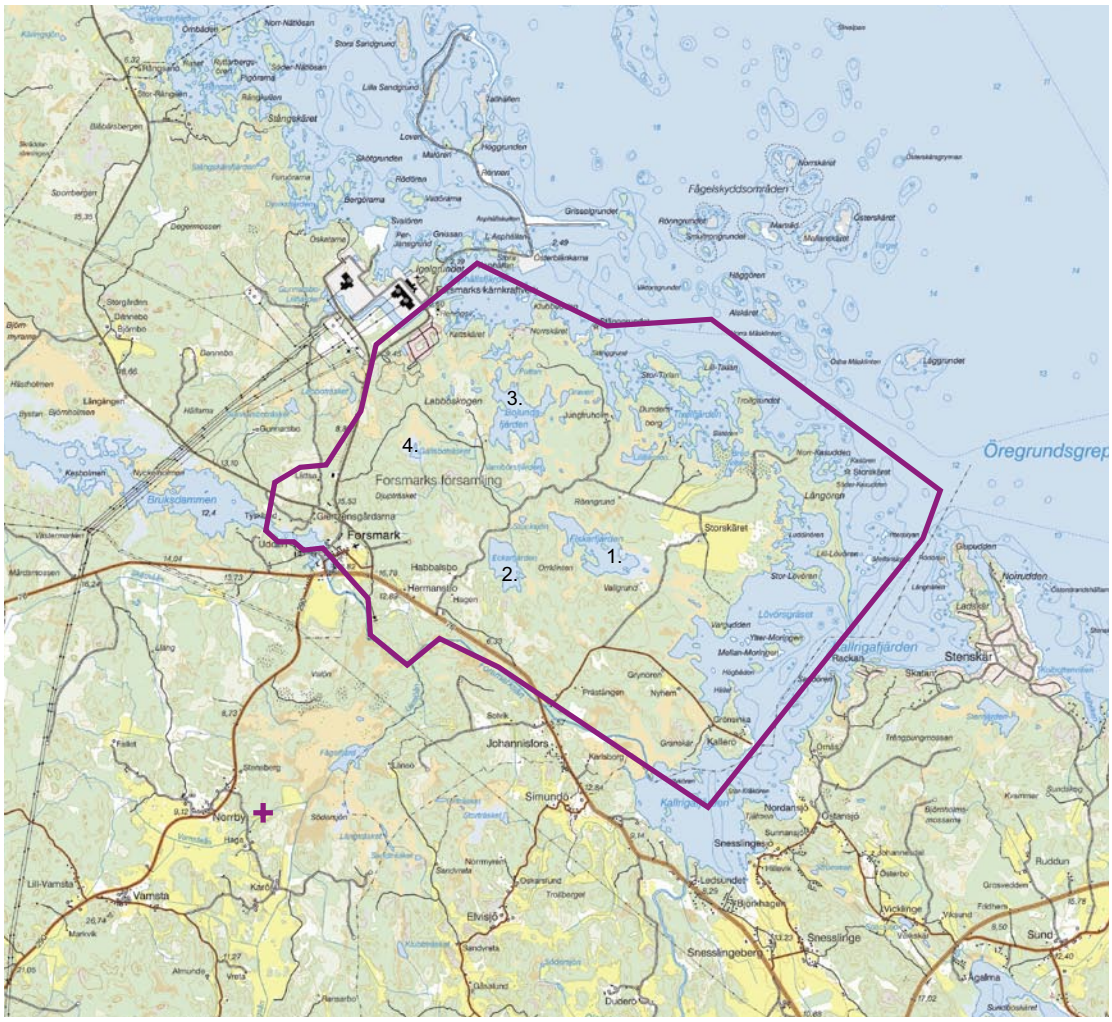

Figure 4-2. *Location of area studied – Local scale. General map of area studied (Lantmäteriverket). The purple line denotes the extension of the area studied. It is located in Sweden, in the North East of the Uppland province, approximately 50 km North of Stockholm, and close to the Forsmark nuclear power plant. The lake marked as 1. is Fiskarfjärden and the lake marked as 2. is Eckarfjärden. The lake marked as 3. is Bolundsfjärden and the lake marked as 4. is Gällsboträsket.*

4.2 Topography

The database used for describing the topography was supplied by SKB from the SICADA database; it was defined in the co-ordinate system RT90 2.5gV - RH70 and the grid is 10 m in both x and y direction. It is not exactly the same topography as used in the regional modelling of the area studied /see Holmén et al. 2003/, as the regional model used a topographic database with a grid size of 50×50 m.

The elevation of the sea floor (depths) is also taken from the SICADA database; this data was also used in the feasibility study of the Östhammar municipality. Originally the data comes from the Swedish Maritime Administration. The data is coarse and represents two depth curves, the 6 m and 20 m depth curves.

The position the shoreline, taken from the general map of the area studied, see Figure 4-2, was added to the topographic database. The elevation of the shoreline was set to 0 masl. In addition extra data points defining the elevation of the sea floor were added to the database, especially close to the shoreline. These data points were also taken from the general map of the area.

The small volume of data, describing the elevation of the sea floor, is a minor problem for this modelling; since in the model a constant specified head condition would be defined along the sea floor. Even if the topography varies in the model along the sea floor, the groundwater head at the sea floor is the same and defined to 0 masl (the elevation of the Baltic Sea).

The topography of the area studied and its surroundings are shown in Figure 4-3. The figure covers an area of 12×10 km. The topography is not very dramatic. North of the regional water divide it is a smooth lowering of the elevations of the ground surface, with some local topographic undulation, towards the shoreline.

The lowest elevations within the area studied are below the sea; the lowest elevation of the sea floor is below –16 masl. The highest elevation is about 27 masl, and it takes place about 3,500 m from the shoreline, which produces a topographic gradient towards the sea of approximately 0.8%

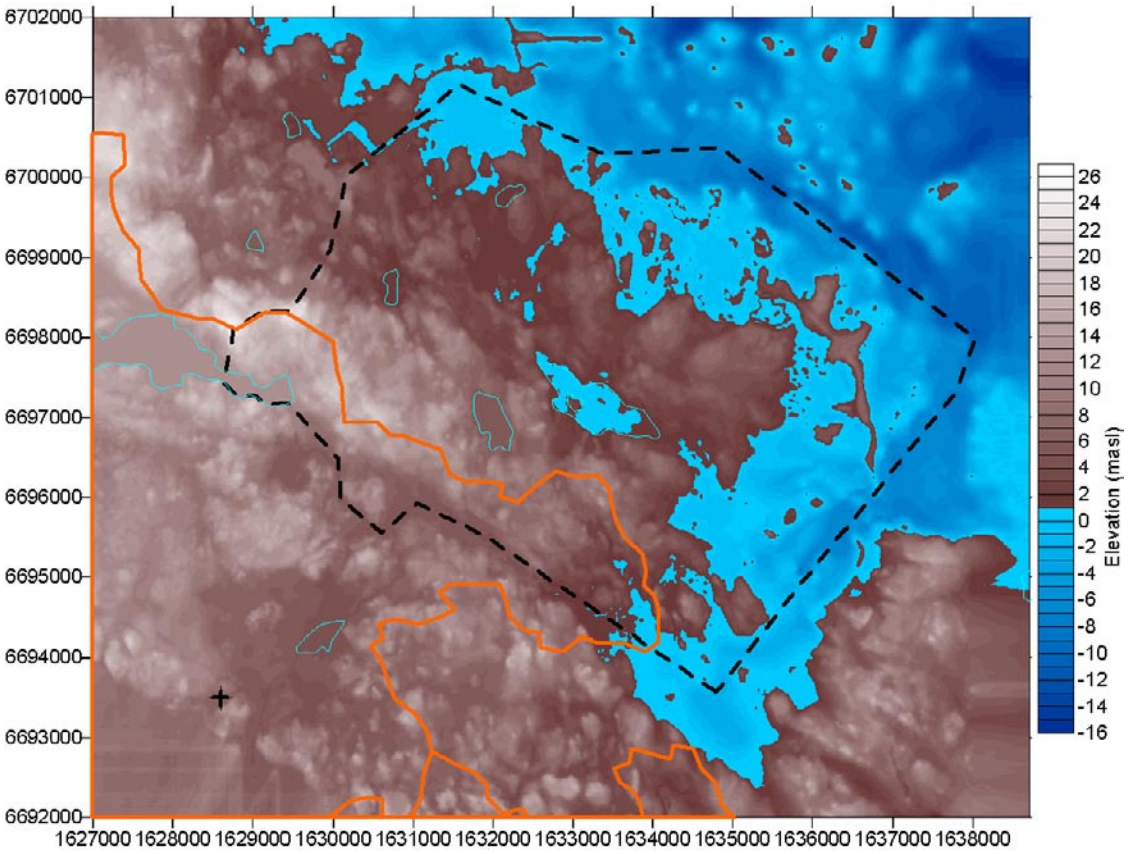

Figure 4-3. *Topography of the area studied. The orange lines denote the regional surface water divides. The topography below the sea is denoted by shades of blue. The black dotted line denotes extension of model.*

4.3 Topographic water divides

The regional topographic surface water divides are presented in Figure 4-3 and in Figure 4-4. The divides are the major surface water divides according to SMHI. (Personal communication with Sten Lindell, SMHI, 2002-04-17 confirmed that no revisions have been made to this data.)

4.4 Fracture zones

The extension of the regional lineaments (regional fracture zones) are defined in different reports, but all data comes primarily from SGU. In this study, the data defining the zones are taken from the file "sprickzon_r99_53fig8_4.shp", as provided by SKB. The definitions of the regional fracture zones used in this study are identical to the definitions used in the regional modelling of the area studied /Holmén et al. 2003/. The definitions of the zones, as provided by SGU, were simplified to a large number of straight lines; duplicate zone definitions were also removed from the data. The extension of the regional zones, as defined in the model, is shown in Figure 4-4. Details of the inclination and depths of the regional zones are not known; in the established model all zones are defined as vertical and extends to the base of the model. The presence and extension of sub-horizontal zones were not well known at the time of the modelling, no such zones were included in the study. As can be seen in Figure 4-4, below, most of the regional fracture zones are located along low-lying parts of the topography.

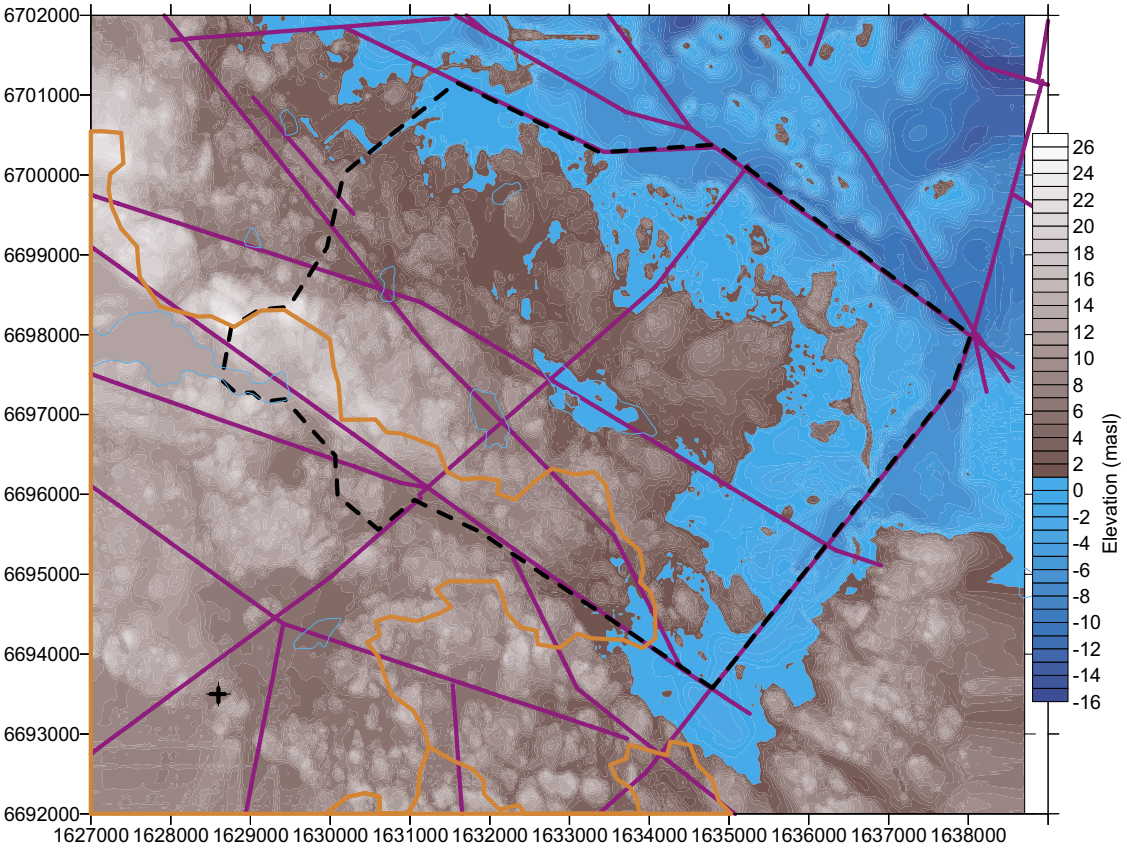

Figure 4-4. *Topography, surface water divides and regional fracture zones. Purple lines denote the horizontal extensions of the zones. Light blue lines denote extension of lakes. The black dotted line denotes extension of model.*

4.5 Lakes

The data describing the extension of the lakes are taken from the general map over the area studied, from a file called SJO1_C.shp, provided by Lantmäteriverket. Figure 4-4 presents the lakes within the area studied. It should be noted that the area with low elevation at 1632000, 6699000 (Bolundsfjärden, Lake 3 in Figure 4-2) is not a lake according to the information provided by Lantmäteriverket), but a part of the sea. However, according to the topographic database, the elevation of the water surface in this area is somewhat above the level of the sea. This illustrates the influence of the shorelevel progress and the somewhat fluctuating water level of the Baltic Sea. The area discussed above used to be a part of the sea, but due to the shorelevel progress and sediment accumulation, it is more and more transformed into a lake. In the model of this study, the area is defined as a swamp/lake with a water level somewhat above the sea level.

4.6 Clays

The low permeable quaternary deposits, i.e. the clays are taken into account in the model since these may be a discriminative factor for water to enter or leave the groundwater system of the model. The distribution of the clays is taken from the map over the quaternary deposits provided by the Lantmäteriverket. The data was delivered in 6 different files called, j1211i_lera.shp, j12hno_lera.shp, j12ino_lera.shp, j12inv_lera.shp, j13iso_lera.shp and j13siv_lera.shp. The distribution in the domain represented by the model is shown in Figure 4-5. It should be noted that the local continuity of the clay layers is not known in detail.

Investigations of the seabed at SFR have revealed that the fractured rock is mainly covered by a glacial till (morain) of varying thickness with a large amount of boulders and a small amount of fine grained material, /Sigurdson, 1987/; at present, no continuous layer of fine-grained sediments, e.g. clay, occur at the seabed above the SFR.

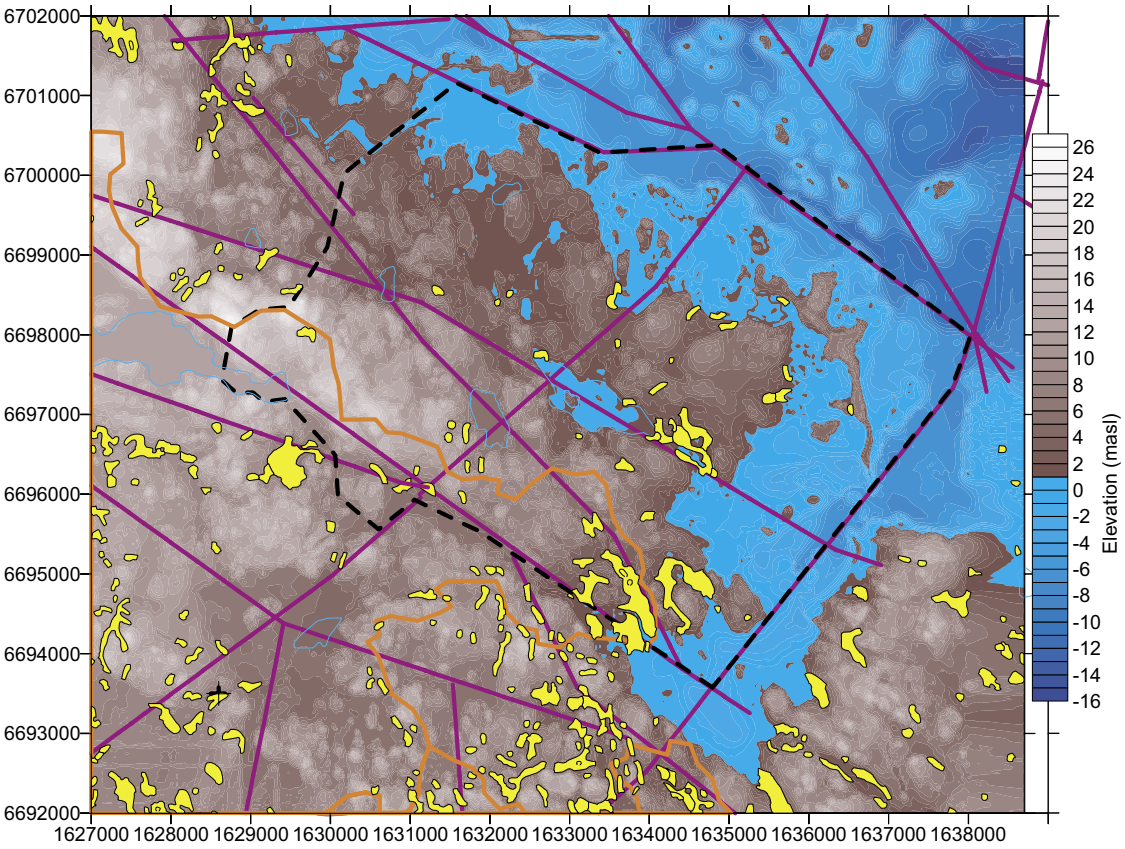

Figure 4-5. *Topography and the areas above the sea which are covered with clay (yellow). Surface water divides (orange), fracture zones (purple), boundary of lakes (light blue) and boundary of model (black dotted line).*

5 Hydrometeorology and water balance modelling

5.1 Average run-off

The concept of run-off and groundwater recharge is defined and discussed in Section 2.3. Run-off is often defined as "That part of the precipitation that flows towards the stream on the ground surface (surface run-off) or within the soil and rock (subsurface run-off)" /Nordic Glossary of Hydrology, 1984/. Hence, the run-off is equal to the surface run-off (surface flows) plus the subsurface run-off (groundwater flow). According to /Brandt et al. 1994/, for the period 1961–1990, the average precipitation in the Östhammar municipality, which includes the Forsmark area, is 600–700 mm/year; the average run-off is 200–300 mm/year. For the province of Uppland, which includes the domain studied, Figure 5-1 presents the average run-off, as measured and estimated by /SMHI, 1999/. The average run-off, for the domain studied, is approximately 250 mm/year.

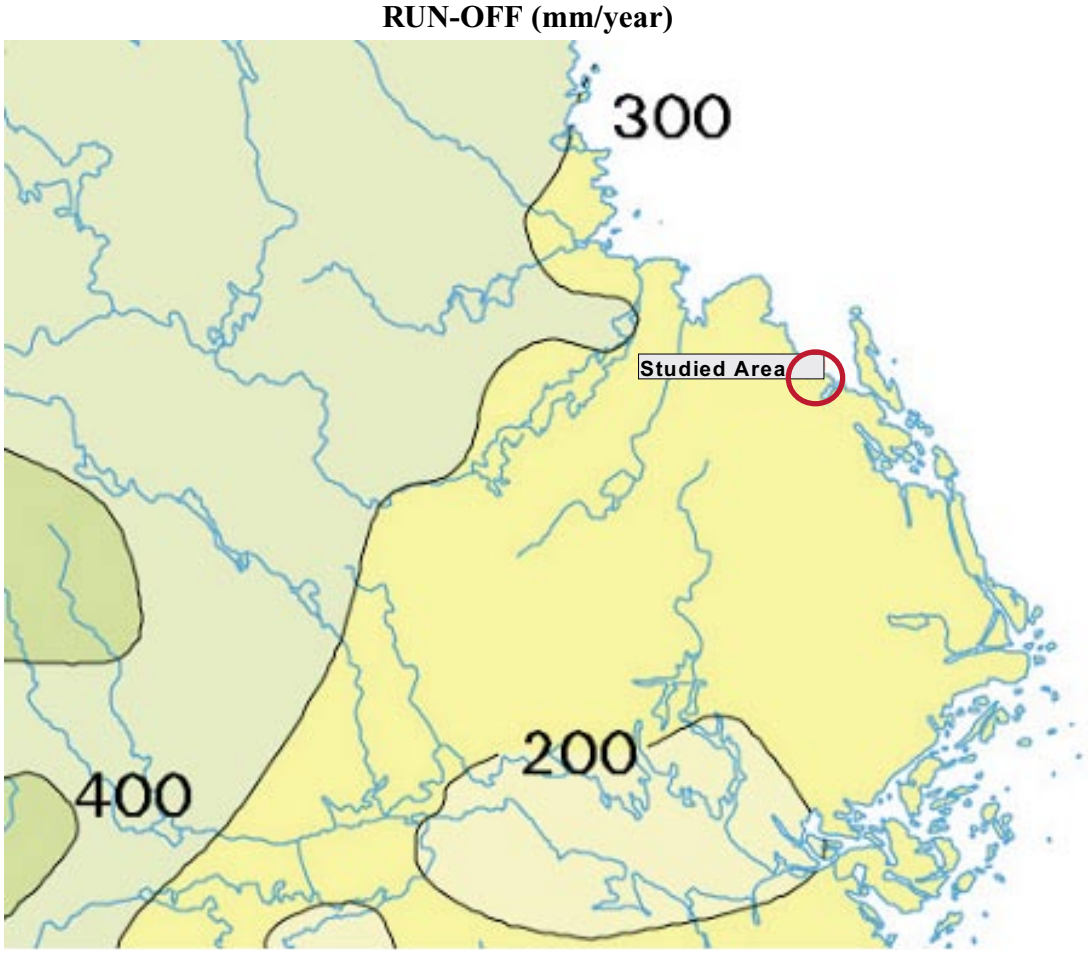

Figure 5-1. *The average run-off (the potential recharge) for the province of Uppland, /SMHI, 1999/. The red dot denotes the position of the area studied. The average run-off, for the domain studied, is approximately 250 mm/year.*

5.2 Statistical analysis of precipitation

To obtain three significantly different groundwater recharge periods for the transient groundwater simulations (GEOAN) we have derived a normal, a dry and a wet precipitation period based on a statistical analysis of available data. In the subsequent section these precipitation periods form a basis for the water balance calculations.

The analysis is based on a time series of precipitation and potential evapotranspiration. (Potential evapotranspiration is defined in Section 2.5.) The analysed data covers the period 1961–2000, i.e. a total of 40 years. The data was obtained from the Sicada database, and is based on SMHI's data from the Lövsta monitoring station (PFM010725) in the Forsmark area.

A probability plotting /e.g. Chow et al. 1988/ of the 40 yearly precipitation values is shown in Figure 5-2 and in Figure 5-3. The statistical analysis was based on the logarithm of the precipitation, i.e. the probability plotting shows that the precipitation data is approximately log-normally distributed. The solid lines represent a perfect lognormal distribution, and the markers represent the data. (The standard normal variable z is calculated according to an approximation given by /Chow et al. 1988, p 390/, and the exceedence probability is calculated using Blom's formula).

One may obtain the precipitation for the 1,000 year return period by extrapolating the theoretical lines. (A return period of 1,000 years corresponds to approx. z = 2.61). This, however, gives a dry year precipitation that is 10% higher than the lowest data value (Figure 5-2), and a wet year precipitation that is 3% lower than the highest data value (Figure 5-3). This result seems unrealistic, and the reason is probably that the extrapolation results in a magnification of errors in the calculation of the theoretical distribution. Therefore, the extrapolated values are not used in the subsequent calculations.

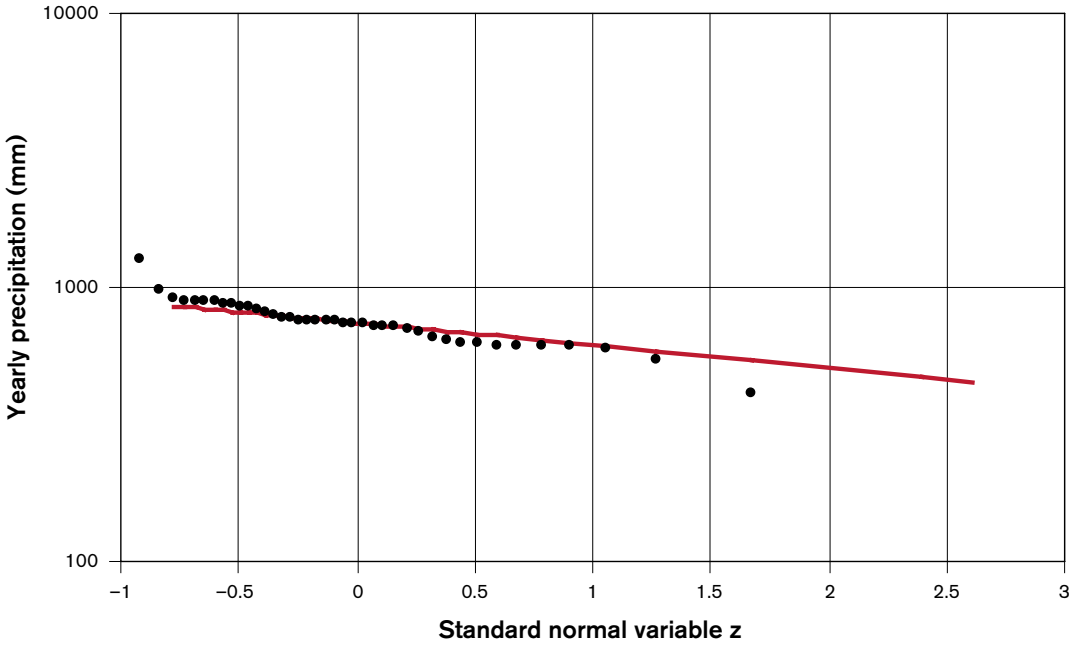

Figure 5-2. *Yearly precipitation at the Forsmark area. A dry-year with return period of 1,000 years is obtained by extrapolation. Markers represent data and the solid line represent the theoretical lognormal distribution.*

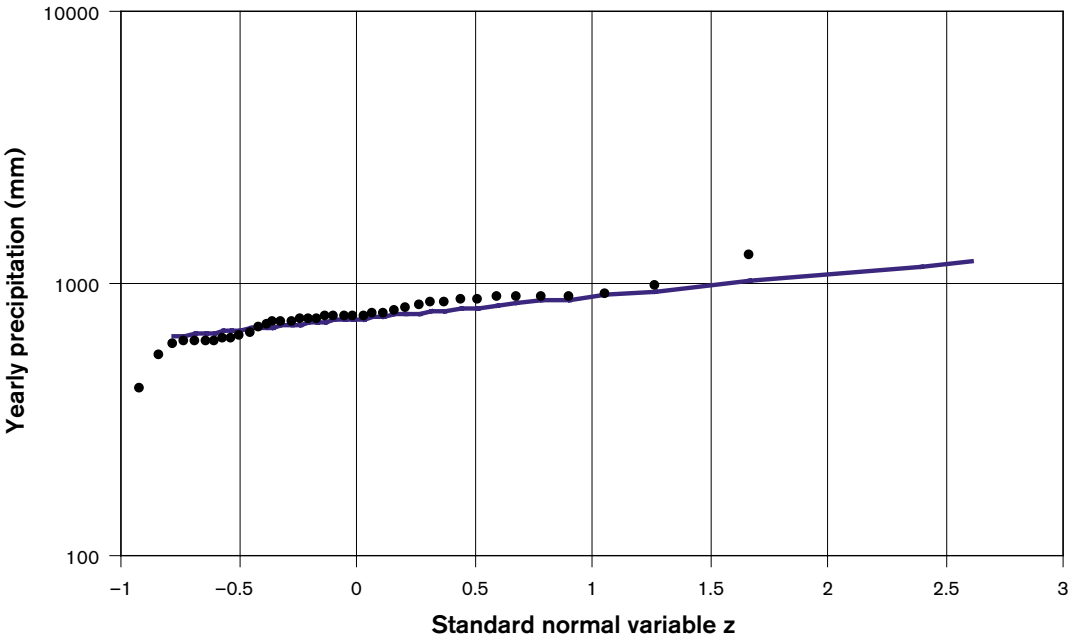

Figure 5-3. *Yearly precipitation at the Forsmark area. A wet-year with return period of 1,000 years is obtained by extrapolation. Markers represent data and the solid line represent the theoretical lognormal distribution.*

An alternative method is to apply a frequency analysis using frequency factors /Chow et al. 1988/. The magnitude of a precipitation event may be represented by

$$x_T = \overline{x} + K_T s_x \qquad \text{Equation 5-1}$$

which is the sum of the mean and the product of the frequency factor and the standard deviation. The frequency factor may be defined by the extreme value Type I distribution according to /Chow, 1988, p 391/:

$$K_T = -\frac{\sqrt{6}}{\pi}\left\{0.5772 + \ln\left[\ln\left(\frac{T}{T-1}\right)\right]\right\} \qquad \text{Equation 5-2}$$

In which T (year) is the return period of the precipitation event. Because the measured precipitation time series is approximately log-normally distributed, we conducted the calculation in (Equation 5-1) with logarithmic data. The antilog of the result achieved in this way gives the dry and wet rain periods. This data forms the basis for the water balance calculations.

The monthly medians of precipitation and the monthly means of potential evapo-transpiration, for the period 1961–2000, is given in Figure 5-4. The temporal distribution (monthly values) of the statistically derived precipitation for the normal-year, the dry-year and the wet-year, were based on the temporal distribution of the monthly medians precipitation values, for the period 1961–2000.

In this way we obtained the distributions for the dry and wet-year depicted in Figure 5-5 and in Figure 5-6, respectively. However, the same evapotranspiration distribution (mean) was utilized for all three cases.

Table 5-1. Yearly precipitation periods derived by the statistical analysis.

Normal year (median)	Dry, with 1,000 year return period	Wet, with 1,000 year return period	Minimum (1961–2000)	Maximum (1961–2000)
750 mm	294 mm	1,870 mm	411 mm	1,252 mm

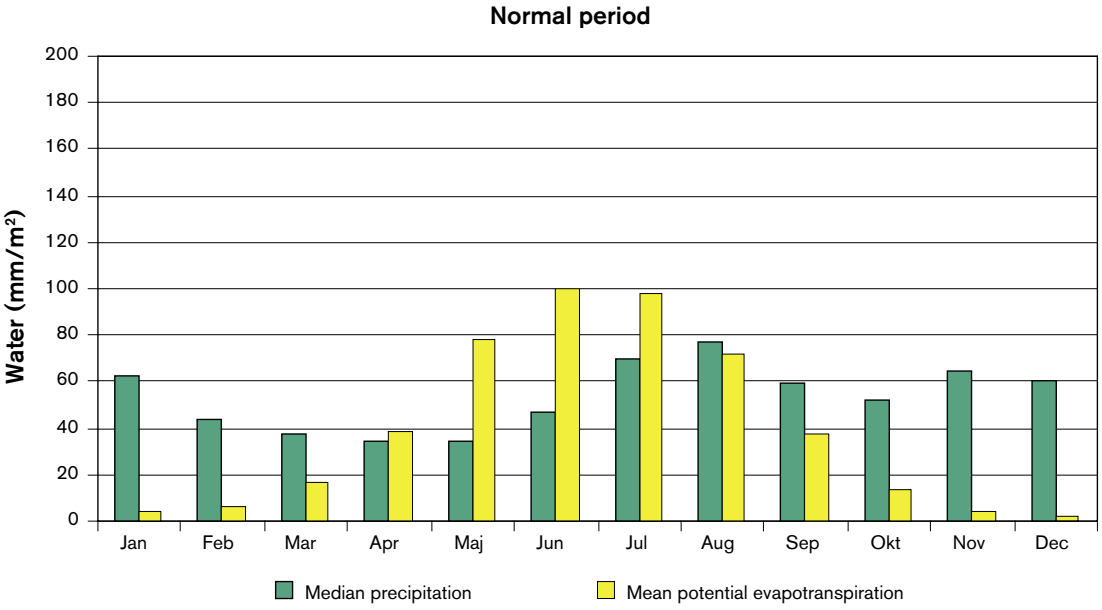

Figure 5-4. *Precipitation (median) and potential evapotranspiration (mean) based on the period 1961–2000. Data from the Sicada database.*

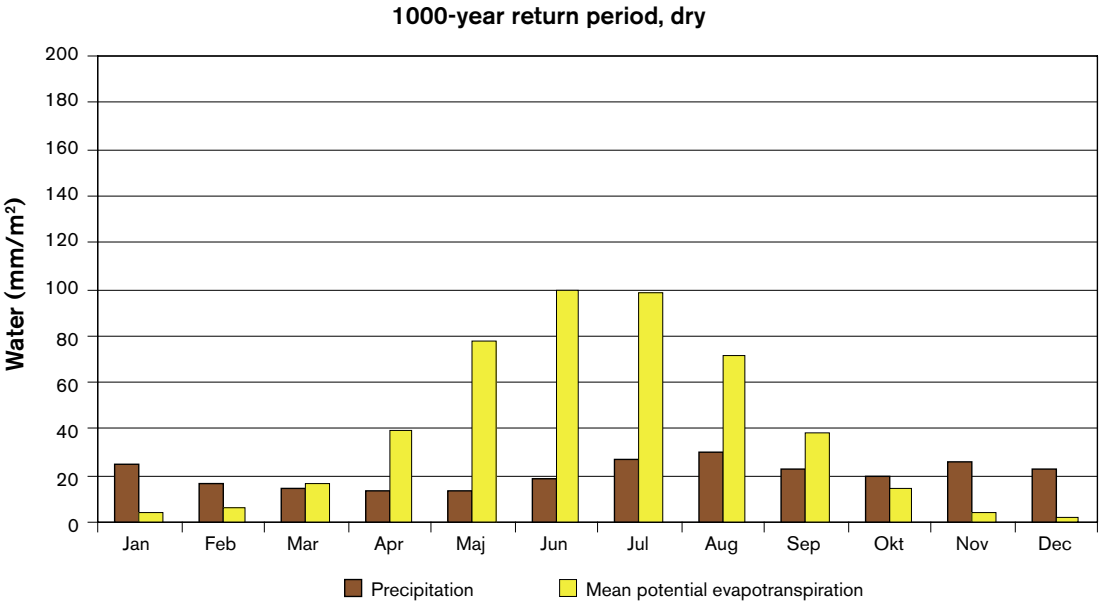

Figure 5-5. *Calculated dry-year precipitation and potential evapotranspiration (mean) based on the period 1961–2000. Data from the Sicada database.*

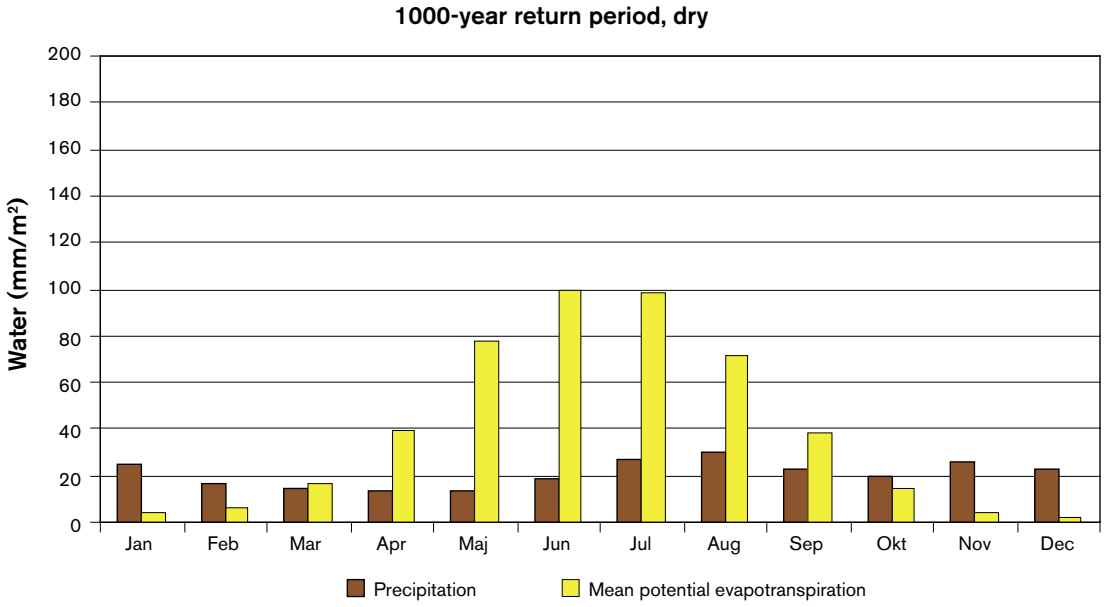

Figure 5-6. *Calculated wet-year precipitation and potential evapotranspiration (mean) based on the period 1961–2000. Data from the Sicada database.*

5.3 Water balance modelling

A water balance calculation is the same thing as a hydraulic budget, the purpose is to estimate and quantify the conceptual flows of a studied area. If we limit ourselves to a catchment area (drainage basin, watershed) in which the surface-water divides and groundwater divides coincide, and for which there are no external inflows or outflows of groundwater, the water balance equation for a studied period would take the form:

$$P = Q + E_{actual} + \Delta S \qquad \text{Equation 5-3}$$

P = Precipitation

Q = Run-off

E_{actual} = Evapotranspiration (actual)

ΔS = Change in storage

We have in the previous section estimated the precipitation, based on measured values from the Lövsta monitoring station (SMHI); we have also presented the potential evapotranspiration for the same monitoring station (as calculated by SMHI). The potential evapotranspiration is an entity that is usually estimated from climatological data alone (Evapotranspiration and potential evapotranspiration is defined in Section 2.5.).

The (actual) evapotranspiration is related to the potential evapotranspiration, it depends not only on the potential evapotranspiration, but also on the available precipitation and soil moisture content.

To be able to calculate the run-off produced during an extreme period, we need to: (i) estimate the actual evaporation of that period and (ii) apply Equation 5-3 for calculation of the run-off.

To obtain a temporal distribution of the runoff, we have conducted a time dependent water balance calculation. We have used two basic equations implemented in an algorithm. The algorithm uses a large number of small time steps to smoothly model the changes in actual evapotranspiration, soil moisture content and run-off:

For a time step of a given length, the actual evapotranspiration was calculated according to:

$$\frac{E_{actual}}{E_{potential}} = \left(\frac{SM - WP}{FC - WP} \right)^n \qquad \text{Equation 5-4}$$

In which E_{actual} is the actual evapotranspiration (mm/m^2), $E_{potential}$ is the potential evapotranspiration (mm/m^2), SM is the soil moisture content (mm/m^2), WP is the wilting point for the soil (minimum soil moisture required for plant survival), FC is the field capacity of the soil (mm/m^2), i.e. the pore water storage capacity, and n is an arbitrary constant. $n < 1$ implies a non-linear relationship between the actual evapotranspiration and the soil moisture content. At high levels of soil moisture, the potential evaporation decreases slowly for decreasing levels of soil moisture, and the opposite for low levels of soil moisture. The water balance calculation was carried out based on monthly values.

For a time step of a given length, the run-off was calculated according to:

$$Q = P - E_{actual} + \Delta SM \qquad \text{Equation 5-5}$$

Q = Run-off (mm/m^2)

P = Precipitation (mm/m^2)

E_{actual} = Evapotranspiration (actual) (mm/m^2)

ΔSM = Change in soil moisture content (mm/m^2)

The calculations were based on the assumed parameter values in Table 5-2. The assumed field capacity and wilting point correspond to glacial till (moraine), according to /Grip and Rodhe, 1985/. The root depth, which was used as a calibration parameter, given in (Table 5-2) corresponds to shallow (0.2–0.6 m) to moderately (0.5–1.0 m) rooted crops and the chosen value of the constant n corresponds to that of a mixed soil (loam).

The calibration of the water balance model was conducted for the normal year. This was done by fitting the root depth to a yearly runoff of 250 mm, which corresponds to an average value of runoff, estimated from SMHI data (see Section 5.1).

In the water balance calculations we have assumed that during months with an average temperature below zero degrees Celsius (at Lövsta monitoring station, SMHI), the precipitation is stored as a snow storage. The snow storage is released during the first month with an average temperature above zero. The release of the snow storage will create a large run-off during the spring.

A balanced normal year occurs when the state of the system studied (soil moisture content and snow storage etc) is the same at the beginning of the year and at the end of the year. To achieve this by means of the calibration procedure, several normal years are modelled in series until a balanced normal year is obtained. The result obtained in this way for the area studied is presented in Figure 5-7.

To produce corresponding results for 1,000 year return periods, the parameters in Table 5-2 are utilised for one-year simulations. The simulations of an extreme year are conducted in connection to a balanced normal year. The initial conditions in the water balance model

were the state of the system studied (soil moisture content and snow storage) at the end of the balanced normal year. Hence, we have modelled an extreme year that follows after a normal year. The results for the dry-year and wet-year are shown in Figure 5-8 and in Figure 5-9, respectively, as well as in Table 5-3 (potential recharge per year) and in Table 5-4 (potential recharge per month).

Table 5-2. Parameter values utilized in the water balance calculations.

Root depth (m)	Field capacity (%)	Wilting point (%)	*n* (–)
0.45	30	4	0.4

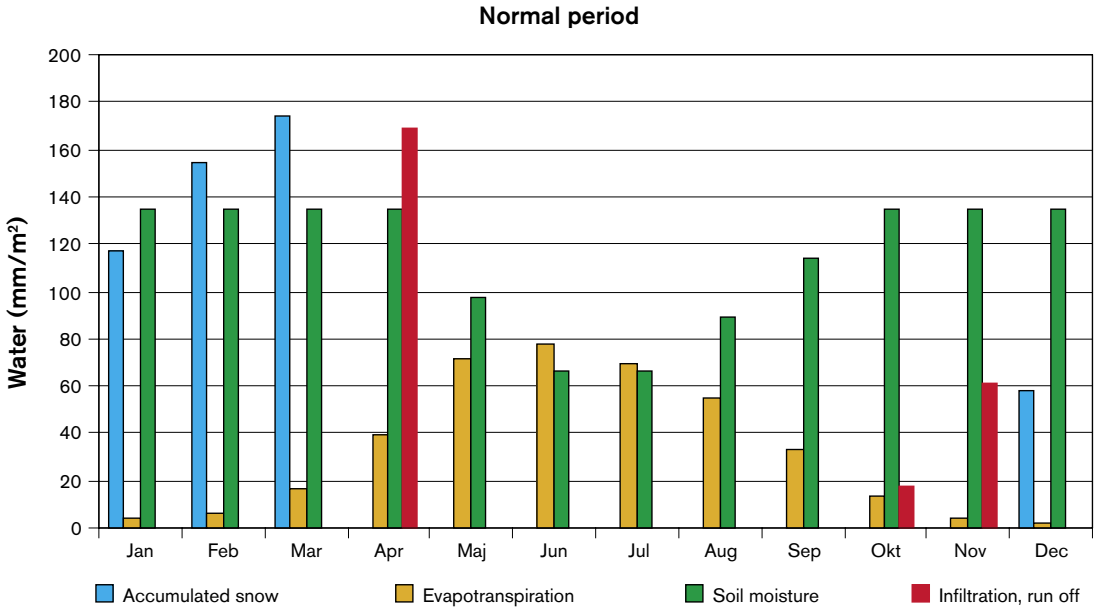

Figure 5-7. *Results from the water balance calculations for the normal precipitation period.*

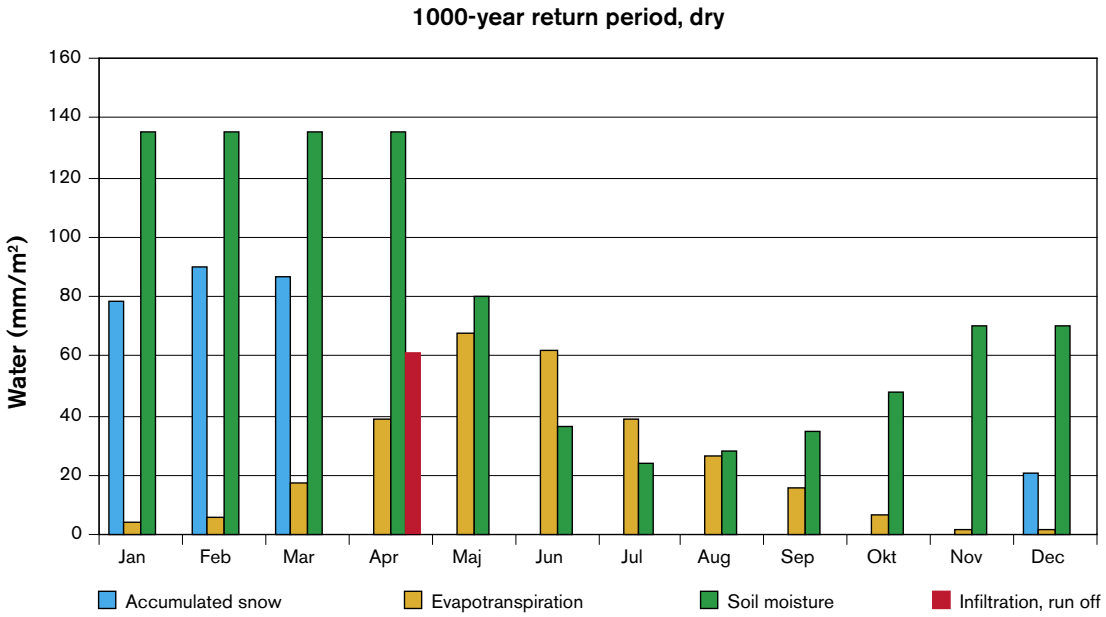

Figure 5-8. *Results from the water balance calculations for the dry 1,000 year return period.*

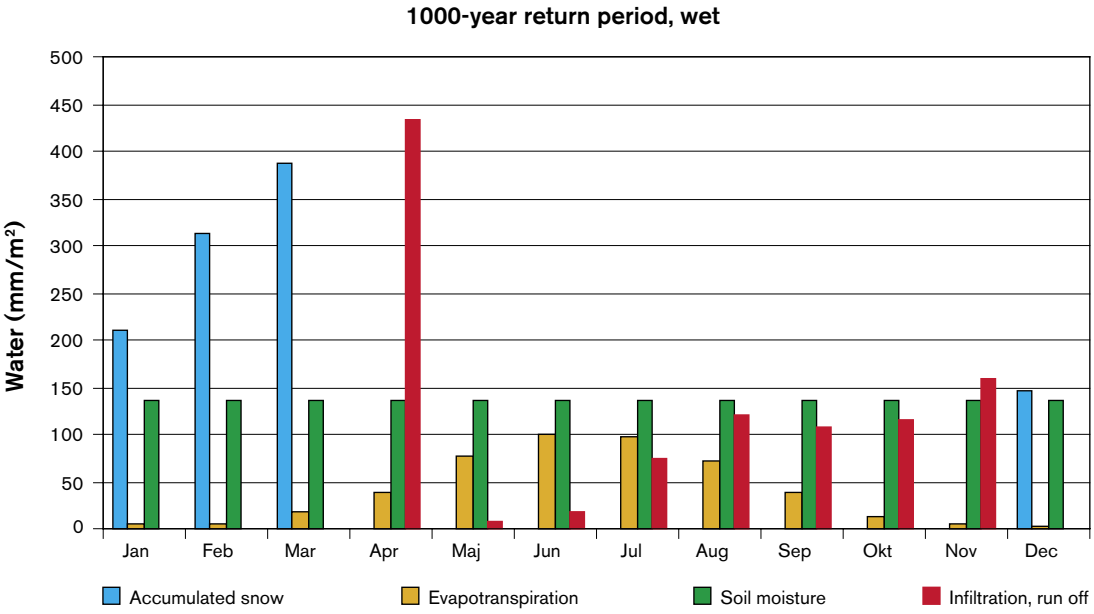

Figure 5-9. *Results from the water balance calculations for the wet 1,000 year return period.*

Table 5-3. Yearly runoff (potential recharge) derived by the water balance modelling.

Runoff (average) as estimated by SMHI	Runoff, normal year as calculated by calibrated water balance model	Runoff, dry-year, with 1,000 year return period	Runoff, wet-year, with 1,000 year return period
About 250 mm/year	240 mm/year	61 mm/year	1,036 mm/year

Table 5-4. Monthly runoff (potential recharge) derived by the water balance modelling.

Potential recharge (mm)	Jan	Feb	Mar	Apr	May	Jun	Jul	Aug	Sep	Oct	Nov	Dec	Tot
Normal year Potential recharge				160						18	61		240
Dry-year Potential recharge				61									61
Wet-year Potential recharge				433	7	18	75	121	108	116	158		1,036

- The runoff of the wet year is about 4 times larger than that of the normal year.
- The runoff of the dry year is about 25% of that of the normal year.
- The run off of the wet year is a factor 17 larger than that of the dry year.

The calculated run-off will be included in the groundwater modelling as a potential groundwater recharge; the applied values are given in Table 5-3 (potential recharge per year) and in Table 5-4 (potential recharge per month).

The potential recharge is a result of the water balance modelling; the potential recharge as an input to the groundwater modelling, the actual recharge is calculated by the groundwater model.

6 Properties of the groundwater model

6.1 Size of model and boundary conditions

6.1.1 Size of model

The outer vertical boundary of the model coincides with regional fracture zones, large surface water bodies or water divides These boundaries give the model a length in a north-south direction that is close to 8 km, and in the west-east direction the maximum length of the model is close to 10 km. The model represents an area of 40.5 km^2. The upper boundary of the model is an undulating surface, the outer boundaries of the model are vertical and the lower boundary is an undulating surface.

6.1.2 Outer vertical boundary – Lateral boundaries

As stated above, the outer vertical boundary of the model (lateral boundaries) coincides with different important hydrogeological structures: (i) Surface water divides. (ii) Regional valleys with streams. And (iii) Regional fracture zones. The lateral boundaries of the model are given in Figure 4-3 and in Figure 4-4 (extension of model).

The lateral boundaries as defined in the model, correspond to important hydrogeological structures. In the model we assume that these structures are boundaries for the groundwater flow, accordingly in the model the lateral boundaries are defined as no-flow boundaries and in the model no groundwater flow (or surface water flow) will pass these boundaries.

This assumption is based on the observation that: (i) Surface water divides are along significant topographic ridges and it is not likely that large amounts of groundwater will flow across a significant topographic ridge. (ii) A regional valley with a stream is an important discharge area for groundwater, and it is not likely that large amounts of groundwater will flow across a significant discharge area. (iii) Some regional fracture zones are also used as lateral boundaries in the model; these zones are along low laying parts of the topography (also considering the topography below the sea). Regional fracture zones along low lying parts of the topography are important discharge areas and it is not likely that large amounts of groundwater will flow across a significant discharge area.

Nevertheless, it is possible that in the reality some groundwater flow may take place across the surfaces that we have defined as the models lateral boundaries. It is however likely that such flows are small.

6.1.3 Boundary at base of model

The base level of the model is defined at a certain depth below the ground surface (600 m). Along the base of the model, the no-flow boundary condition is applied.

6.1.4 Boundary condition along the top of the model

The top boundary condition used for the model is either: (i) the specified head condition, representing the seawater table and the lakes or (ii) a non-linear boundary condition, representing the ground surface above the sea and the varying actual groundwater recharge that may take place along an area with an undulating topography. By use of the non-linear

boundary condition we will not force a certain value of recharge or head condition upon the model. The model will calculate the actual recharge and the corresponding position of the groundwater surface as a part of its solution of the flow field (and these properties may vary with time). The extensions and positions of recharge and discharge areas will also be calculated by use of the non-linear boundary condition.

The precipitation and the evapotranspiration produce a potential recharge, a certain amount of the potential recharge may infiltrate at the ground surface (into the quaternary deposits) and create the actual recharge. The actual recharge varies depending on, the potential recharge, the topography, the conductivity of the material at the ground surface and the state of the groundwater system. For the areas not covered by the sea, the non-linear boundary condition used by the GEOAN model reproduces closely the interaction between: (i) the state of the groundwater system, (ii) the potential groundwater recharge and (iii) the ground surface topography. The non-linear boundary condition calculates the actual recharge and the position of the groundwater surface by the use of an iterative algorithm.

The iterative algorithm

First step: The model calculates the position of the groundwater surface and compares it to the topography, thereby estimating the extension of recharge areas and discharge areas.

Second step: The model estimates the actual recharge.

- Discharge areas: the model will use the specified head boundary condition at discharge areas. The head is set equal to the ground elevation and the model calculates the recharge-discharge components. The maximum recharge is equal to the potential recharge plus surface water flows at the point studied. The discharge is larger than zero.
- Recharge areas: the model will use a continuous boundary condition at recharge areas. The recharge is set equal to the potential recharge plus surface water flows at the point studied. The model calculates the head. The maximum head is equal to the ground surface. The discharge is equal to zero.

The steps are repeated.

For the areas covered by the sea, the model will use the specified head boundary condition, representing the seawater table (assigned to the cells along the sea floor). For the areas defined as lakes, the model will use the specified head boundary condition representing the water levels of the lakes.

6.1.5 Surface water flows

The model will include surface water flows (above the shoreline), as a part of the boundary conditions along the top of the model. The amount of the potential discharge that will not infiltrate at a certain location, or groundwater that discharges out of the groundwater system, will be moved (in the model) as a surface flow. In the model, the movement of surface water takes place in the direction of the topographic gradient. The surface flows will be added to the potential groundwater recharge along the flow direction of the surface flows, hence if the conditions are favourable water that did not infiltrate at one position may infiltrate at another, along the topographic gradient. At the outer boundary of the model, or at the shoreline, the surface flows are stopped and included in the global mass balance of the model as a discharge out of the model.

6.1.6 Boundary at lakes

The lakes are defined on the models upper surface. In the model, the lakes are in contact with the underlying groundwater system (see Figure 6-1 below). In the groundwater model, the contact between the lake and the groundwater system is defined as follows.

Along the lake perimeter, the groundwater system is in direct contact with the lake via a highly permeable material (a wave eroded material). The lake perimeter is defined with the specified head boundary condition, and the specified head corresponds to the surface water level of the lake.

Along the base of the lake, the contact between the groundwater system and the lake takes place through a material having a low permeability; this material represents sediments at the base of the lake. The groundwater system below the lake (and inside of the lake perimeter) is partly confined by the lake sediments, but some groundwater flow may take place across the sediments and the magnitude of this flow depends primarily on the permeability of the lake sediments. Inside of the lake perimeter, the boundary condition is the specified head boundary condition (as along the perimeter), and the specified head corresponds to the surface water level of the lake.

In the model, inflow and outflow of groundwater to a lake will primarily take place along the lake perimeter, but some flow may also take place across the base of the lake via the lake sediments.

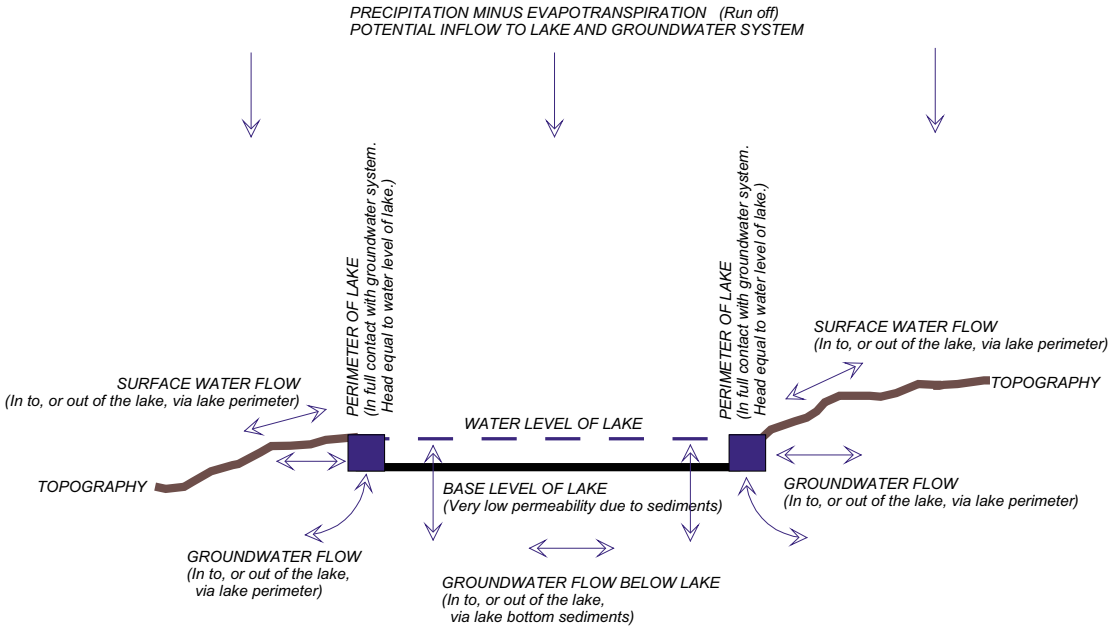

Figure 6-1. *A lake, as defined in the models.*

6.1.7 Boundary condition at surface areas with clay

In the model some areas are defined as carrying a surface clay layer. The boundary condition for these areas are the same as for all other surface areas above the shoreline that are not defined as lakes (see Section 6.1.4). However, as the permeability of the clay is very small, the model will assign these areas the specified head condition, and the head will correspond to the topographic elevation.

In the model, inflow and outflow of groundwater will take place at cells carrying a clay layer, but these flows are very small due to the small permeability of the clay.

It should be noted that the local continuity and permeability of the clay is not known in detail. In this model we have however assumed that the clay is homogeneous and without any disruptions.

6.2 Discretization of domain studied

6.2.1 The Grid

A three-dimensional grid (mesh) of cells (elements) represents the domain studied.

- *Horizontal discretization*. In the central part of the model, the horizontal cell size is 25×25 m. Outside of this area, the cells are either 50×25 m or 50×50 m (horizontal extension).
- *Vertical discretization*. The models contain 10 different layers of cells. The elevations of the layers are defined in relation to the surface topography, hence all cells of a layer have the same vertical extension, but the elevation varies with the topography. The model grid is not regular in the vertical plane. The vertical extension of cells of the different layers varies with depth. The total vertical extension of the model is 600 m below ground surface. The vertical extension of the layers of the model are as follows: Layer 10 (upper layer) = 0.5 m, Layer 9 = 1 m, Layer 8 = 1.5 m (surface near layers)
- Layer 7 = 3 m, Layer 6 = 6 m, Layer 5 = 13 m, Layer 4 = 25 m, Layer 3 = 50 m,
- Layer 2 = 140 m, Layer 1 (layer at base of model) = 360 m.

The horizontal discretization of the Base case model is given below in Figure 6-2. The total number of cells in one layer is 34,200. The total number of cells is 342,000.

6.2.2 Discretization of the lakes

The model will calculate which parts of the grid that represents a lake. For these calculations we have applied the condition that all cells that contains a part of a lake will be assigned as lakes. This will lead to an overestimation of the lake area, but as the lakes are limited in size and do not have many “fingers”, the method will produce an acceptable result. The extension of the lakes as defined in the Base case is given below in Figure 6-3.

6.2.3 Discretization of the areas that carries a surface clay layer

The model will calculate which parts of the grid that represents an area covered by clay. For these calculations it is not possible to apply the condition that all cells that contains a part of the clay areas will be assigned as clay-cells, because this will lead to a large overestimation of the extension of the clay areas. This is because of the complicated geometry of the clay

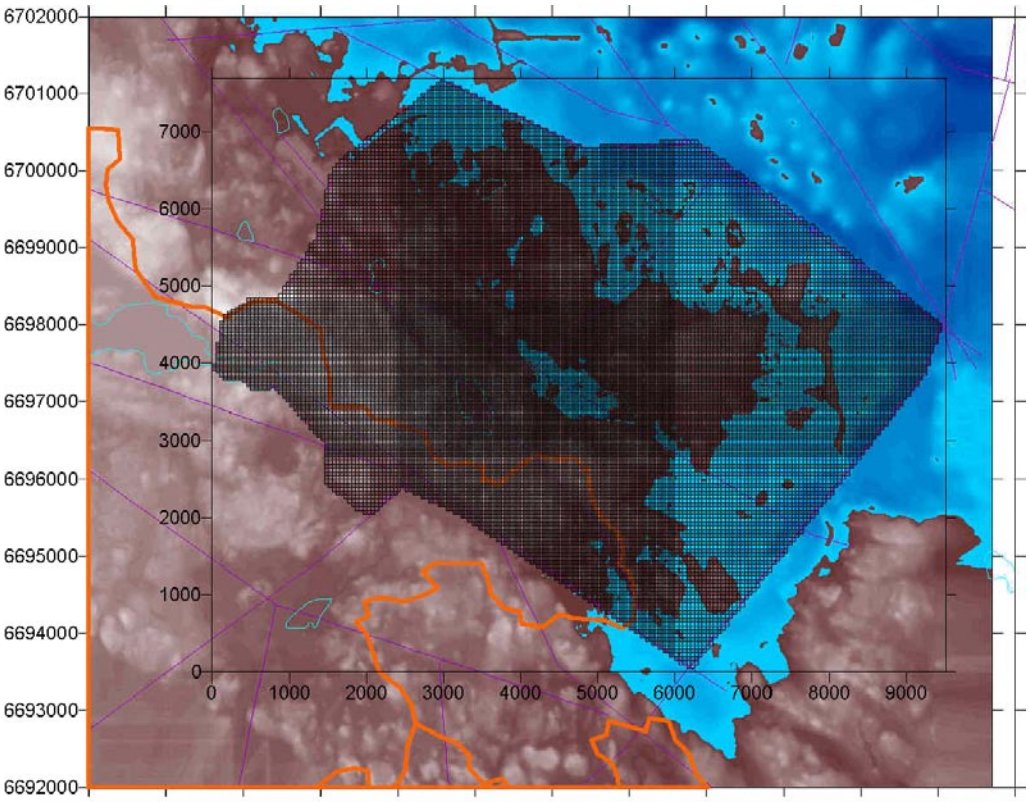

Figure 6-2. *Horizontal discretization of the model (the grid). In the central part of model the cell size is 25×25 m. Outside of this area, the cells are either 50×25 m or 50×50 m (horizontal extension).*

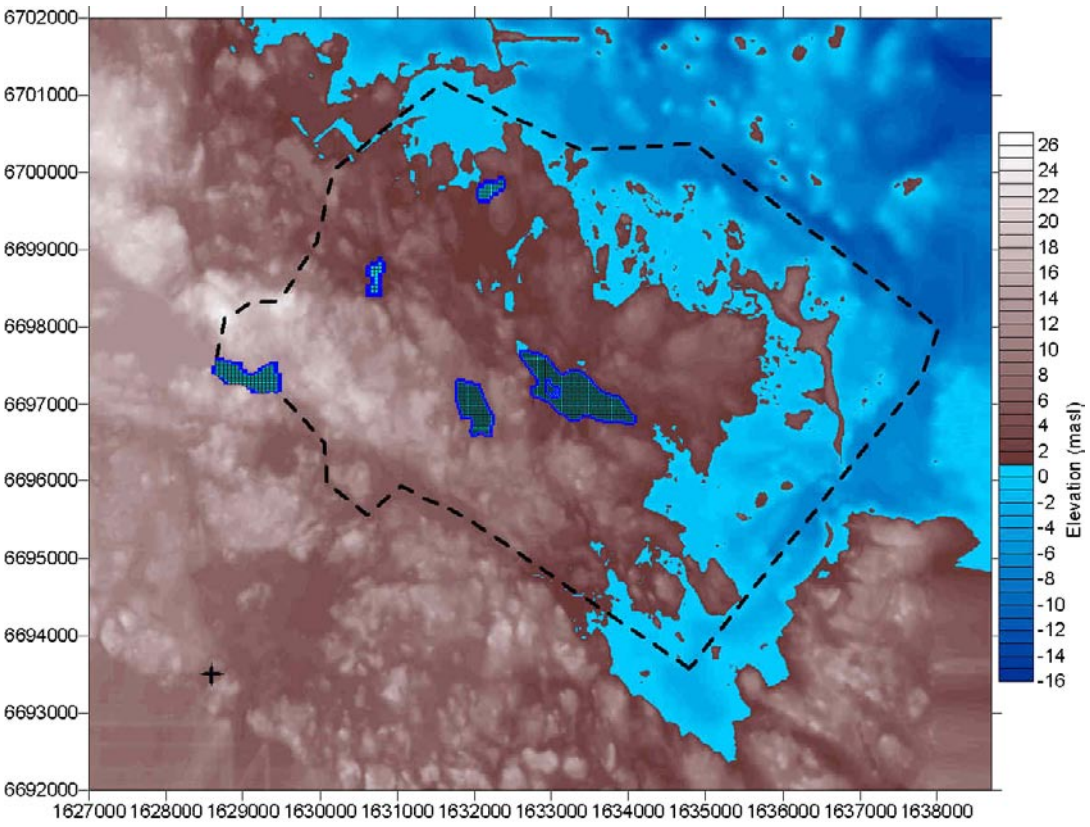

Figure 6-3. *Extension of lakes in model. The lakes perimeters are denoted by a dark blue colour.*

areas with “fingers”. Instead a method was applied in which certain conditions regarding amount of clay in cell studied and the shape of the clay areas were considered before assigning a cell as a clay cell; still the clay areas in the model are larger than the actual areas. The extension of the clay areas as defined in the Base case model is given below in Figure 6-4.

6.2.4 Discretization of the fracture zones

The model will calculate which cells the regional fracture zones intersect. In the models, the fracture zones are defined as separate continuous structures, by use of an implicit formulation as regards the conductivity of the cells intersected by the fracture zones.

Hence, a cell that represents a zone may also partly represent the surrounding rock mass. The calculation of the properties of such a cell is based on the condition that the transport capacity of the cell should include both the transport capacity of the zone and that of the surrounding rock mass. If the cell is small its properties will be dominated by the properties of the zone. If the cell is large and the zone is small, the properties of the cell will be dominated by the properties of the rock mass. Since the horizontal width of the cells of the established model (25 m or 50 m) are of approximately the same size as the width of the regional fracture zones (30 m through 50 m), the properties of the cells will be dominated by the properties of the fracture zones. Cells intersected by a fracture plane will get an anisotropic conductivity formulation, in which some faces of the cells represent the rock mass only, and other faces represent both the zone and the rock mass. Even if the defined fracture zones forms a complicated geometry in three dimensions, by use of the implicit formulation the mesh can be defined as regular and the geometry of the mesh will not cause numerical difficulties.

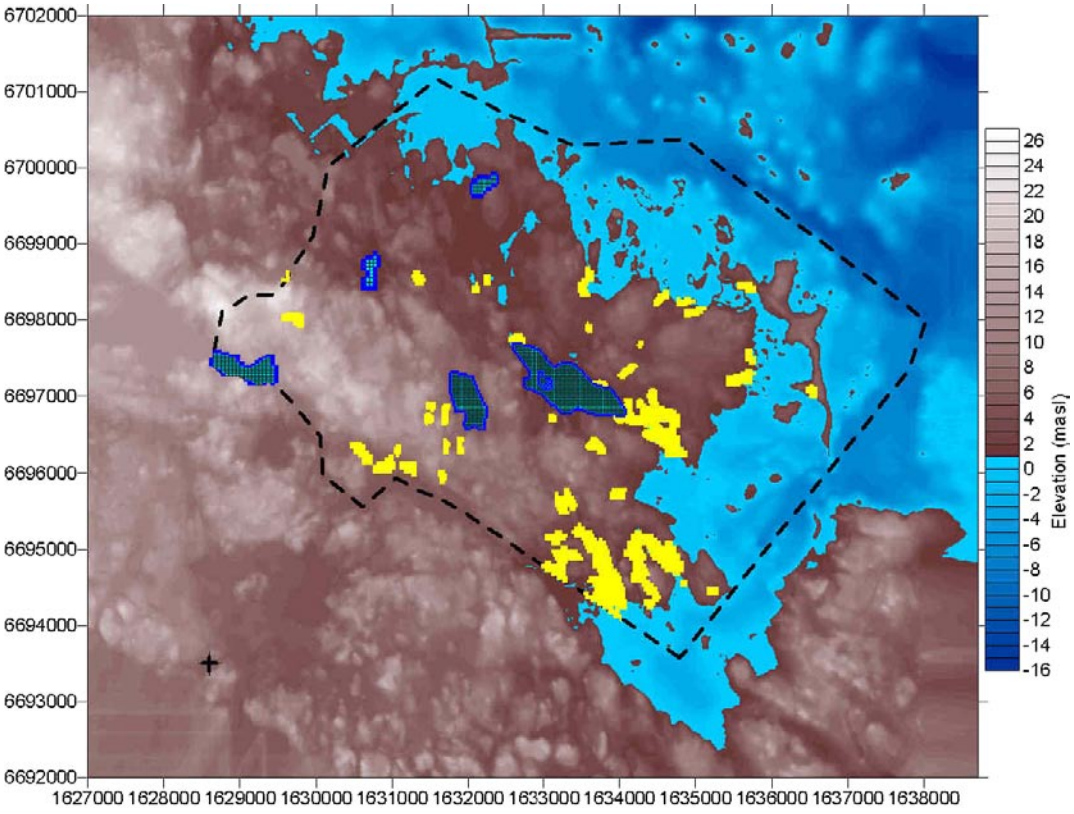

Figure 6-4. *Extension of clay areas as defined in the model. The clay areas are denoted as yellow.*

In the model the fracture zones are defined as vertical planes in the rock mass, all the way down to the base of the model. It should be noted that the uppermost 3 layers are not defined as rock mass, but as quaternary deposits; hence there are no fracture zones in the uppermost 3 layers. Cells intersected by regional fracture zones are denoted below in Figure 6-5 (these cells are below the quaternary deposits).

6.2.5 Representation of the topography

The topography of the area studied is given in Figure 4-3, it is based on a data-grid of size 10×10 m. By use of a non-linear spatial interpolation this data-grid was transferred to the grid (mesh) of the models. The method for the spatial interpolation was based on the inverse distance between data points and by use of a weighting power equal to 2.0. The same method was used for the more sparse data below the shoreline.

In the GEOAN model, the topography is defined at the centre of each cell of the grid. Hence, the exactness of the representation of the topography depends on the cell size; a grid with small cells will produce a better representation of the actual topography than a grid with large cells.

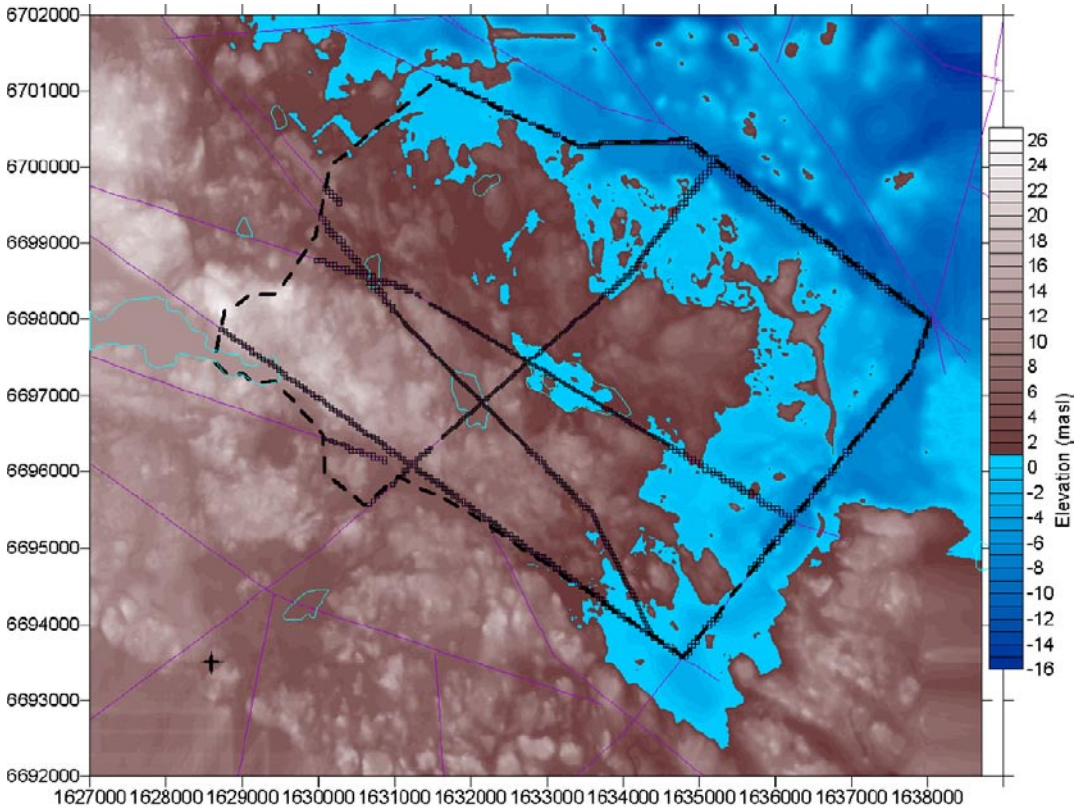

Figure 6-5. *The regional fracture zones (purple lines) and the cells intersected by the zones (black squares).*

6.3 Permeability and porosity of flow domain

6.3.1 Introduction

We have establish a model with such resolution that the model is capable of reproducing the flow of groundwater in the quaternary deposits, and at the same time include some aspects of the groundwater flow at great depth. The hydraulic properties of the quaternary deposits of the established model are based on a conceptual model of the near surface groundwater flow system discussed in Section 2.6, this conceptual model includes a very permeable layer close to the ground surface, having a thickness of a few decimetres. Accordingly, we have in our model defined the uppermost 0.5 m with a very large permeability.

6.3.2 Permeability and depth of quaternary deposits

The quaternary deposits at the area studies are predominately glacial till (moraine) and clay. The conductivity of moraine, close to the ground surface, has been studied by /Lind and Lundin, 1990/, see Figure 6-6. In the established model, the permeability of the highly permeable surface layer (the uppermost 0.5 m) was based on the study of /Lind and Lundin, 1990/ and a sensitivity analysis, presented in Chapter 7.

In the model the quaternary deposits extends over a depth of 0 to 3 metres, and is represented by 3 layers. The hydraulic conductivity at different depths (of the quaternary deposits) as defined in the model is given in Table 6-1. A summary of the permeability of the model is given in Figure 6-6.

6.3.3 Permeability of rock mass

In the models the conductivity of the rock mass between the regional fracture zones was set to 5×10^{-9} m/s. This represents the conductivity of a rock mass without large fracture zones. It is the same value as the value used by /Holmén and Stigsson, 2001/ for the conductivity of the rock mass without fracture zones, in their model of the future groundwater flow at SFR (Forsmark), the same value was also used in the regional modelling of the area studied by /Holmén et al. 2003/. The value was derived based on the measured groundwater inflow to the tunnels at SFR /see Holmén and Stigsson, 2001/. No depth trend is introduced to the hydraulic conductivity of the flow media. This decision is based on observations at different sites in Sweden, see /Walker et al. 1997/. It is however possible that rock permeability is reduced at extreme depths, i.e. depths below approximately 8 km. The vertical extension

Table 6-1. Hydraulic conductivity and depth of quaternary deposits, as defined in the model (the Base case).

	Type	Depth	Hydraulic conductivity
Quaternary deposits	Highly permeable layer close to ground surface	0–0.5 m	1E–4 m/s
	Upper moraine	0.5–1.5 m	5E–7 m/s
	Lower moraine and weathered rock	1.5–3 m	5E–8 m/s
	Moraine below lakes (Not lake bottom sediments)	0–1.5 m	5E–7 m/s
	Clay	0–0.5 m	1E–9 m/s
	Lake bottom sediments	Resistance = 1E+10 seconds [1]	

[1] The concept of resistance includes both thickness and conductivity. Resistance = Thickness/Conductivity. (Units: Time = Length/(Length/Time)

of the models is however not so large that it is necessary to reduce the permeability of the rock mass due to extreme depth. A summary of the permeability of the model is given in Figure 6-6.

6.3.4 Permeability of regional fracture zones

In the model, the regional fracture zones are assumed to have the same properties as the Singö zone, which is a regional zone just off the coast, close to Forsmark. Hence, in the model the conductivity and width of the regional fracture zones are defined in accordance to the measure and estimated properties of the Singö zone.

According to the SFR safety report /SKB, 1993/ the Singö zone is assumed to consist of three parts: a core with a large conductivity and two outer parts with a somewhat smaller conductivity (this assumption goes back at least to /Carlsson et al. 1986/). The thickness of the different parts are: 14 m (outer part), 2.4 m (core) and 14 m (outer part), which together gives a thickness of 30.5 m. All together the three parts produces a total transmissivity of 2.4×10^{-5} m^2/s. The corresponding conductivity becomes 7.87×10^{-7} m/s.

In the models of this study, the regional zones are defined with a theoretical width of 30 m and a conductivity of 8.0×10^{-7} m/s. No depth trend is introduced to the hydraulic conductivity of the flow media. This principle is based on observations at different sites in Sweden, see /Walker et al. 1997/. A summary of the permeability of the model is given in Figure 6-6.

It should be noted that the fracture zones are more permeable than the quaternary deposits, except for the highly permeable layer close to the ground surface. Hence, the quaternary deposits will partly act as a low permeable lid above the fracture zones.

6.3.5 Porosity, yield and storativity

General

The porosity, the yield and the storativity of the different materials that takes place in the established model need to be defined. The applied values were selected based on the nature of the different materials and the hydraulic conductivity of the materials.

Effective porosity

The effective porosity (kinetic porosity or transport porosity) is defined as the ratio of the volume of interconnected pore-space available for fluid transmission to bulk volume of the soil or the rock. The calculated advective breakthrough times are directly proportional to the effective porosity. A summary of the effective porosity of the model is given in Figure 6-7.

- Close to the ground surface, a highly permeable material is defined in the model, except were clay occur at the surface. The highly permeable layer has a depth of 0.5 m. The effective porosity of this material is set to 25% (0.25).
- There is an Upper moraine below the highly permeable material. The thickness of the Upper moraine is 1 m. The effective porosity of the Upper moraine is set to 20% (0.20).
- There is a Lower moraine below the Upper moraine. The Lower moraine may also include some weathered rock. The thickness of the Lower moraine is 1.5 m. The effective porosity of the Lower moraine is set to 15% (0.15).
- Clay occurs at some parts of the model, close to ground surface (depth 0.5 m). The effective porosity of the clay is set to 5% (0.05).

Below the quaternary deposits there are rock masses. In the models a single value of the effective porosity was used for the whole domain of rock mass, both for the rock mass between regional fracture zones and for the fracture zones. This value is equal to 0.1% (0.001). The value should be looked upon as a possible value; it was partly chosen to facilitate a comparison with other studies in which this value has been used. The calculated breakthrough times of the flow paths in the rock mass are directly proportional to the effective porosity, and as the effective porosity is set as constant in the whole of the rock mass (with zones), the breakthrough times (through the rock mass) for other values of the effective porosity are easily calculated based on the following formula:

$t_{new} = (n_{new}/0.001)\ t_{given}$

t_{new} = Breakthrough time through rock mass with new value of effective porosity

n_{new} = New value of effective porosity

t_{given} = Breakthrough time through rock mass given in this study

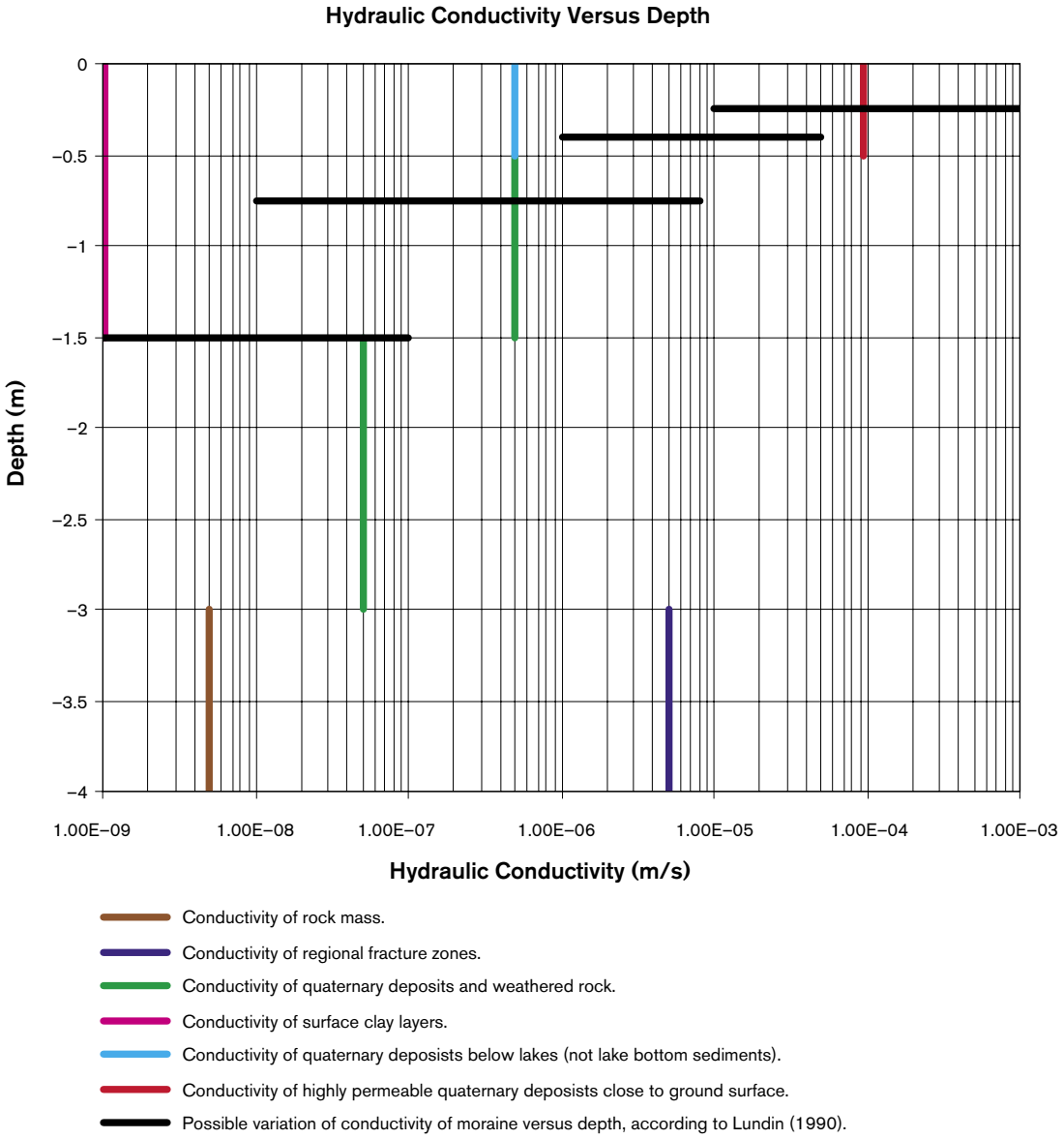

Figure 6-6. *Hydraulic conductivity versus depth, as defined in the model; and the range within which the conductivity of the moraine may vary, according to /Lind and Lundin, 1990/.*

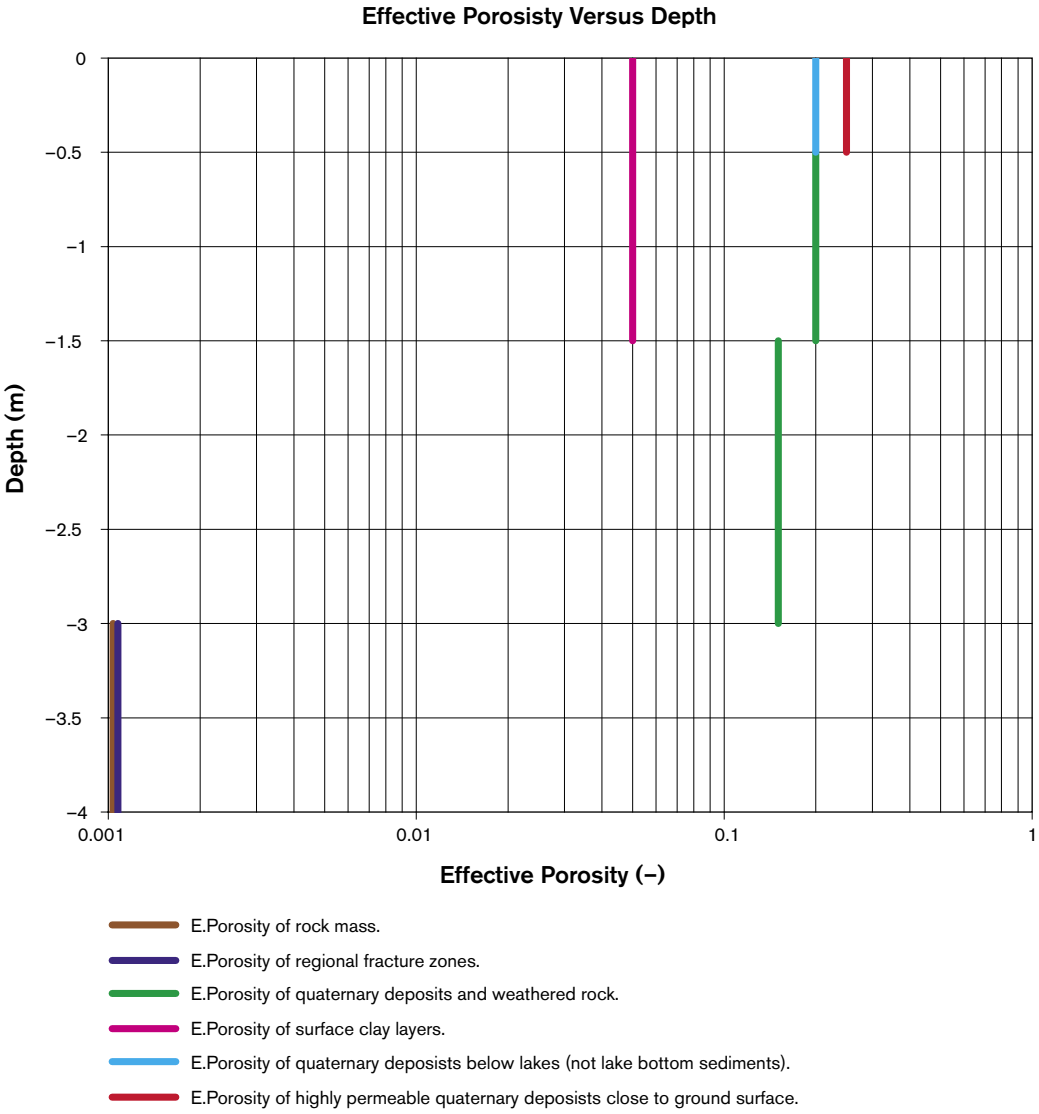

Figure 6-7. *Effective porosity versus depth, as defined in the model.*

It should be noted that the effective porosity assigned to the fracture zones is probably on the small side of a likely range of values. /Carlsson and Gustafsson, 1984/ present a likely range of 0.001 through 0.01 for a fracture zone in a crystalline rock mass.

The specific yield and the storativity are properties that should be included in a time-dependent model.

Specific yield

The specific yield defines the amount of water that is released/stored in the flow medium when the groundwater surface moves. This property is mainly related to the porosity. In this study we have set the specific yield equal to the effective porosity.

Storativity

The storativity defines the amount of water that is released/stored in the flow medium when the groundwater head changes. This property is related to soil and rock stresses; we have set the storativity equal to 5×10^{-4} (1/m), for all materials in the established model.

6.4 Principle lay-out of model

The principle layout of the model is given in Figure 6-8, below.

Flow of water takes place as:

- Recharge and discharge to the upper boundary of the model.
- Surface flow on the top of the model (on the quaternary deposits).
- Groundwater flow in the quaternary deposits.
- Groundwater flow in rock mass and fracture zones.

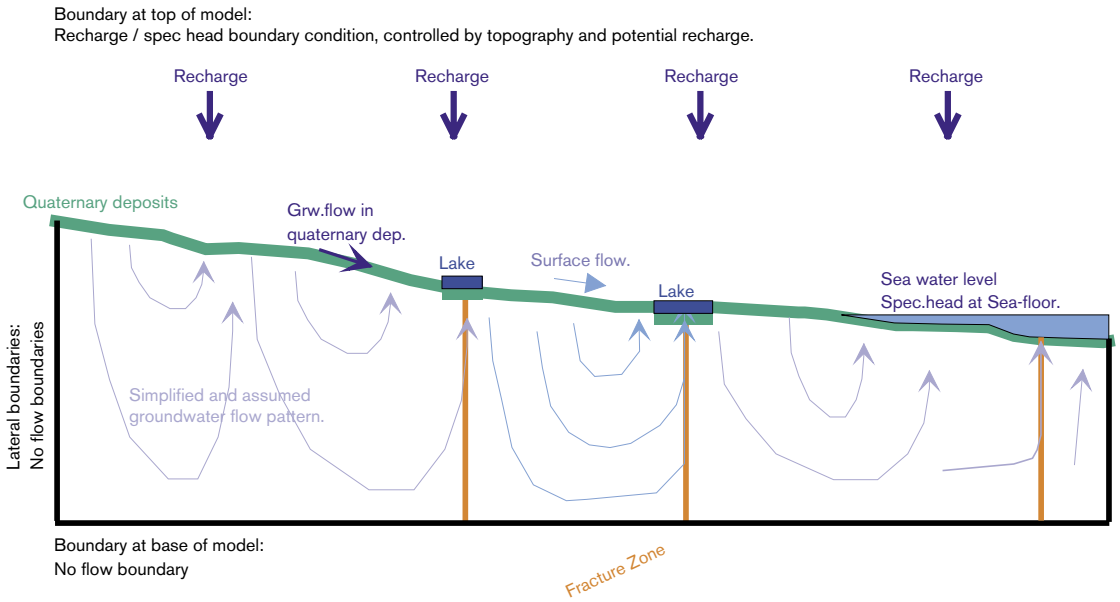

Figure 6-8. *Figure presenting a 2-dimensional view of the principle lay-out of model.*

7 Calculation of recharge areas and discharge areas, thickness of unsaturated zone

7.1 Introduction

The hydraulic properties of the quaternary deposits of the established model are based on a conceptual model of the near surface groundwater flow system discussed in Section 2.6, the conceptual model includes a very permeable layer close to the ground surface, having a thickness of a few decimetres. Accordingly, we have in our model defined the uppermost 0.5 m with a very large permeability. There are several reasons for a large permeability close to the ground surface, see Section 6.3.1.

The potential recharge is a result of the water balance modelling; the potential recharge as an input to the groundwater modelling, the actual recharge is calculated by the groundwater model.

The amount of recharge areas and discharge areas depend on the permeability of the uppermost part of the flow medium. This chapter presents a sensitivity analysis. The purpose is to calculate:

- size of discharge areas and recharge areas, as well as size of unsaturated zone, and compare these to,
- the corresponding different values of the hydraulic conductivity of the uppermost 0.5 m of the model. (The uppermost 0.5 m represents a part of the quaternary deposits with a very large permeability see Section 6.3.1.)

The concept of recharge and discharge areas is also discussed in Section 2.4.

7.2 Amount of recharge areas and discharge areas, and thickness of unsaturated zone; versus conductivity of the uppermost 0.5 m – Steady state solution

Four different cases have been established. All these cases are identical to the Base case presented in previous section (see Figure 6-6), except for the permeability of the uppermost 0.5 m. The hydraulic conductivity (of the uppermost 0.5 m) of the cases studied is as follows:

The different cases

- Case A (M30b) Conductivity of uppermost 0.5 m is set to 5E–6 m/s.
- Case B (M30) Conductivity of uppermost 0.5 m is set to 5E–5 m/s.
- Case C (M52e) Conductivity of uppermost 0.5 m is set to 1E–4 m/s. (Base case)
- Case D (M30c) Conductivity of uppermost 0.5 m is set to 5E–4 m/s.

Potential groundwater recharge corresponds to that of a normal year.

The amount of discharge and recharge areas were calculated by use of the routine discussed in Section 6.1.4. Results are given in Table 7-1, Figure 7-3 and in Figure 7-1.

For the Base case, the spatial extension of the discharge areas is given in Figure 7-2.

Table 7-1. Calculated amount of discharge area and depth of unsaturated zone. Steady state solution normal year.

Case	Conductivity of uppermost 0.5 m (m/s)	Calculated amount of discharge areas (%)	Calculated depth of unsaturated zone [1] (m)	
			Percentile 60th	Percentile 99th
Case A (*M30b*)	5E–6	95	0	0.08
Case B (*M30*)	5E–5	57	0.02	0.78
Case C (*M52e*) Base case [2]	1E–4	43	0.16	0.88
Case D (*M30c*)	5E.4	20	0.40	1.05

[1] Distribution of depth of unsaturated zone includes the whole of the area studied, both saturated and unsaturated areas. Hence, in Case C 43% of the unsaturated zone has a depth equal to zero.
[2] See Figure 7-2.

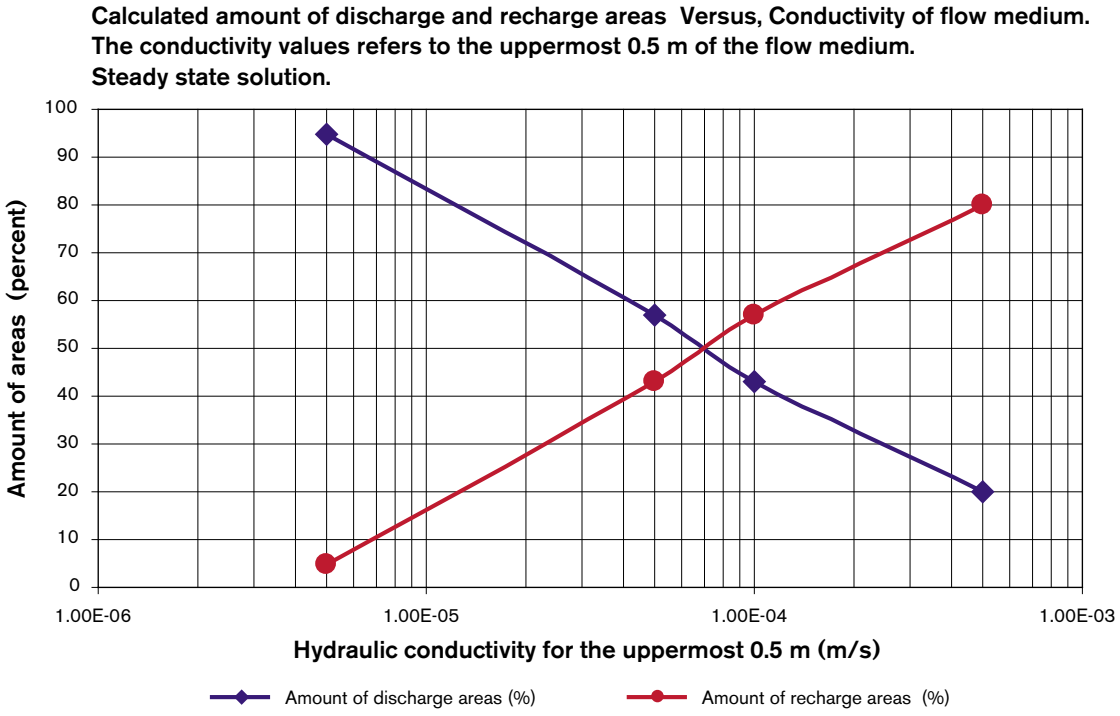

Figure 7-1. *Calculated amount of groundwater discharge areas versus conductivity of the uppermost 0.5 m of the flow medium. Steady state solution normal year.*

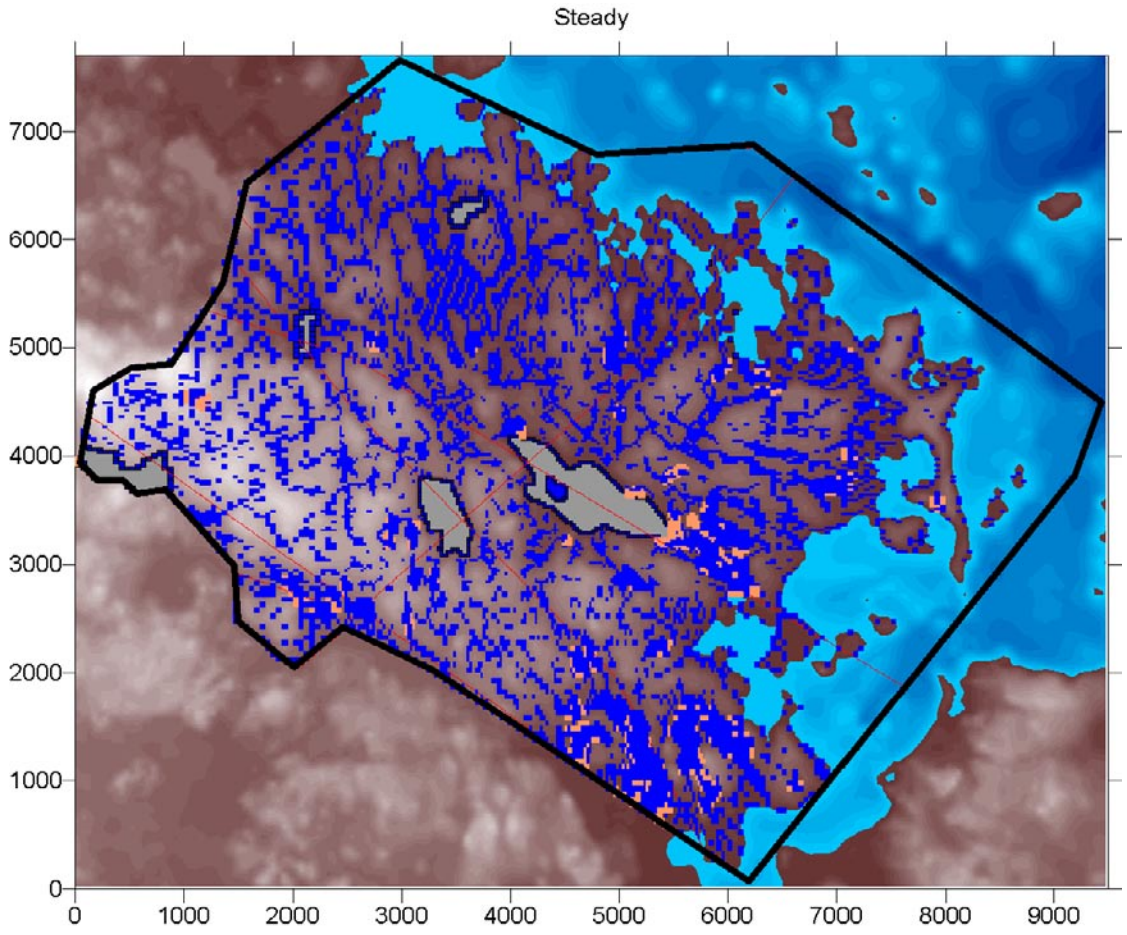

Figure 7-2. *Base case – Normal year – Steady State solution – Groundwater discharge areas. Blue squares denote discharge areas above the sea, areas that are not defined as lakes. Discharge will also take place below the sea and at the lakes. Lakes are defined with a dark blue boundary and a grey interior. Orange denotes areas with clay.*

The model was solved for a steady state situation. Results derived via a steady state solution do not represent any particular moment during a year, but is to be looked upon as a sort of average representation of the actually varying situation. We will in later in this chapter also include the transient behaviour of the system studied.

The amount of discharge areas and recharge areas depends on the conductivity of the uppermost part of the flow medium (assuming everything else being equal); this is well demonstrated by Figure 7-1 (and also discussed in Section 2.4).

- If the conductivity is large, a large amount of the precipitation and surface waters will infiltrate and create groundwater. For such a situation, the amount of recharge areas will be large (but it cannot be 100%, as there must always be discharge areas). And for such a situation the discharge areas will be few, but the outflow of groundwater is large at these areas.
- If the conductivity is small, only a small amount of the precipitation will be able to infiltrate, it follows that most of the areas will be saturated up to the ground surface, consequently for such a situation most areas will be discharge areas, even if the discharge is small.

The amount of false discharge areas, or saturated recharge areas, (defined in Section 2.4.1) is minimal, because the potential recharge (7.93E–9 m/s) is small compared to the conductivity of the uppermost layer.

Figure 7-3 presents the calculated thickness (depth) of the unsaturated zone versus depth. The calculated distribution of depth of unsaturated zone represents the whole of the area studied, both saturated and unsaturated areas. Hence, in Case C 43% of the unsaturated zone has a depth equal to zero (as these areas are discharge areas).

(The analysis of the extension of the unsaturated zone is based on 50,000 values for each studied case, each value represents an area of 25×25 m.)

Considering Case C (the Base case), Figure 7-3 demonstrates that for 10% of the area studied, the unsaturated zone has a depth (thickness) larger than 0.5 m. It follows that the highly permeable surface layer is completely unsaturated at only 10% of the areas studied.

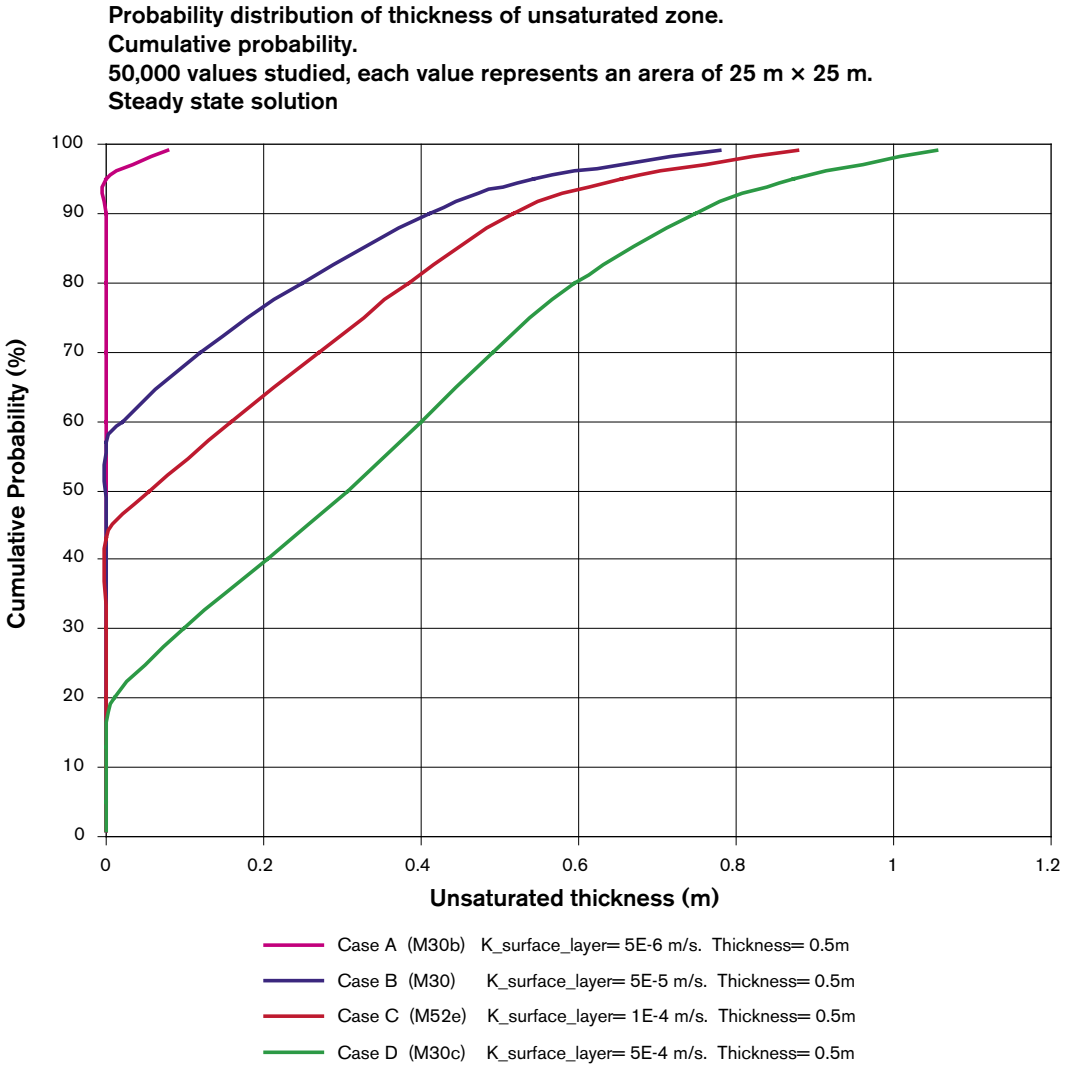

Figure 7-3. *Probability distribution of thickness (depth) of the unsaturated zone, for different values of conductivity of the uppermost 0.5 m. (Case C is the Base case). (Steady state, normal year.)*

For Case C (the Base case), the distribution of the unsaturated zone is also presented in Figure 7-4. It is demonstrated by the figure that for 43% of the area, the depth (thickness) of the unsaturated zone is zero. These 43% are the discharge areas. Hence, 57% of the areas are recharge areas. The cell with the largest unsaturated zone takes place at a regional surface water divide, at this place the unsaturated zone extends down to a depth of 3 m.

Based on the relationship demonstrated in Figure 7-1 we may derive the following conclusion: For values of conductivity (of the uppermost 0.5 m) between 5E–6 m/s and 5E–4 m/s, the amount of discharge areas (in percent of all areas) is approximately linear proportional to the logarithms of the conductivity of the uppermost 0.5 m. The conclusion produces the following approximate relationship applicable between K = 5E–6 m/s and K = 5E–4 m/s.

$$A_{dis} = C_1 \, {}^{10}Log(K)+C_2 \qquad \text{Equation 7-1}$$

Where:

A_{dis} = Amount of discharge areas in percent

C_1 = A constant derived from Figure 7-1 , C_1 = –38.46

K = Hydraulic conductivity (m/s) of uppermost 0.5 m

C_2 = A constant derived from Figure 7-1 , C_2 = –110.85

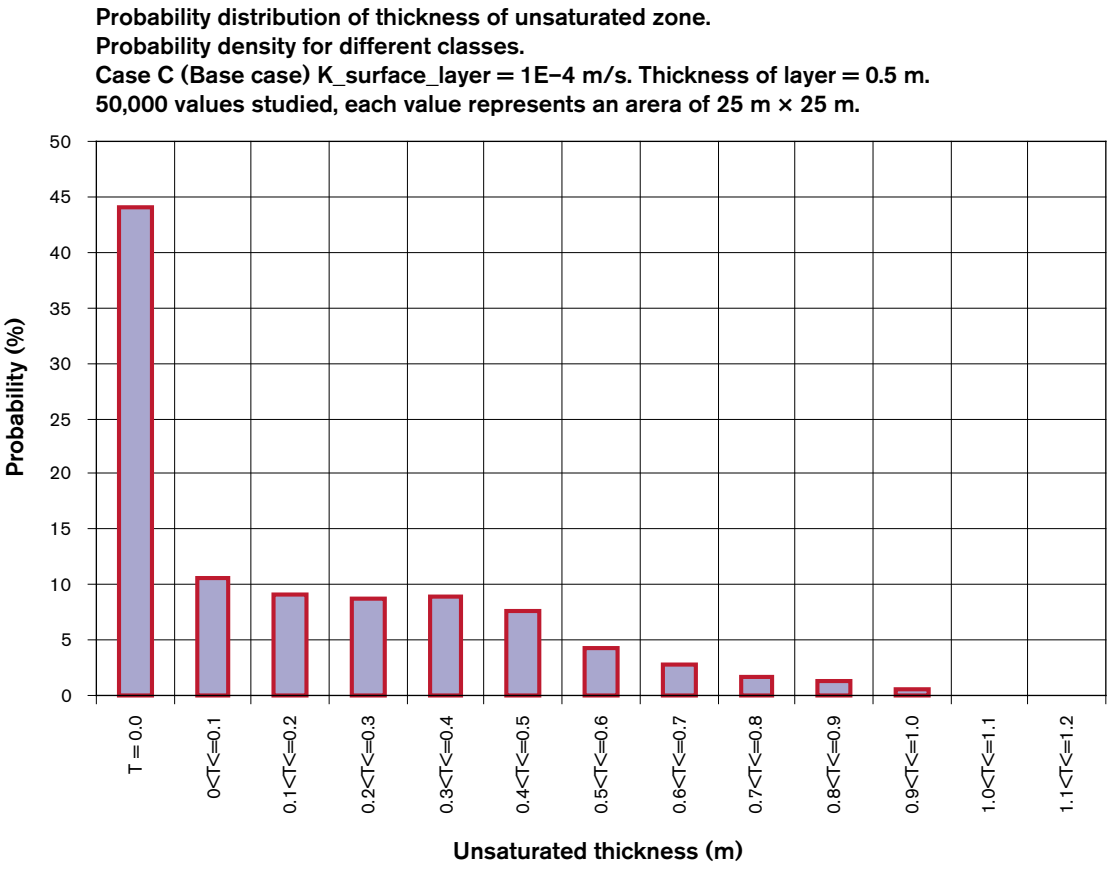

Figure 7-4. *Probability distribution of thickness of unsaturated zone, considering Case C (Base case). Probability density for different classes. (Steady state, normal year.)*

A similar relationship is demonstrated between the total transmissivity of the quaternary deposits and the amount of discharge areas. Reformulating the relationship above for the total transmissivity of the quaternary deposits, will produce the following equation, applicable between T = 3E–6 m^2/s and T = 2.5E–4 m^2/s.

$$A_{dis} = C_1 \, {}^{10}Log(T) + C_2 \qquad \text{Equation 7-2}$$

Where:

A_{dis} = Amount of discharge areas in percent

C_1 = A constant, C_1 = –41.19

T = Total hydraulic transmissivity (m^2/s) of the quaternary deposits

C_2 = A constant, C_2 = –133.94

7.3 Amount of recharge areas and discharge areas, and thickness of unsaturated zone; versus time – Normal year

7.3.1 Methodology of transient simulation

Transient calculations were carried out for the Base case (Case C). The simulation represents a normal year. Potential groundwater recharge was specified according to the results of water balance modelling: 160 mm during May, 18 mm during October and 61 mm during November. (Note that these values are the potential recharge and not the actual recharge, this will be further discussed in the next chapter.) The initial conditions were the results of the steady state simulation of a normal year. The modelled period included two years – in order to equalize the temporal storage and to obtain a balanced normal year. For a balanced normal year, the system studied starts and ends at the same state. The presented results represent a balanced normal year. The transient model did not include any frozen ground during the winter months. In the model discharge of groundwater took place during the winter as well.

7.3.2 Results

Considering the Base case and a balanced normal year, the temporal variation in amount of discharge areas is given in Figure 7-7 below. For the balanced normal year (Base case), the spatial extensions of the discharge areas are given in Figure 7-5 and in Figure 7-6. As can be seen in the figures, the discharge areas are the largest during the early spring, at the end of April 76% of the areas above the shoreline are discharge areas (not including the lakes). During the summer, the amount decreases and at the end of September the discharge areas make up 24% of all areas. Then follows the autumn with increasing amount of discharge areas, at the end of November the amount of discharge areas is 47%. The smallest amount of discharge areas occurs at the end of Mars, before the spring (23%).

The amount of discharge areas predicted with the steady state solution is also given in Figure 7-7, it is 43%; as can be seen in the figure, the steady state solution is a sort of average value of the variation during the year. It is however not the same thing as an arithmetic average based on monthly values, which is equal to 38%; but it is close to the geometric average of the monthly values, which is equal to 45%. The median of the monthly values is 32%.

The thickness of the unsaturated zone will also vary during the year; this is illustrated in Figure 7-8. At the end of March, the groundwater levels are at their lowest; for 99% of the area studied the thick ness of the unsaturated zone is less than 0.98 m. At the end of April the groundwater levels are at their highest, for 99% of the area studied the thickness of the unsaturated zone is less than 0.48 m. The thickness of the unsaturated zone of the steady state solution is also presented in the figure. The steady state solution produces an average representation that is between the maximum and minimum states of the transient solution.

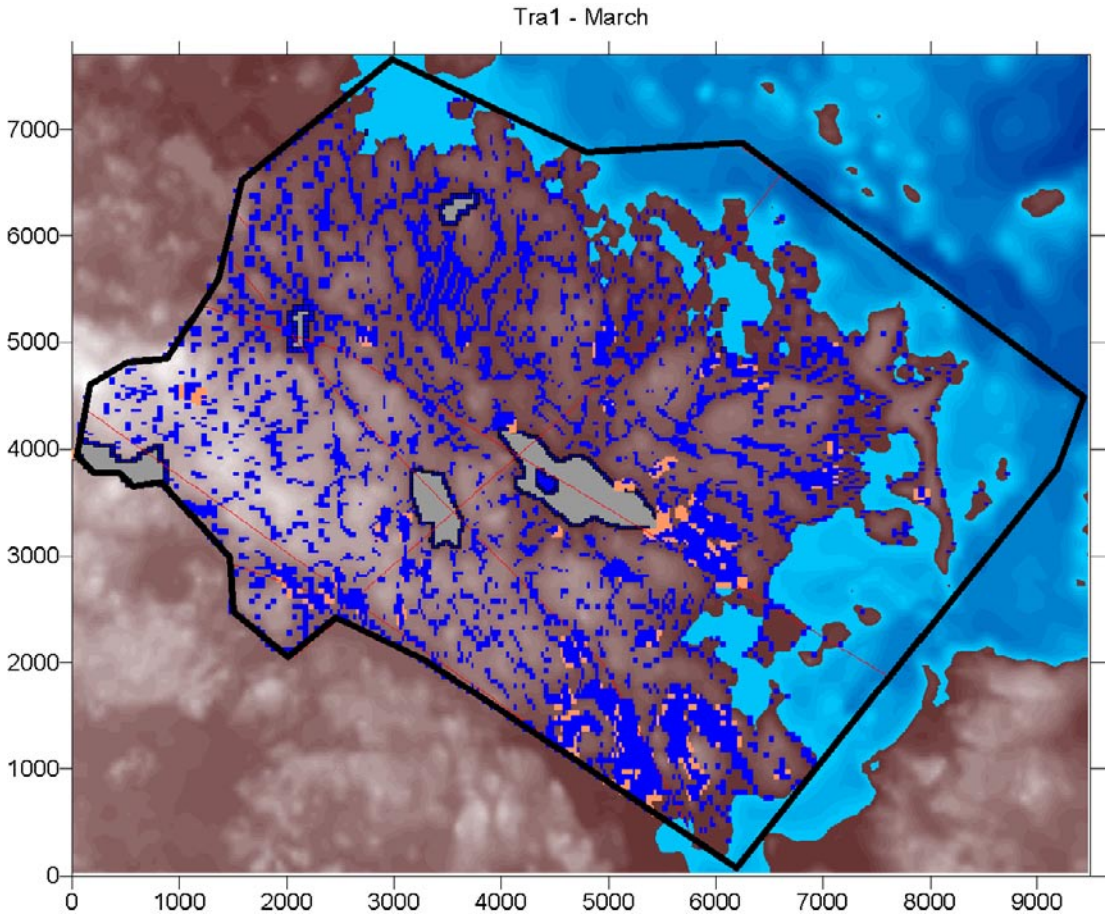

Figure 7-5. *Base case – Normal year – April – Groundwater discharge areas. Blue squares denote discharge areas above the sea, areas that are not defined as lakes. Discharge will also take place below the sea and at the lakes.*

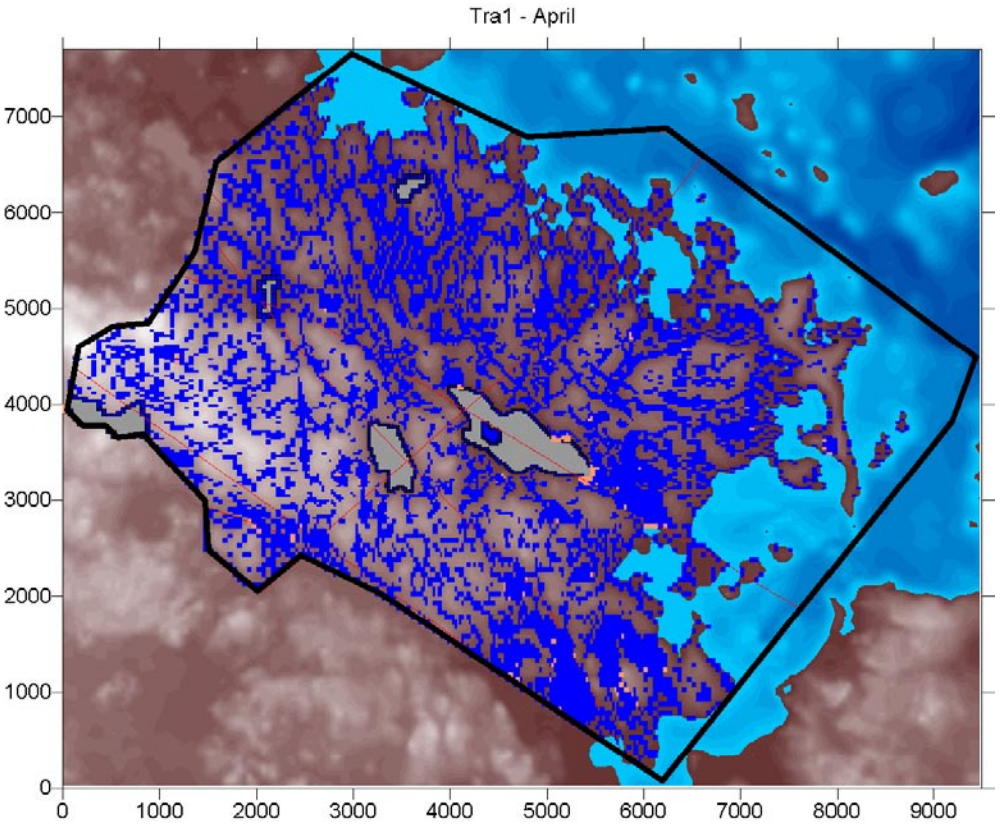

Figure 7-6. *Base case – Normal year – March – Groundwater discharge areas. Blue squares denote discharge areas above the sea, areas that are not defined as lakes. Discharge will also take place below the sea and at the lakes.*

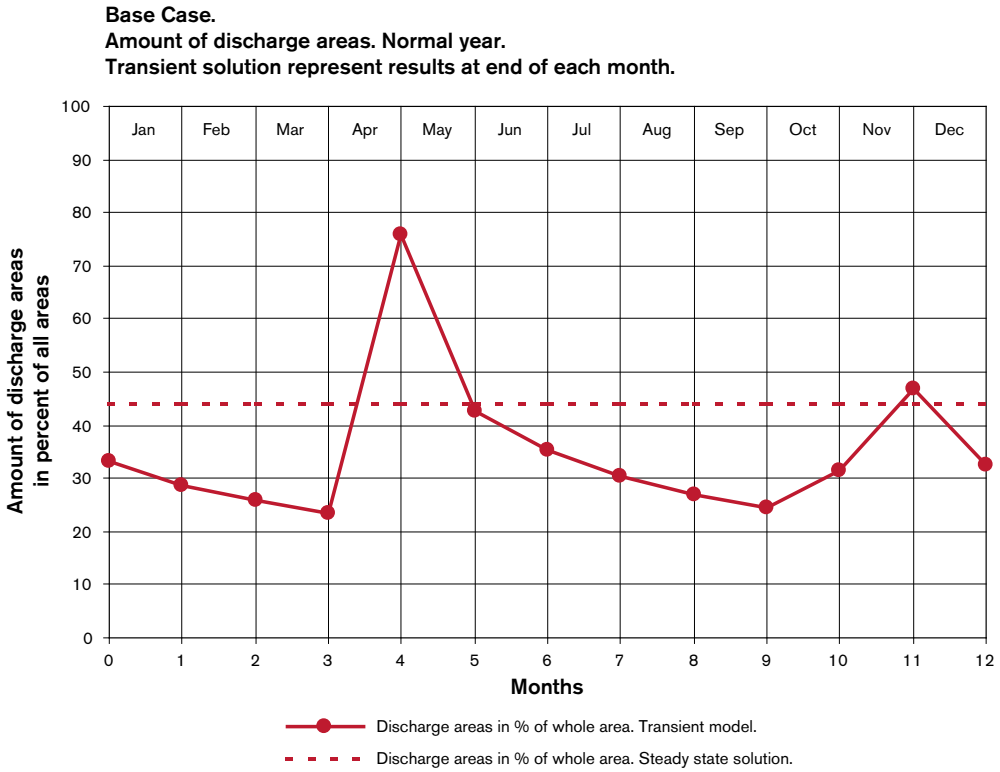

Figure 7-7. *Variation of amount of discharge areas during a normal year (Base case).*

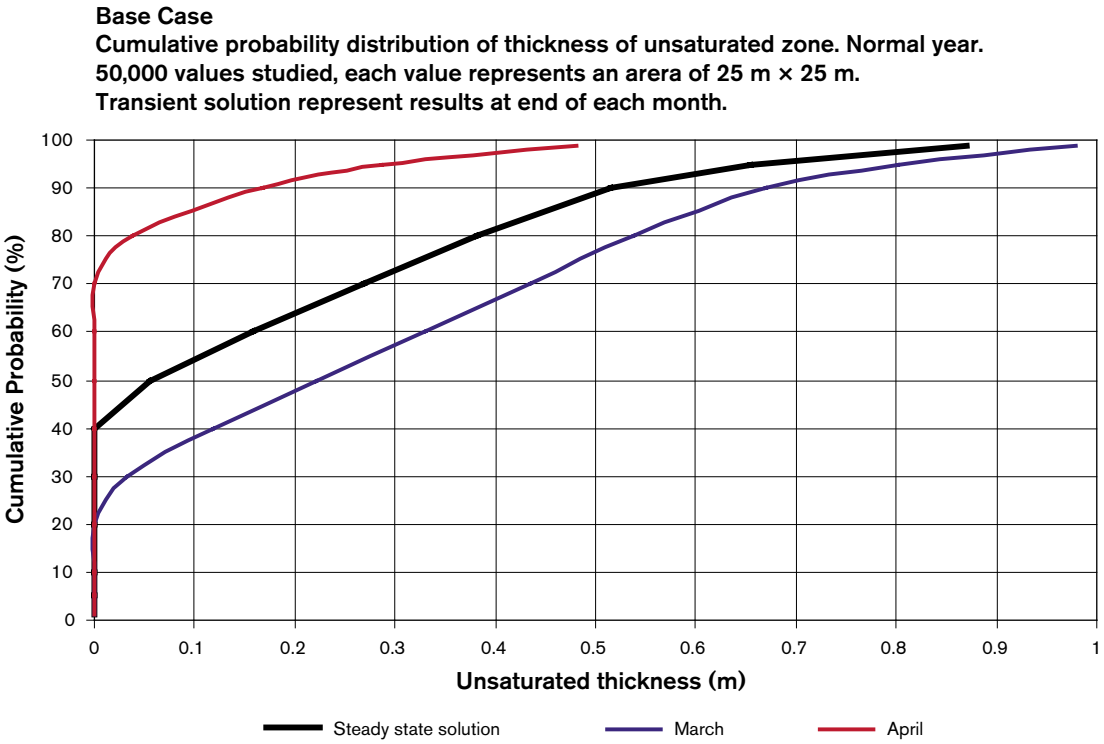

Figure 7-8. *Probability distribution of thickness of unsaturated zone, considering the Base case and a transient solution and a normal year. Results are given for March (largest thickness) and April (smallest thickness), also the results of a steady state situation is given in the figure.*

7.4 Selection of Base case

The balance of recharge/discharge areas depends not only of the amount of precipitation, the temperature (freezing or not) and permeability of the flow media, but also on the topography; and in addition also on the history of the studied system.

It follows that field observations of amount of discharge areas represents the area studied only (the place), and also only the state of the system studied at the studied occasion (time). An example of field estimates of the amount of discharge areas is given in /Grip and Rhode, 1985/. Saturated discharge areas were estimated for six Swedish catchment areas (drainage basins). The sizes of the catchment areas varied between 0.03 km^2 and 6.6 km^2, and they were all dominated by glacial till and coniferous forest (pine forest). For the field investigations, the definition of a discharge area was "an area at which water occurred on or at the ground surface". According to these field investigations the amount of discharge areas varied between 10 through 35 percent of the catchment areas studied. The investigations were carried out when the flow of water in the local streams were larger than average. It is stated in /Grip and Rhode, 1985/ that the estimates probably represent a situation when the discharge areas are close to their maximum extension. To what degree these field investigations are applicable to the area analysed in this study we cannot say. However, they indicate that the amount of discharge areas can be large during a wet season.

We have selected a Base case considering both the results of the above-presented steady state simulations and the transient simulations. We have selected Case C as our Base case. Case D may also have been a good choice as well as Case B. We selected however the case with a conductivity in the uppermost 0.5 m that correspond to the geometric mean of the range of possible conductivity values as estimated by /Lind and Lundin, 1990/.

7.5 Simulation of wet-year

7.5.1 Methodology of transient simulation – Wet-year

Transient calculations were carried out for the Base case (Case C). The simulation represents a wet-year (probability 1/1,000). Potential groundwater recharge was specified according to the results of water balance modelling as follows: April = 433 mm, May = 7 mm, June = 18 mm, July = 75 mm, August = 121 mm, September = 108 mm, October = 116 mm, November = 158 mm. (Note that these values are the potential recharge and not the actual recharge, this will be further discussed in the next chapter.) The initial conditions were the state of the studied groundwater system at the end of the balanced normal year. Hence, we have modelled a wet-year that follows after a normal year. The transient model did not include any frozen ground during the winter months. In the model discharge of groundwater took place during the winter as well.

7.5.2 Results

Considering the Base case and a wet-year, the temporal variation in amount of discharge areas is given in Figure 7-9, below.

As can be seen in the figure, the discharge areas are the largest during the early spring, at the end of April all of the areas above the shoreline are saturated with groundwater. During May and June, the amount of discharge areas decreases and at the end of June the discharge areas make up 50% of all areas. Then follows the late summer and autumn with increasing amount of discharge areas, at the end of November the amount of discharge areas is 90%. The smallest amount of discharge areas occurs at the end of Mars, before the spring (23%). (The amount of discharge areas predicted with the steady state solution is also given in the figure, 43%).

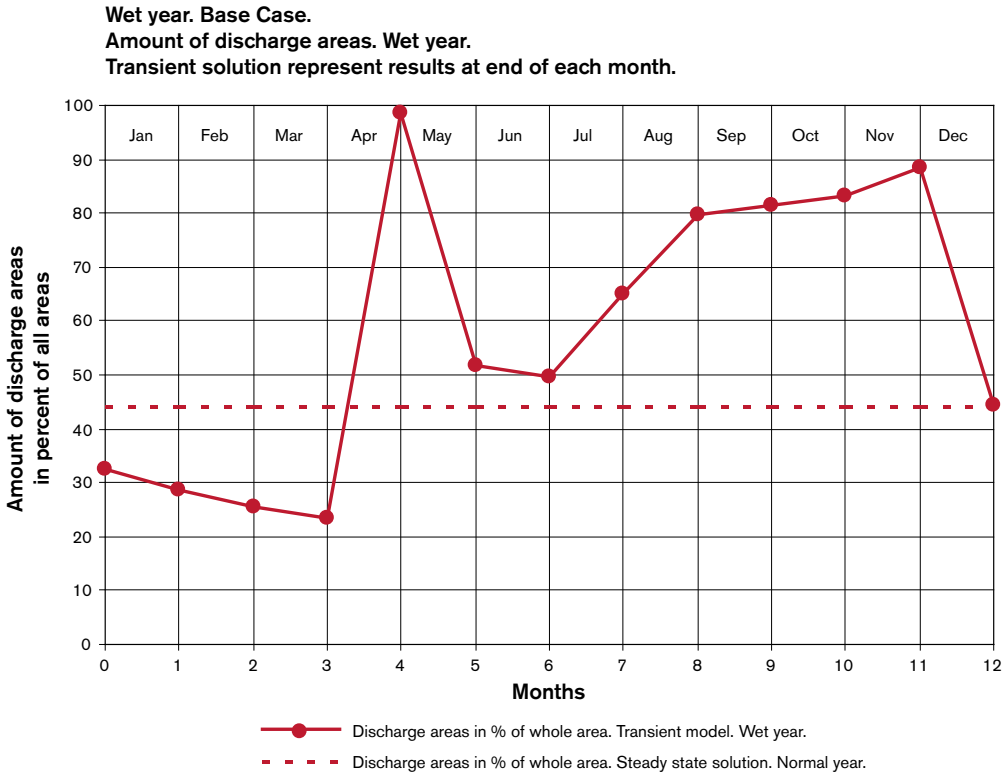

Figure 7-9. *Variation of amount of discharge areas during a wet-year.*

7.6 Simulation of dry-year

7.6.1 Methodology of transient simulation – Wet-year

Transient calculations were carried out for the Base case (Case C). The simulation represents a dry-year (probability 1/1,000). Potential groundwater recharge was specified according to the results of water balance modelling as follows: 61 mm during April. (Note that this value is the potential recharge and not the actual recharge, this will be further discussed in the next chapter.) The initial conditions were the state of the studied groundwater system at the end of the balanced normal year. Hence, we have modelled a dry-year that follows after a normal year. The transient model did not include any frozen ground during the winter months. In the model discharge of groundwater took place during the winter as well.

7.6.2 Results

Considering the Base case and a dry-year, the temporal variation in amount of discharge areas is given in Figure 7-11, below, the spatial extension of the discharge areas are given in Figure 7-10.

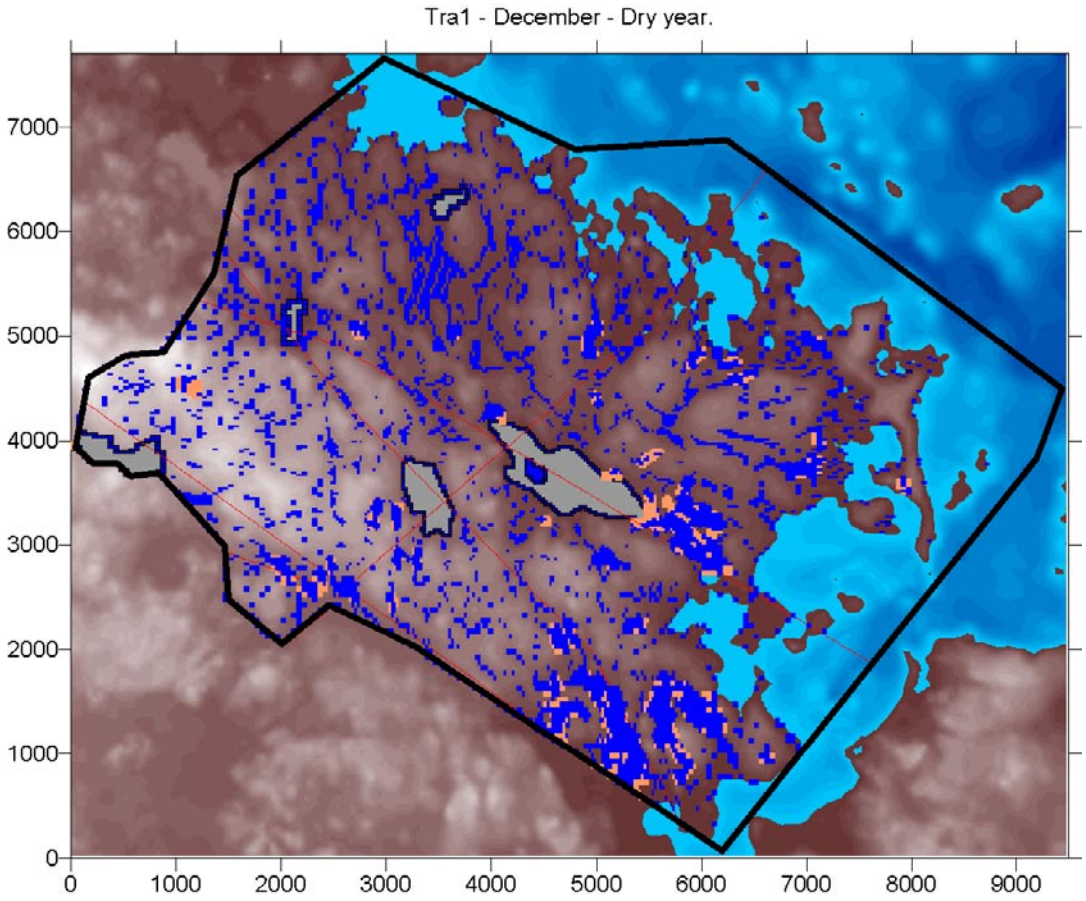

Figure 7-10. *Base case – Dry-year – December – Groundwater discharge areas. Blue squares denote discharge areas above the sea, areas that are not defined as lakes. Discharge will also take place below the sea and at the lakes.*

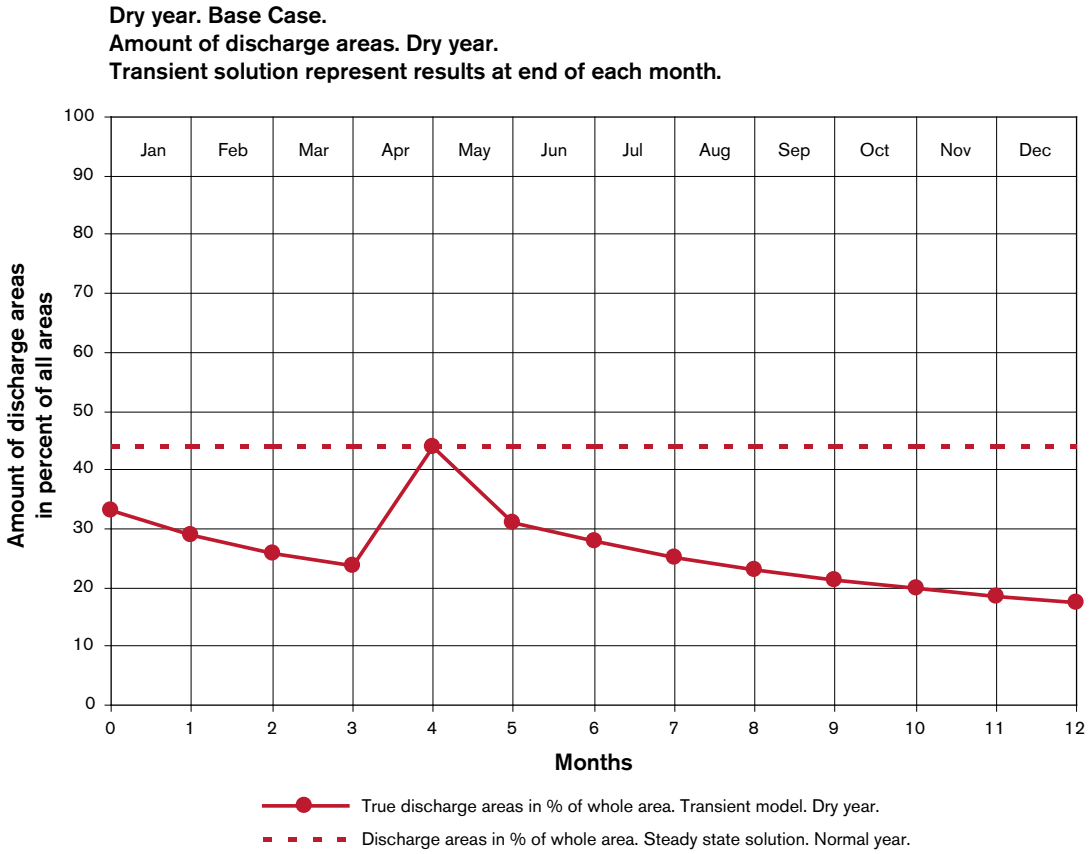

Figure 7-11. *Variation of amount of discharge areas during a dry-year.*

As can be seen in the figure, the discharge areas are the largest during the early spring. At the end of April 43% of the areas above the shoreline are saturated with groundwater. During the special year studied – the dry-year – the amounts of discharge areas decreases steadily during the summer and the autumn; since no groundwater recharge takes place during the autumn. At the end of the dry-year, the amount of discharge areas is 18%. (The amount of discharge areas predicted with the steady state solution is also given in the figure 43%).

During the dry-year, the thickness of the unsaturated zone will vary; this is illustrated in Figure 7-12. At the end of April the groundwater levels are at their highest, for 99% of the area studied the thickness of the unsaturated zone is less than 0.79 m. At the end of the year (December), the groundwater levels are at their lowest; for 99% of the area studied the thickness of the unsaturated zone is less than 1.02 m. As a reference, the thickness of the unsaturated zone of the steady state solution of the normal year is also presented in the figure.

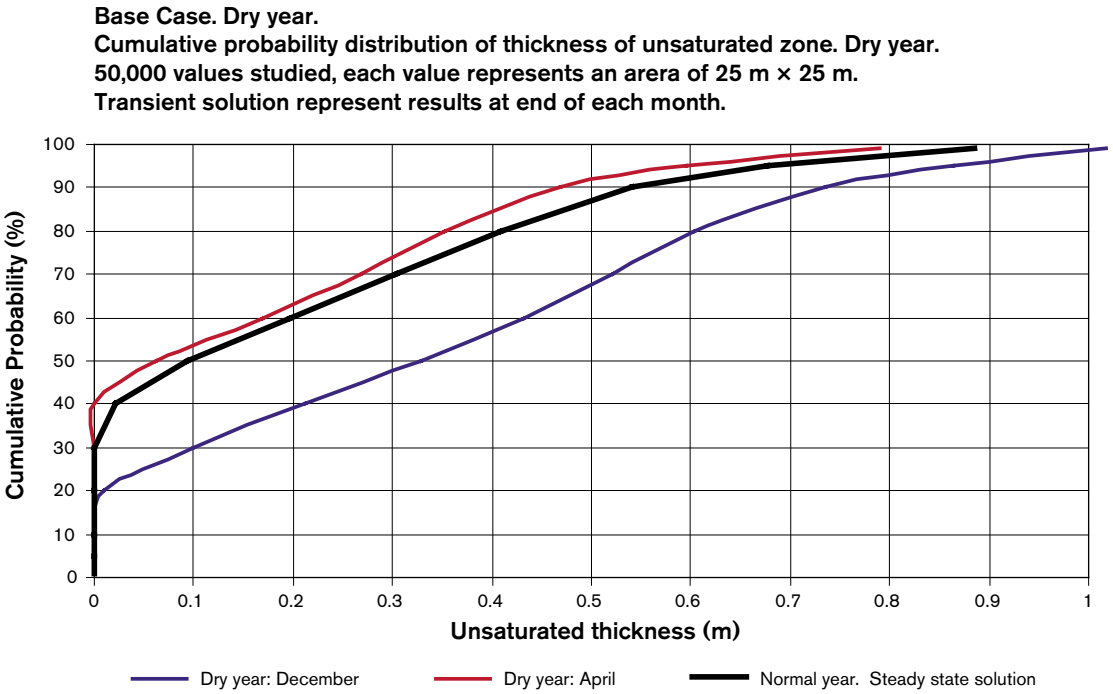

Figure 7-12. *Probability distribution of thickness of unsaturated zone, considering the Base case and a transient solution and a dry-year. Results are given for December (largest thickness) and April (smallest thickness), also the results of a steady state situation is given in the figure.*

8 Calculated groundwater recharge

8.1 Introduction

In the previous chapter we discussed the amount of recharge areas and discharge areas. At recharge areas, water is added to the groundwater system. At discharge areas water leaves the groundwater system. In this chapter we will calculate the size of the recharge (the flow). The recharge will be given in the units (mm/year) or (mm/month); the length (mm) corresponds to the height of water taken over an area. Hence, a flow of 1 mm/month is the same thing as 1 litre per square metre and month, and taken over an area of 1,000 m^2 it corresponds to a flow of 1 m^3/month. The concepts of recharge areas and discharge area, as well as groundwater recharge (flow) are also discussed in Sections 2.3 and 2.4. The potential recharge is a result of the water balance modelling; the potential recharge as an input to the groundwater modelling, the actual recharge is calculated by the groundwater model.

8.2 Size of recharge (flow); versus conductivity of the uppermost 0.5 m – Steady state solution

Four different cases have been established – the same cases as discussed in Section 7. All cases are identical to the Base case presented in Section 6 (see Figure 6-6), except for the conductivity of the uppermost 0.5 m. The cases studied are as follows:

The different cases

- Case A (M30b) Conductivity of uppermost 0.5 m is set to 5E–6 m/s.
- Case B (M30) Conductivity of uppermost 0.5 m is set to 5E–5 m/s.
- Case C (M52e) Conductivity of uppermost 0.5 m is set to 1E–4 m/s. (Base case)
- Case D (M30c) Conductivity of uppermost 0.5 m is set to 5E–4 m/s.

Potential groundwater recharge corresponds to that of a normal year. We have calculated the size of the actual groundwater recharge by use of the routine discussed in Section 6.1.4. The calculations presented in this section (8.2) were carried out under steady state conditions. Results derived via a steady state solution do not represent any particular moment during a year, but is to be looked upon as an average representation of the actually varying situation. We will in the following sections of this chapter also include the transient behaviour of the system studied. Table 8-1 presents the calculated actual groundwater recharge and the corresponding amount of discharge areas, for the four different cases studied. The calculated actual groundwater recharge is also presented in Figure 8-1, in the figure the recharge is given as a function of the conductivity of the uppermost 0.5 m of the quaternary deposits.

Considering an area large enough to contain both recharge areas and discharge area, the actual recharge cannot be larger than the potential recharge, since the potential recharge defines the maximum available amount of water; the actual recharge is smaller than the potential recharge because of the limited transport capacity of the flow medium and because

of the presence of discharge areas. The size of the recharge depends on the conductivity of the uppermost part of the flow medium (assuming everything else being equal); this is demonstrated by Figure 8-1.

- If the conductivity is large, a large amount of the precipitation and surface waters will infiltrate and create groundwater. Size of recharge and amount of recharge areas will be large for such a situation. The discharge areas will be few, but the outflow of groundwater is large at these areas.
- If the conductivity is small, only a small amount of the precipitation will be able to infiltrate – the recharge will be small. It follows that most of the areas will be saturated up to the ground surface; consequently for such a situation most areas will be discharge areas, even if the discharge is small.

Table 8-1. Calculated actual groundwater recharge and amount of discharge areas, considering four different values of hydraulic conductivity of the uppermost 0.5 m. Steady state solution, normal year.

Case	Conductivity of uppermost 0.5 m. (m/s)	Calculated actual groundwater recharge (mm/year)	Calculated amount of discharge areas (%)
Case A (*M30b*)	5E–6	28	95
Case B (*M30*)	5E–5	104	57
Case C (*M52e*) Base case	1E–4	122	43
Case D (*M30c*)	5E.4	169	20

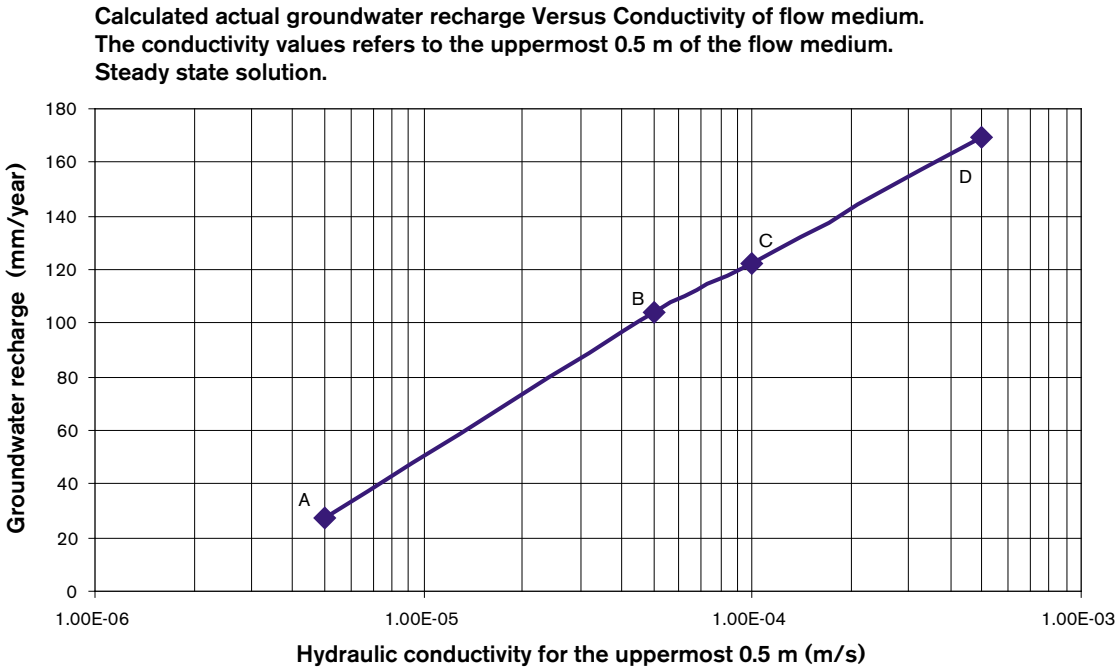

Figure 8-1. *Calculated actual groundwater recharge for the four different cases studied (A, B, C and D), versus conductivity of the flow medium. The conductivity values refer to the uppermost 0.5 m of the quaternary deposits. Steady state solution, normal year.*

Based on the relationship demonstrated in Figure 8-1 we may derive the following conclusion: For values of conductivity (of the uppermost 0.5 m) between 5E–6 m/s and 5E–4 m/s, the amount of actual groundwater recharge (in mm per year) is approximately linear proportional to the logarithms of the conductivity of the uppermost 0.5 m. The conclusion produces the following approximate relationship applicable between K = 5E–6 m/s and K = 5E–4 m/s.

$$R = C_1 \, {}^{10}Log(K) + C_2 \qquad \text{Equation 8-1}$$

Where:

R = Groundwater recharge (mm/year)

C_1 = A constant derived from Figure 8-1, C_1 = 72.54

K = Hydraulic conductivity (m/s) of uppermost 0.5 m

C_2 = A constant derived from Figure 8-1, C_2 = 412.15

A similar relationship is demonstrated between the total transmissivity of the quaternary deposits and the recharge. Reformulating the relationship above for the total transmissivity of the quaternary deposits, will produce the following equation, applicable between T = 3E–6 m^2/s and T = 2.5E–4 m^2/s.

$$R = C_1 \, {}^{10}Log(T) + C_2 \qquad \text{Equation 8-2}$$

Where:

R = Groundwater recharge (mm/year)

C_1 = A constant, C_1 = 77.68

T = Total hydraulic transmissivity (m^2/s) of the quaternary deposits

C_2 = A constant, C_2 = 455.70

8.3 Size of recharge with alternative top boundary condition

The Base case model carries, above the shoreline, a non-linear boundary condition (see Section 6.1.4). For the purpose of comparison we have established a model (M53ep1sh) identical to the Base case, but with specified head as the top boundary condition, and the specified head is set to the varying topographic elevation (no unsaturated zone in this model). We have calculated the recharge produced by this model. With the specified head condition on top of model, the recharge to the quaternary deposits will be 241 mm/year, an increase of about 100% compared to the Base case. This follows from the higher heads at the top of the specified head model, as that model has no unsaturated zone. The recharge to the rock mass, below the quaternary deposits, will increase with 25% (recharge to the rock mass is discussed in Section 8.6).

8.4 Size of recharge and amount of discharge areas versus conductivity of flow medium, steady state solution

We have combined Figure 7-1 (amount of discharge areas versus conductivity) and Figure 8-1 (size of recharge versus conductivity) into Figure 8-2. This figure demonstrate the relationships between: (i) size of recharge and (ii) amount of discharge areas, versus (iii) hydraulic conductivity of the uppermost 0.5 m of the flow medium.

It is demonstrated by the figure that the larger the conductivity of the flow medium, the larger the recharge and the smaller the amount of discharge areas. If follows, that the larger the amount of discharge areas, the smaller the groundwater recharge (this is self-evident as recharge can only take place at recharge areas).

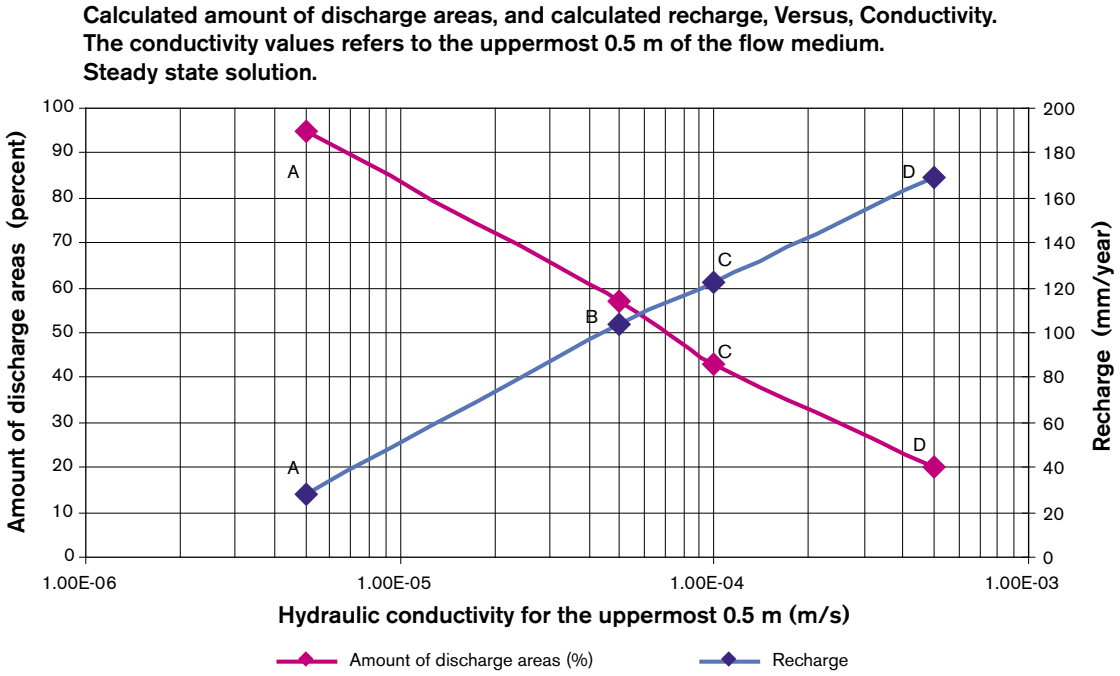

Figure 8-2. *Calculated amount of discharge areas and calculated groundwater recharge, versus conductivity of the uppermost 0.5 m of the flow medium (quaternary deposits). The letters (A, B, C and D) refers to the different cases studied. Steady state solution, normal year.*

8.5 Size of recharge versus time

8.5.1 Normal year

8.5.1.1 Methodology of transient simulation – Normal year

Transient calculations were carried out for the Base case (Case C). The simulation represents a normal year. Potential groundwater recharge was specified according to the results of water balance modelling: 160 mm during May, 18 mm during October and 61 mm during November. The initial conditions were the results of the steady state simulation of a normal year. The modelled period included two years – in order to equalize the temporal storage and to obtain a balanced normal year. For a balanced normal year, the system studied starts and ends at the same state. The presented results represent a balanced normal year. The transient model did not include any frozen ground during the winter months. In the model discharge of groundwater took place during the winter as well.

8.5.1.2 Results

Considering the Base case and a balanced normal year, the temporal variation in size of groundwater recharge is given in Table 8-2 and in Figure 8-3, below.

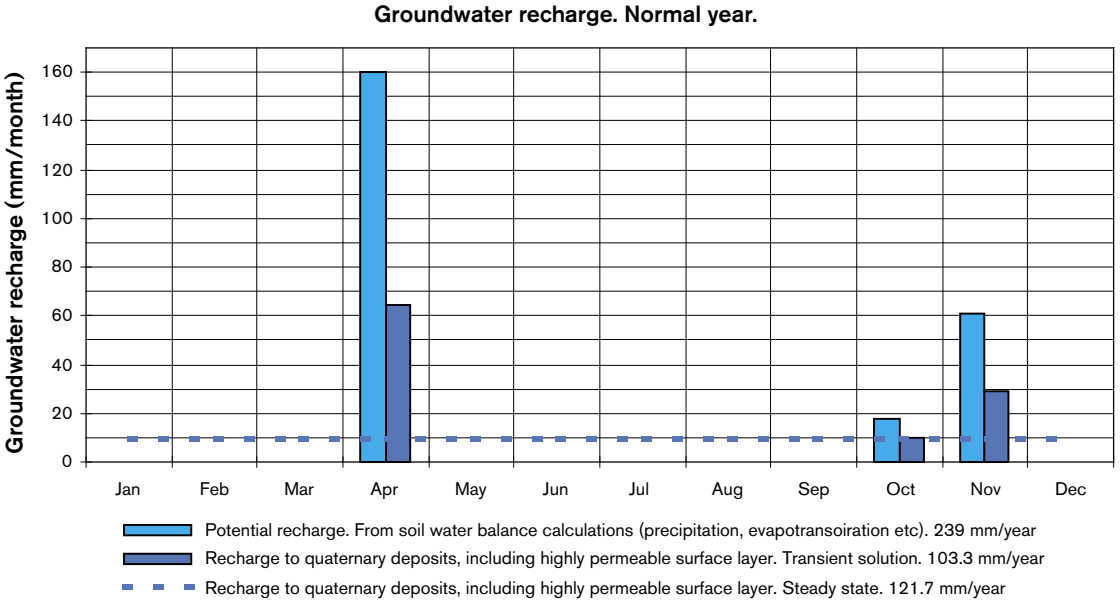

Figure 8-3. *Groundwater recharge during a normal year. The potential recharge is from the water balance calculations and the actual recharge is as calculated by the model.*

Table 8-2. Groundwater recharge during a normal year. The potential recharge is from the water balance calculations and the actual recharge is as calculated by the model.

Potential and calculated actual recharge (mm)													
Normal year	**Jan**	**Feb**	**Mar**	**Apr**	**May**	**Jun**	**Jul**	**Aug**	**Sep**	**Oct**	**Nov**	**Dec**	**Tot**
Potential recharge				160						18	61		239
Actual recharge steady	10.1	10.1	10.1	10.1	10.1	10.1	10.1	10.1	10.1	10.1	10.1	10.1	121.7
Actual recharge transient	< 1	< 1	< 1	64.5	< 1	< 1	< 1	< 1	< 1	9.7	29.0	< 1	103.3

According to the water balance calculations, potential recharge is only available during the spring (April) and during the autumn (October and November). It follows that the nearly all of the actual recharge will take place during those periods. However, as the model includes surface water flows, actual recharge will also take place during months with zero potential recharge. This recharge comes from the flow of surface water; it is water that has been transported as a surface flow that infiltrates into the groundwater system of the model (e.g. along hill sides and streams). The size of this recharge is however small and always less than one millimetre per month.

As can be seen in the figure above, both the intensity and the total volume of recharge are the largest during the spring. During the month of April the potential recharge is 160 mm, and out of this 64.5 mm will infiltrate and produce groundwater recharge. During October and November, the potential recharge is 79 mm, and out of this 38.7 mm will infiltrate and produce groundwater recharge.

The size of the actual recharge as predicted with the steady state solution is also given in the table and in the figure above; per month the steady state actual recharge is equal to 10.1 mm/year. The value derived from the steady state solution is a sort of average value of the variation during the year. It is however not the same thing as an arithmetic average based on the transient monthly values, which is equal to 8.6 mm/month.

8.5.2 Wet-year

8.5.2.1 Methodology of transient simulation – Wet-year

Transient calculations were carried out for the Base case (Case C). The simulation represents a wet-year (probability 1/1,000). Potential groundwater recharge was specified according to the results of water balance modelling as follows: April = 433 mm, May = 7 mm, June = 18 mm, July = 75 mm, August = 121 mm, September = 108 mm, October = 116 mm, November = 158 mm. The initial conditions were the state of the studied groundwater system at the end of the balanced normal year. Hence, we have modelled a wet-year that follows after a normal year. The transient model did not include any frozen ground during the winter months. In the model discharge of groundwater took place during the winter as well.

8.5.2.2 Results

Considering the Base case and a wet-year, the temporal variation in size of groundwater recharge is given in Table 8-3 and in Figure 8-4 (note that the scale is not the same in Figure 8-4 and in Figure 8-3). For the wet-year, the water balance modelling produces a potential recharge for all months, except the winter months. A very large potential recharge takes place during April when the snow melts, and during the whole summer there will be a potential recharge (especially in August), and as for the normal year, the potential recharge is large during the autumn. For all months with a potential recharge, there will be an actual recharge calculated by the model. In total the potential recharge is 1,036 mm/year for the wet-year, and the corresponding actual recharge is 207 mm/year.

Table 8-3. Groundwater recharge during a wet-year. The potential recharge is from the water balance calculations and the actual recharge is as calculated by the model.

Potential and calculated actual recharge (mm)													
Wet-year	**Jan**	**Feb**	**Mar**	**Apr**	**May**	**Jun**	**Jul**	**Aug**	**Sep**	**Oct**	**Nov**	**Dec**	**Tot**
Potential recharge				433	7	18	75	121	108	116	158		1,036
Actual recharge transient	< 1	< 1	< 1	65	3	8	24	28	25	26	29	< 1	207

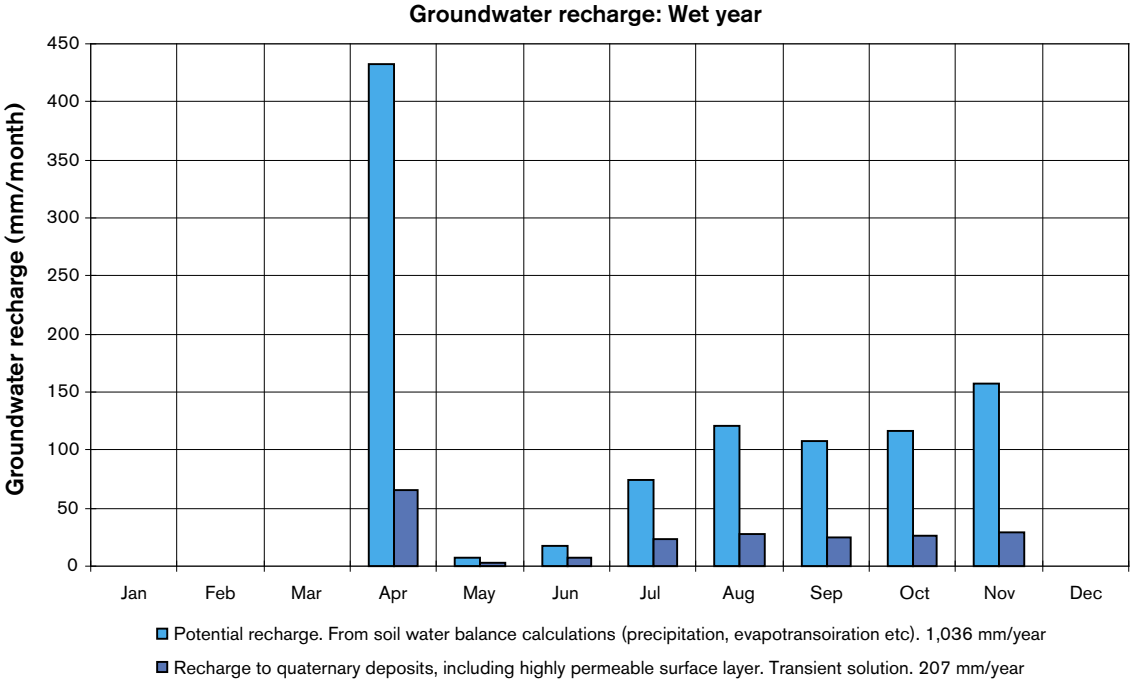

Figure 8-4. *Groundwater recharge during a wet-year. The potential recharge is from the water balance calculations and the actual recharge is as calculated by the model.*

8.5.3 Dry-year

8.5.3.1 Methodology of transient simulation – Dry-year

Transient calculations were carried out for the Base case (Case C). The simulation represents a dry-year (probability 1/1,000). Potential groundwater recharge was specified according to the results of water balance modelling, and these calculations demonstrates that potential recharge will only take place during the month of April (61 mm). The initial conditions were the state of the studied groundwater system at the end of the balanced normal year. Hence, we have modelled a dry-year that follows after a normal year. The transient model did not include any frozen ground during the winter months. In the model discharge of groundwater took place during the winter as well.

8.5.3.2 Results

Considering the Base case and a dry-year, the temporal variation in size of groundwater recharge is given in Table 8-4 and in Figure 8-5, below.

Table 8-4. Groundwater recharge during a dry-year. The potential recharge is from the water balance calculations and the actual recharge is as calculated by the model.

Potential and calculated actual recharge (mm)													
Dry-year	**Jan**	**Feb**	**Mar**	**Apr**	**May**	**Jun**	**Jul**	**Aug**	**Sep**	**Oct**	**Nov**	**Dec**	**Tot**
Potential recharge				61									61
Actual recharge transient	< 1	< 1	< 1	29.8	< 1	< 1	< 1	< 1	< 1	< 1	< 1	< 1	29.8

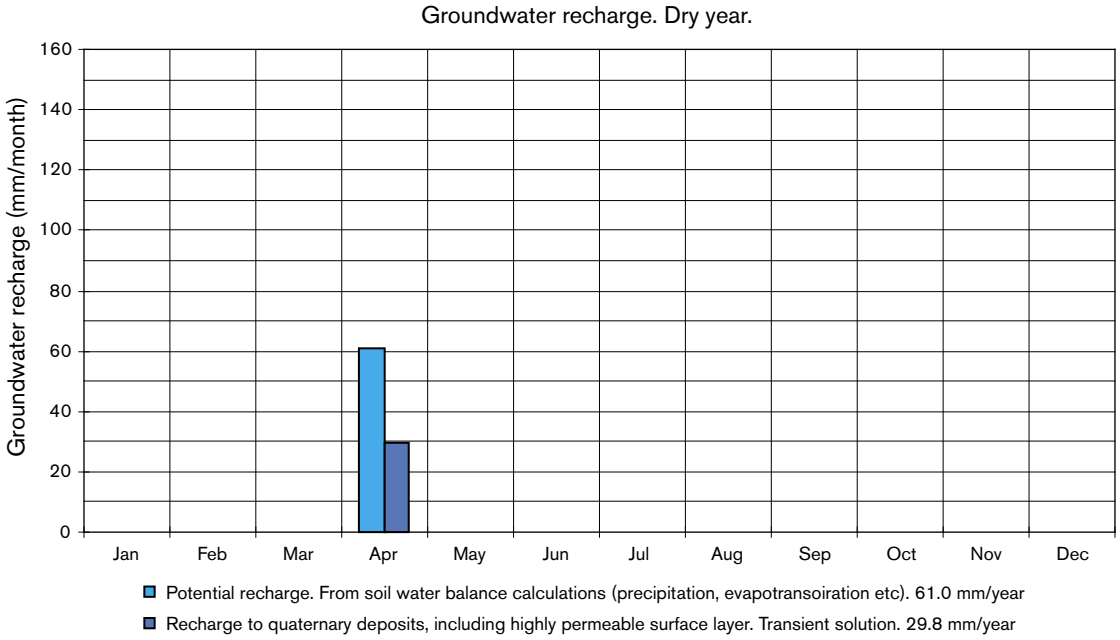

Figure 8-5. *Groundwater recharge during a dry-year. The potential recharge is from the water balance calculations and the actual recharge is as calculated by the model.*

For the dry-year, the water balance modelling produces a potential recharge for the month of April, only. It follows that actual recharge will take place during April. In total the potential recharge is 61 mm/year for the dry-year, and the corresponding actual recharge is 29.8 mm/year.

8.6 Recharge to the rock mass

8.6.1 Introduction

As stated in Section 2.3, recharge is often defined as: “A process, natural or artificial by which water is added from outside to the zone of saturation, either directly into a formation or indirectly by way of another formation” /Nordic Glossary of Hydrology, 1984/. Hence, we may define recharge to the rock mass as the groundwater that flows from the quaternary deposits to the rock mass. When we discuss groundwater recharge and rock mass, we mean recharge to the fracture zones and the rock between these zones. It is easily done in the established models to calculate the groundwater flow between the quaternary deposits and

the rock mass. The flow is first calculated in the unit: volume/time, in a second step the flow is divided by the horizontal area between the two formations, thereby producing a flow in the units: length/time, which can be compared to the recharge to the quaternary deposits (see previous sections).

8.6.2 General behaviour of the system

The size of recharge to the rock mass depends not directly on the potential recharge (and the precipitation etc), but on the size of groundwater head in the quaternary deposits in relation to the head in the rock mass (the gradient). Hence, the recharge to the rock mass is indirectly coupled the potential recharge, via the groundwater heads of the quaternary deposits that depend on the potential recharge. Since the variation in groundwater gradient between the rock mass and quaternary deposits is small, compared to the variation in potential recharge; it follows that the recharge to the rock mass varies much less during a year than the recharge to the quaternary deposits. The recharge to the rock mass is the largest during the spring, when the groundwater heads are the highest, and smallest at the end of the winter and at the end of the summer, as the groundwater heads are the lowest at these times of the year. In addition, as the permeability of the rock mass, on the average, is much smaller than that of the quaternary deposits, the recharge to the rock mass is much smaller than the recharge to the quaternary deposits.

8.6.3 Normal year

Considering the Base case and a balanced normal year, the temporal variation in size of groundwater recharges to the rock mass (with fracture zones) and to the quaternary deposits are given in Table 8-5 and in Figure 8-6, below.

Table 8-5. Groundwater recharge during a normal year. Recharge to quaternary deposits and recharge to rock mass (rock mass includes fracture zones). The potential recharge is from the water balance calculations and the (actual) recharge is as calculated by the model.

Potential and calculated actual recharge (mm)														
Normal year		**Jan**	**Feb**	**Mar**	**Apr**	**May**	**Jun**	**Jul**	**Aug**	**Sep**	**Oct**	**Nov**	**Dec**	**Tot**
Quarternary deposits	Potential recharge				160						18	61		239
	Actual recharge steady	10.1	10.1	10.1	10.1	10.1	10.1	10.1	10.1	10.1	10.1	10.1	10.1	121.7
	Actual recharge transient	< 1	< 1	< 1	64.5	< 1	< 1	< 1	< 1	< 1	9.7	29.0	< 1	103.3
Rock mass	Actual recharge steady	0.21	0.21	0.21	0.21	0.21	0.21	0.21	0.21	0.21	0.21	0.21	0.21	2.50
	Actual recharge transient	0.18	0.18	0.17	0.34	0.21	0.19	0.18	0.18	0.17	0.20	0.26	0.19	2.47

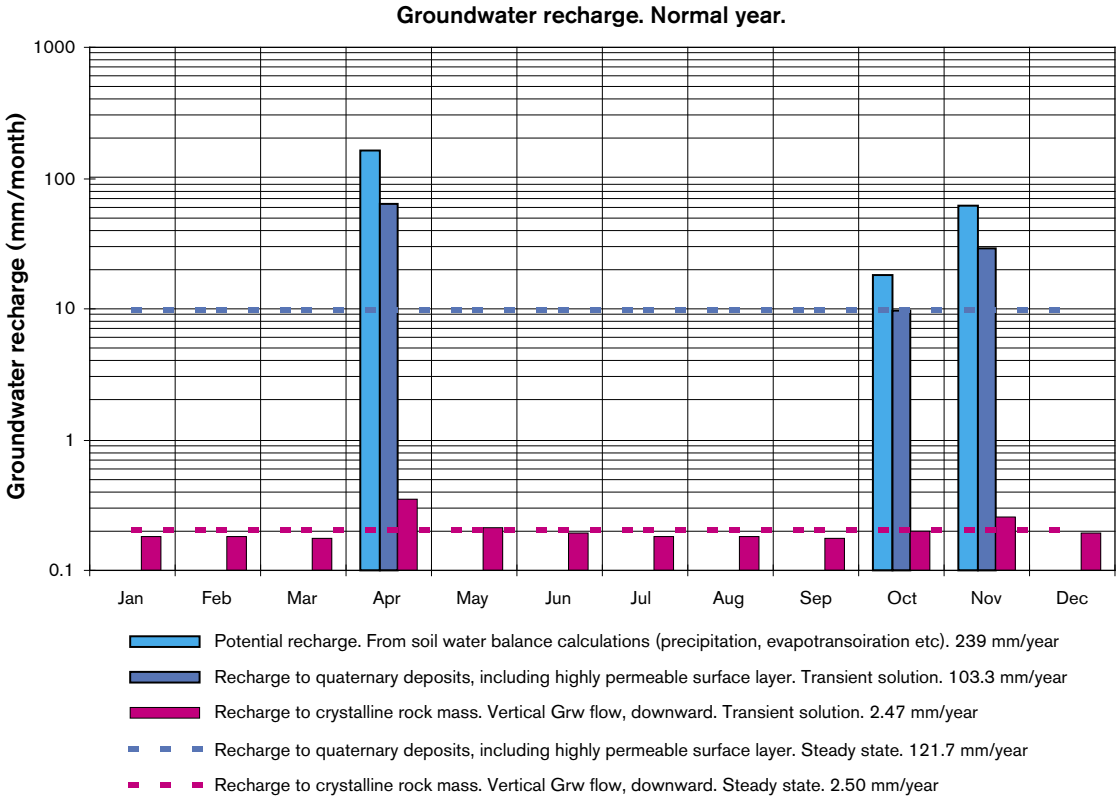

Figure 8-6. *Groundwater recharge during a normal year. Recharge to quaternary deposits and recharge to rock mass (rock mass includes fracture zones). The potential recharge is from the water balance calculations and the (actual) recharge is as calculated by the model.*

The potential recharge (or the run off) is 240 mm/year. The groundwater recharge to the quaternary deposits is equal to 103 mm/year, which is about 45% of the potential recharge. The groundwater recharge to the rock mass is 2.5 mm/year, this is close to 1% of the potential recharge, and close to 2% of the recharge to the quaternary deposits. Hence only a fraction of the groundwater flow of the quaternary deposits will recharge into the rock mass. If all recharge is equally distributed in time (as in a steady state simulation) the recharge during a month is 8.3% of the total recharge during a year. Considering the transient simulations and the quaternary deposits, the maximum recharge during a month is 64.5 mm, which is close to 62% of all the recharge during a year. However, considering transient simulations and the recharge to the rock mass, the maximum recharge during a month is 0.34 mm, which is close to 14% of all the recharge during a year; the minimum recharge during a month is 0.17 mm, which is close to 7% of all the recharge during a year. Hence, the variation in recharge to the rock mass is much less than the variation in recharge to the quaternary deposits.

8.6.4 Wet-year

The initial conditions were the state of the studied groundwater system at the end of the balanced normal year. Hence, we have modelled a wet-year that follows after a normal year. Considering the Base case and a wet-year, the temporal variation in size of groundwater recharges to the rock mass (with fracture zones) and to the quaternary deposits are given in Table 8-6 and in Figure 8-7, below. The total recharge to the rock mass is 2.85 mm/year; this is an increase of only 15% compared to the normal year. (Considering the quaternary deposits, the recharge during the wet-year is close to two times that of the normal year.)

Table 8-6. Groundwater recharge during a wet-year. Recharge to quaternary deposits and recharge to rock mass (rock mass includes fracture zones). The potential recharge is from the water balance calculations and the (actual) recharge is as calculated by the model.

Potential and calculated actual recharge (mm)														
Wet-year		**Jan**	**Feb**	**Mar**	**Apr**	**May**	**Jun**	**Jul**	**Aug**	**Sep**	**Oct**	**Nov**	**Dec**	**Tot**
Quarternary deposits	Potential recharge				433	7	18	75	121	108	116	158		1,036
	Actual recharge transient	< 1	< 1	< 1	65	3	8	24	28	25	26	29	< 1	207
Rock mass	Actual recharge transient	0.18	0.18	0.17	0.35	0.22	0.21	0.26	0.28	0.26	0.26	0.27	0.19	2.85

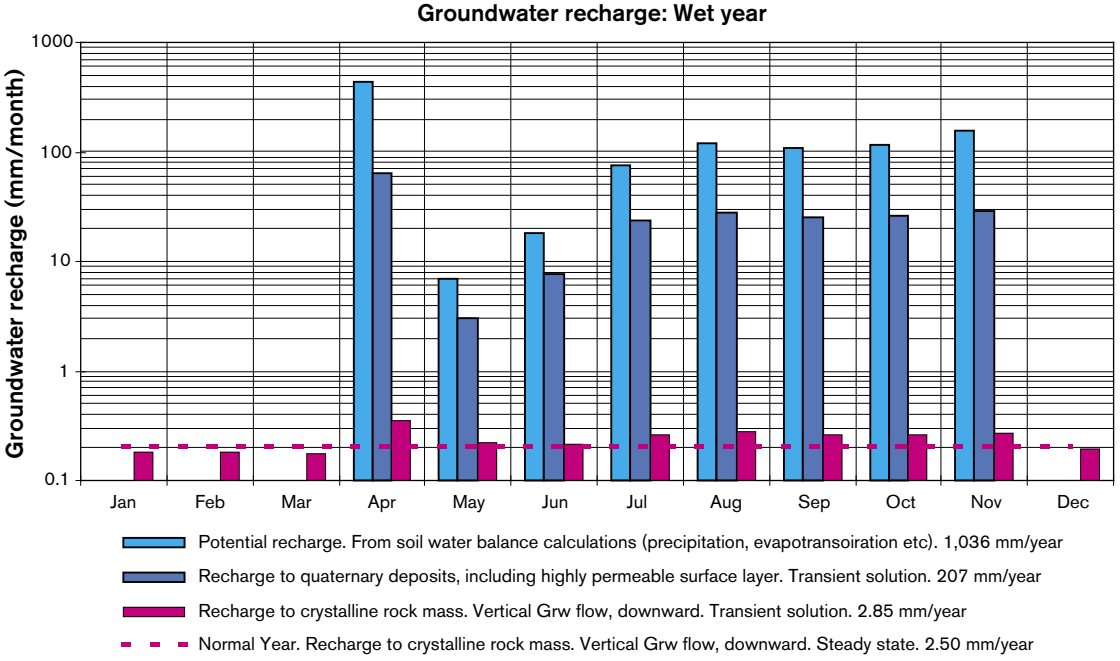

Figure 8-7. *Groundwater recharge during a Wet-year. Recharge to quaternary deposits and recharge to rock mass (rock mass includes fracture zones). The potential recharge is from the water balance calculations and the (actual) recharge is as calculated by the model.*

8.6.5 Dry-year

The initial conditions were the state of the studied groundwater system at the end of the balanced normal year. Hence, we have modelled a dry-year that follows after a normal year. Considering the Base case and a dry-year, the temporal variation in size of groundwater recharges to the rock mass (with fracture zones) and to the quaternary deposits are given in Table 8-7 and in Figure 8-8, below. The total recharge to the rock mass is 2.19 mm/year; this is a reduction of only 13% compared to the normal year. (Considering the quaternary deposits, the recharge during the dry-year is less than one third of the recharge of a normal year.)

Table 8-7. Groundwater recharge during a dry-year. Recharge to quaternary deposits and recharge to rock mass (rock mass includes fracture zones). The potential recharge is from the water balance calculations and the (actual) recharge is as calculated by the model.

Potential and calculated actual recharge (mm)														
Dry-year		**Jan**	**Feb**	**Mar**	**Apr**	**May**	**Jun**	**Jul**	**Aug**	**Sep**	**Oct**	**Nov**	**Dec**	**Tot**
Quarternary deposits	Potential recharge				61									61
	Actual recharge transient	< 1	< 1	< 1	29.8	< 1	< 1	< 1	< 1	< 1	< 1	< 1	< 1	29.8
Rock mass	Actual recharge transient	0.18	0.18	0.17	0.25	0.19	0.18	0.18	0.17	0.17	0.17	0.17	0.16	2.19

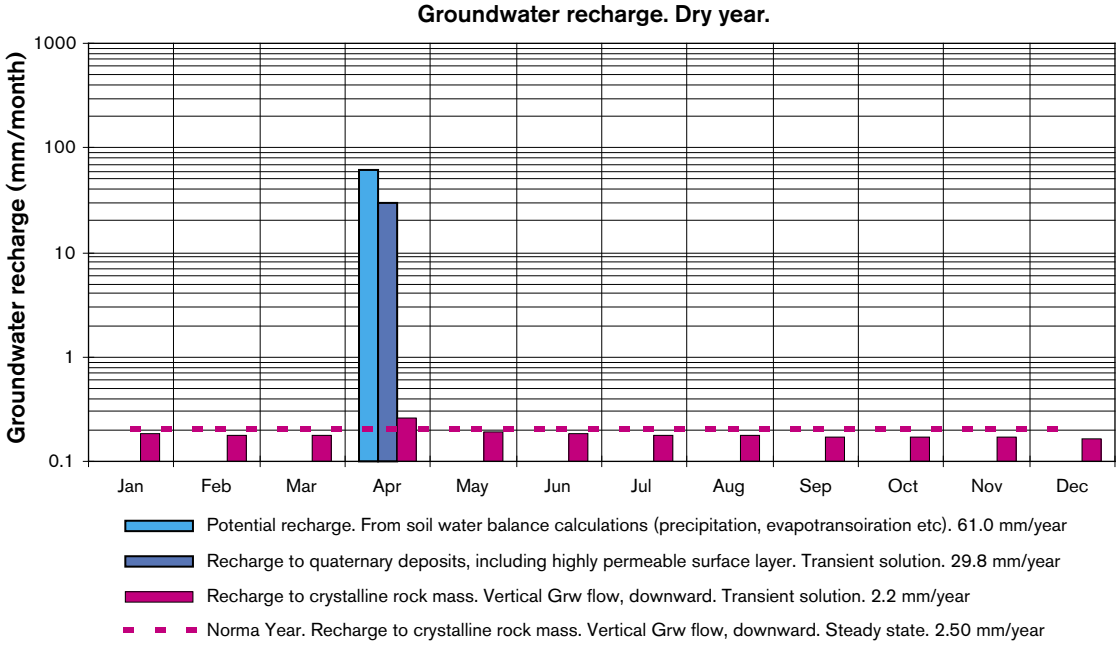

Figure 8-8. *Groundwater recharge during a dry-year. Recharge to quaternary deposits and recharge to rock mass (rock mass includes fracture zones). The potential recharge is from the water balance calculations and the (actual) recharge is as calculated by the model.*

8.6.6 Recharge to rock mass without quaternary deposits

We have established models without any quaternary deposits. The quaternary deposits were changed into rock mass and fracture zones, hence the rock mass and the zones were extended all the way up to the ground surface. These cases have been established for the purpose of comparisons to the Base case, and the models are identical to the Base case, except for the conductivity of the uppermost layers and the boundary conditions of the uppermost layers. The cases are defined in Table 8-8, below. For each case and a steady state situation we have calculated the recharge to the rock mass see Table 8-8, below.

As can be seen in the table above, the recharge to the rock mass as calculated by models without quaternary deposits (Case N1 and N2) is somewhat larger than the recharge obtained for the Base case (with quaternary deposits). The primary reason for this is that the fracture zones have a larger conductivity than the lower part of the quaternary deposits, and hence in the Base case the lower parts of the quaternary deposits limits the recharge to the

Table 8-8. Definition of cases without quaternary deposits, and the recharge to the rock mass calculated by use of these cases (steady state solutions).

Case	Definition of case	Recharge to rock mass (Normal year, Steady state) (mm/year)
Base case (*M52e*)	See Section 6 (This is the Base case. It contains quaternary deposits.)	2.5
N1 *(N53hw)*	As Base case, but quaternary deposits changed into rock mass. Fracture zones extends up to ground surface.	3.4
N2 *(N53hwp)*	As Case N2, except that the boundary condition on top of the model is set to: Specified head = Topography.	3.4
N3 *(N53h)*	As Base case, but quaternary deposits changed into rock mass. No fracture zones in the uppermost 3 m.	2.1
N4 *(N53hp)*	As Case N3, except that the boundary condition on top of the model is set to: Specified head = Topography.	2.1

fracture zones. However, in the cases without quaternary deposits, the fracture zones extend all the way up to the ground surface and the recharge into the fracture zones will be larger than for the Base case (with quaternary deposits).

Two cases are also presented (N3 and N4) for which there are no quaternary deposits (the quaternary deposits were changed into rock mass) and for which the fracture zones ends 3 m below the ground surface. As the permeability of the rock mass (without fracture zones) is smaller than that of the lower parts of the quaternary deposits, the recharge to the zones will be smaller for these cases than for the Base case.

Considering the establishment of a groundwater model and the recharge to the rock mass as well as the properties of the uppermost part of the model, we conclude: It is not always necessary to include the quaternary deposits in a groundwater model. If the purpose of the model is to study the flow in the rock mass, an approximation may be derived without the quaternary deposits. This follows from a flow situation in which the groundwater levels in the quaternary deposits are close the ground surface and the thickness of the quaternary deposits is small compared to thickness of the rock masses. The flow situation in the rock mass below the depth of the quaternary deposits is approximately the same for situations with (i) a large groundwater flow in the upper part of the quaternary deposits or (ii) a large surface flow.

8.6.7 Recharge to rock mass – Concluding remarks

Some concluding remarks are given below:

The recharge to the rock mass depends not directly on the potential recharge (and the precipitation etc), but on the size of groundwater head in the quaternary deposits in relation to the head in the rock mass – the hydraulic gradient between the rock mass and the quaternary deposits.

The permeability of the rock mass is (on the average) much smaller than that of the quaternary deposits, accordingly the recharge to the rock mass is much smaller than the recharge to the quaternary deposits.

Since the variation in groundwater gradient between the rock mass and quaternary deposits is small, compared to the variation in potential recharge; it follows that the recharge to the rock mass varies much less during a year than the recharge to the quaternary deposits. The recharge to the rock mass is the largest during the spring, when the groundwater heads are the highest, and smallest at the end of the winter and at the end of the summer, as the groundwater heads are the lowest at these times of the year.

It follows from the small temporal variation of recharge to the rock mass that the difference is small between the recharge calculated by use of a steady state solution and the recharge calculated by use of a transient solution.

As the recharge to the rock mass is not directly coupled to the potential recharge, the recharge to the rock mass will not vary much even if the potential recharge varies a lot. Considering a wet-year, with a potential recharge that is two times that of a normal year, the recharge to the rock mass will be only 15% larger than the recharge of a normal year. Considering a dry-year with a potential recharge that is less than one third of the recharge of a normal year, the recharge to the rock mass will be only 13% smaller than the recharge of a normal year. As long as there will be groundwater in the quaternary deposits, there will be recharge to the rock mass. A single dry-year, with a very small potential recharge, will not influence the recharge to the rock mass in a dramatic way.

Considering the establishment of a groundwater model and the recharge to the rock mass as well as the properties of the uppermost part of the model, we conclude: It is not always necessary to include the quaternary deposits in a groundwater model. If the purpose of the model is to study the flow in the rock mass, an acceptable approximation may be derived without the quaternary deposits. This follows from a flow situation in which the groundwater levels in the quaternary deposits are close the ground surface and the thickness of the quaternary deposits is small compared to thickness of the rock masses. The flow situation in the rock mass below the depth of the quaternary deposits is approximately the same for situations with (i) a large groundwater flow in the upper part of the quaternary deposits or (ii) a large surface flow. The important property is the size and distribution of the recharge to the rock mass, which may be approximately the same for both situations.

9 Analyses of flow paths from great depth

9.1 Introduction and methodology

9.1.1 Introduction

As a part of this study we have conducted an extensive flow path analysis. The purpose of this analysis is to investigate the movement of the groundwater from great depth, via rock mass and quaternary deposits, to the discharge areas.

9.1.2 Method for calculation of flow paths

The flow pattern of the groundwater can be illustrated by the use of flow paths. The GEOAN model creates flow paths by the use of simulated particles, particles that follow the flow of groundwater through the model. The particle tracking algorithm can be used for estimation of break through times, etc. For calculation of flow paths the GEOAN model provides the user with both a semi-analytical method /Pollock, 1989/ and an iterative numerical method. For all calculations in this study we have used the semi-analytical method. It should also be noted that the length of the groundwater flow paths at discharge areas in the uppermost layer (thickness 0.5) is not known exactly in the numerical solution, due to the non-continuous flow conditions at discharge areas (the head is bounded by the topography). A flow path length is nevertheless estimated for groundwater flow at discharge areas in the uppermost layer, however that estimate includes a numeric uncertainty that depends on cell size.

9.1.3 Method for release of particles

It is a purpose of this study to investigate the flow of ground water from great depth. For that purpose we have (in the model) released particles that demonstrate flow paths from a depth that corresponds to the possible depth of a repository. All analysed particles were released at a depth of 420 m below ground surface.

Particles (flow paths) were released in a regular pattern, one particle in each volume (cell or element) studied, regardless of the flow through the volume studied. Particles were released on-shore, inside of the shore line; no particles were released below the sea. All parts of the model inside of the shore line were covered by release positions (at a depth of 420 m).

The exact locations of the start points were at the centres of the cells; hence in the central part of the model the distance between release points were 25 m. The total number of analysed flow paths, for each case studied, were approximately 28,000. The flow paths were analysed considering different parameters: length, breakthrough time, velocity, point of discharge etc. Different distributions were obtained for the parameters studied. For different cases studied, the properties of these distributions were compared.

9.1.4 Time dependency of flow paths

In the models, flow paths will develop (particles will move) inside a head field that controls the development of the paths. For a time-independent flow path, the path will develop inside a head field that will not change with time. Hence, the head field is constant during the movement of the simulated particle that produces the flow path. For a time-dependent flow path, the head field will change with time during the movement of the simulated particle that produces the flow path.

Theoretically, the actual movement of a particle should take place in a changing head field, because the head field will change while the particle moves through the rock mass. The GEOAN model can simulate both time-dependent and time-independent flow paths. In this study we have generated flow paths that are time-independent as well as time dependent. A time dependent flow path represent the flow field during a studied period. A time independent flow path represent the flow field for a studied moment in time.

9.1.5 Dispersion and retardation

In this study we have examined advective transport only, hence dispersion and retardation have not been included.

9.1.6 The not included heterogeneity of the local domain

Considering the results of the flow path analysis, the approach used for permeability of the domain studied, with a homogeneous rock mass between given fracture zones having different but homogeneous properties, will provide us with good estimates considering average representative results. However, the actual variation of results caused by the local heterogeneity of the rock mass and especially by the heterogeneity inside the fracture zones, is not included in this study. To calculate such a variation also the heterogeneity of the rock mass and the fracture zones need to be included and as such heterogeneity has not been included in this study no such variation is calculated.

9.1.7 Percentiles

The results of the flow path analyses are based on statistical analyses of the properties of each simulated flow path. The properties of the flow paths, e.g. length of paths, create different statistical distributions. The statistical distributions are characterised by percentiles. A percentile is defined as “a value below which a certain percentage of the observations fall”.

9.1.8 Separation of results from flow paths analyses into results for complete paths and results for surface near part of paths

We have analysed flow paths released at a depth of 420 m. We have studies different properties of the flow paths e.g. length and breakthrough time of the paths; and we have done that for the complete paths, but we have also done it for surface near parts of the paths studied. Primary we have studied the properties of the flow paths considering three different domains:

(i) The whole model, with rock mass, fracture zones and quaternary deposits. The derived results (distributions) represent the complete paths, from release positions to points of discharge.

(ii) The uppermost 1.5 m and the uppermost 3 m of the quaternary deposits. The derived results (distributions) represent the same flow paths (released at a depth of 420 m) as in (i), but the derived results (e.g. path length) consider the uppermost 1.5 m, or the uppermost 3 m, of the quaternary deposits, only.

(iii) The quaternary deposits below or outside of the lakes. The vertical extension of these domains corresponds to the vertical extension of the quaternary deposits (depth 3 m). The horizontal extension is given by the horizontal extension of the lakes. The derived results (distributions) represent the same flow paths (released at a depth of 420 m) as in (i), but the derived results (e.g. path length) consider quaternary deposits below or outside of lakes only, and no part of the rock mass.

The separation of the flow paths into complete paths and surface near parts of the paths is presented in Figure 9-1. We have studied the uppermost 1.5 m of quaternary deposits separately, because this zone is important considering biological activity (roots, unsaturated zone etc), and consequently for the interaction between the geosphere and the biosphere. We would like to stress that the results derived for the surface near part of the flow paths, considers flow paths from great depth only. If all the flow in the quaternary deposits had been studied, the results would have been different.

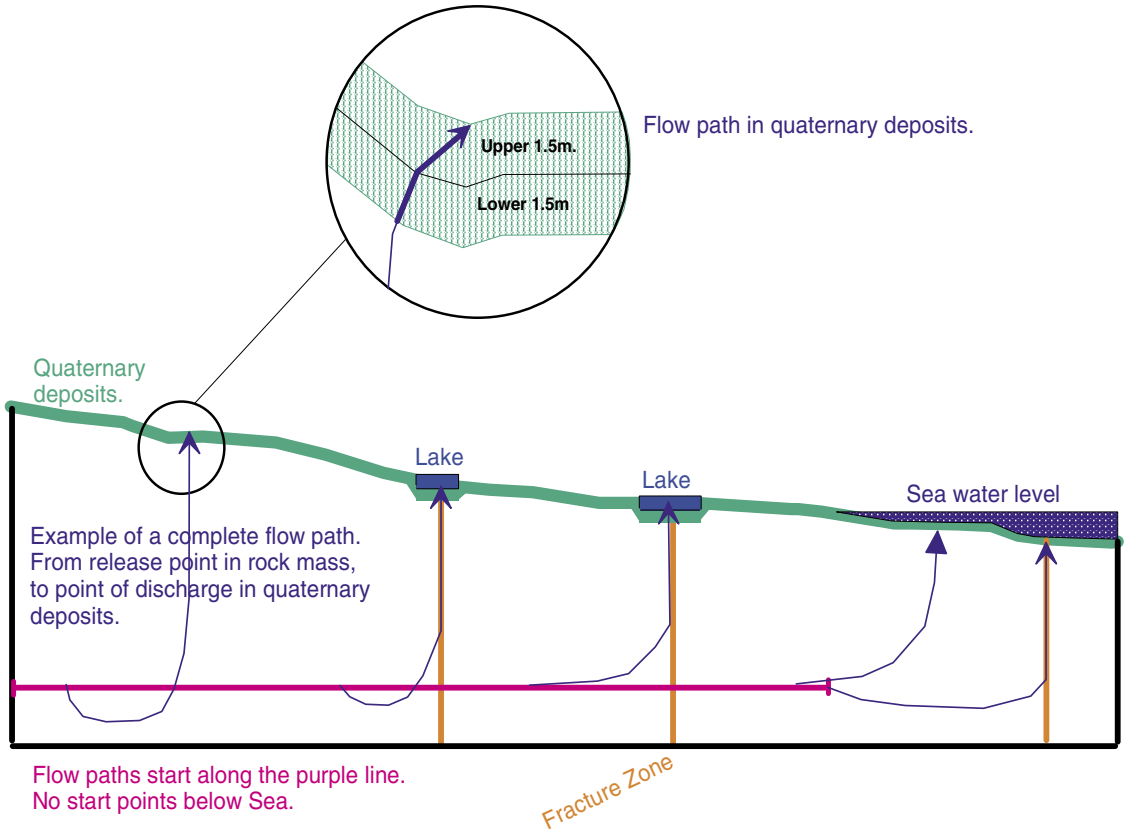

Figure 9-1. *The Principle of the separation of flow paths into complete paths and the surface-near parts of the paths.*

9.2 Steady state and time-independent flow paths

9.2.1 Methodology

The results presented below were derived by use of a steady state simulation. Results derived via a steady state solution do not represent any particular moment during a year, but is to be looked upon as an average representation of the actually varying situation. The flow paths were time independent; they represent the flow field for the studied average situation.

9.2.2 Visualisation of discharge areas and flow paths

The analysed discharge areas and flow paths are given in Figure 9-2, Figure 9-3, Figure 9-4 and Figure 9-5.

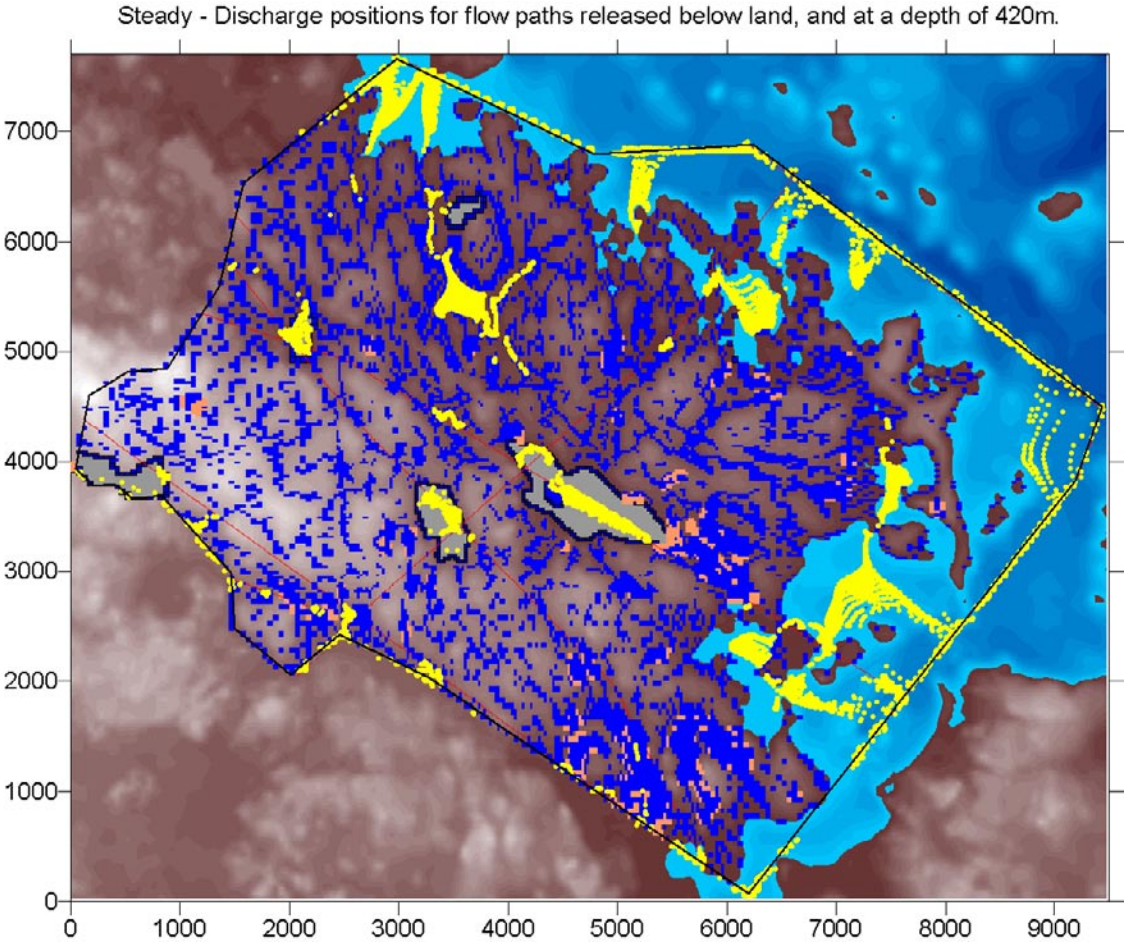

Figure 9-2. *Base case – Normal year – Steady State solution – Discharge areas. Yellow dots denote discharge areas for paths from a depth of 420 m (no release points below the sea). Blue squares denote all discharge areas above the sea, areas that are not defined as lakes.*

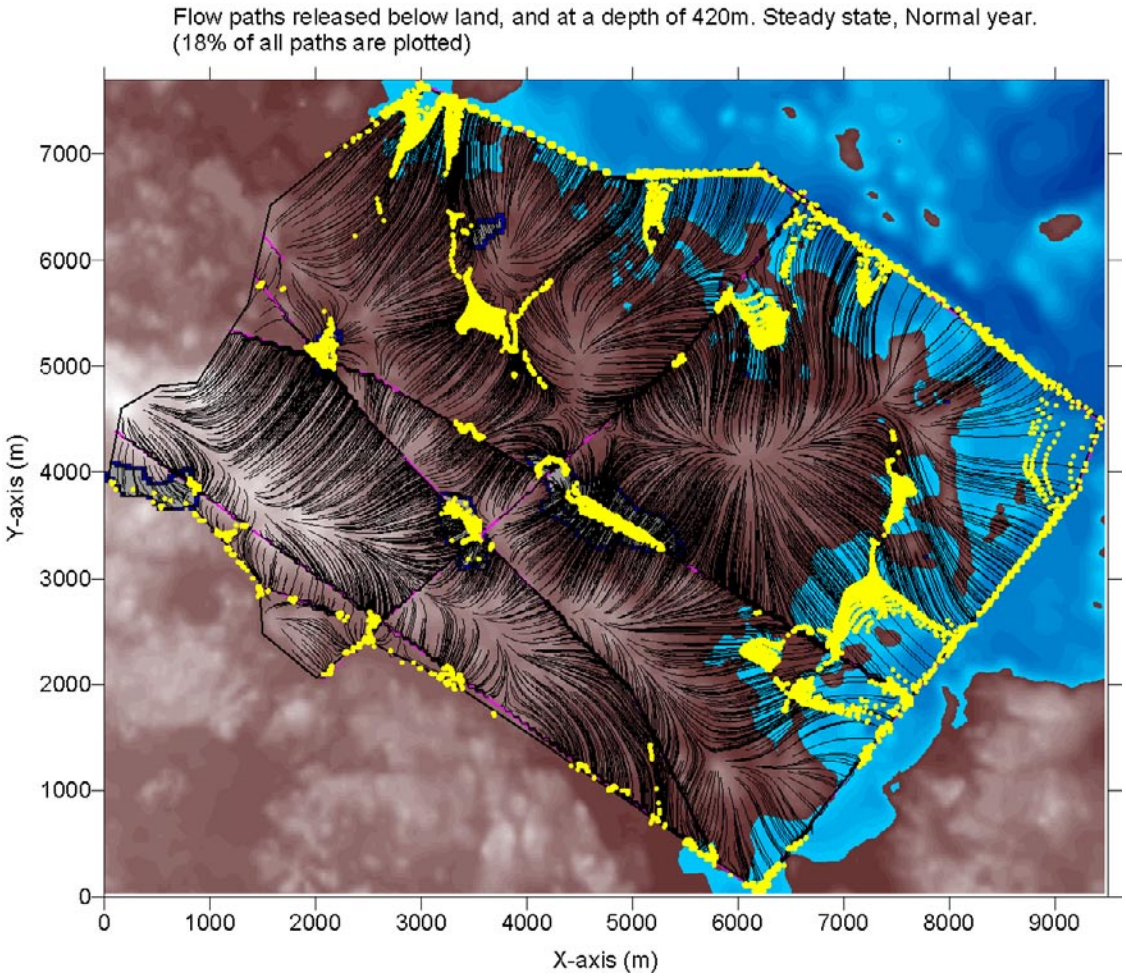

Figure 9-3. *Base case – Normal year – Steady State solution – Flow paths from a depth of 420 m (no release points below the sea). Only 18% of the analysed paths are plotted in the figure. Yellow dots denote discharge areas for all paths released at a depth of 420 m.*

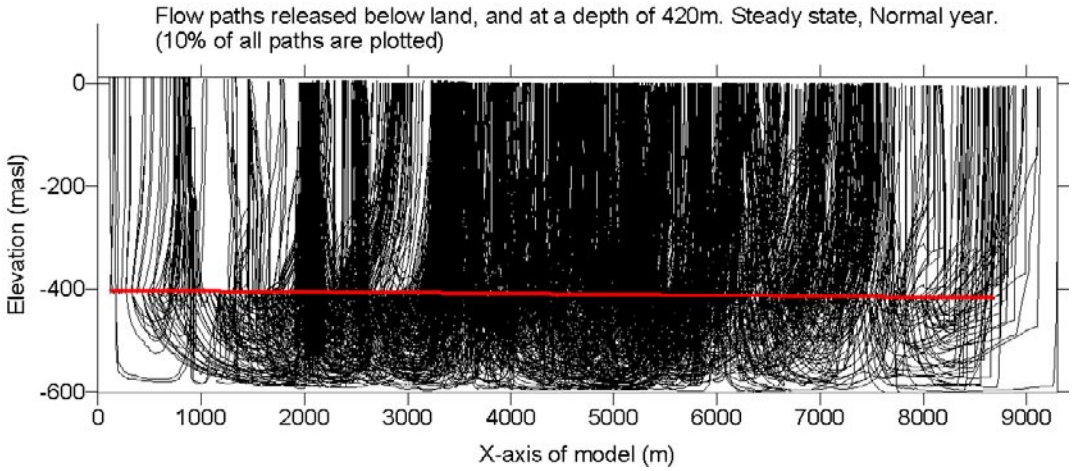

Figure 9-4. *Base case – Normal year – Steady State solution – Flow paths from a depth of 420 m (no release points below the sea). The figure presents a horizontal view through the model (a vertical cross-section along X-axis of model); only 10% of the analysed paths are plotted in the figure. The red line represents the approximate elevations of the start positions of the flow paths. Note that the vertical scale is 5 times larger than the horizontal scale.*

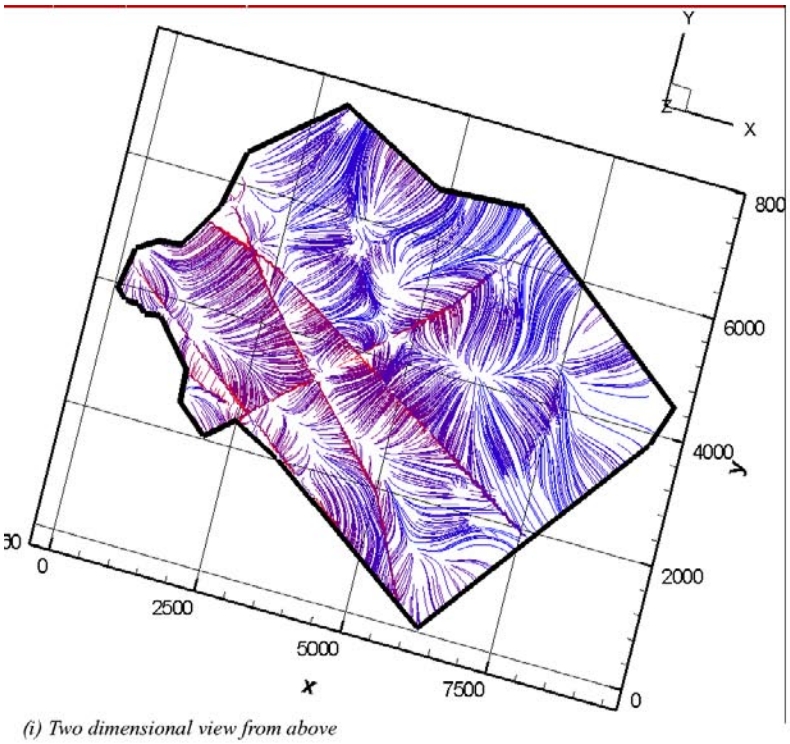

(i) Two dimensional view from above

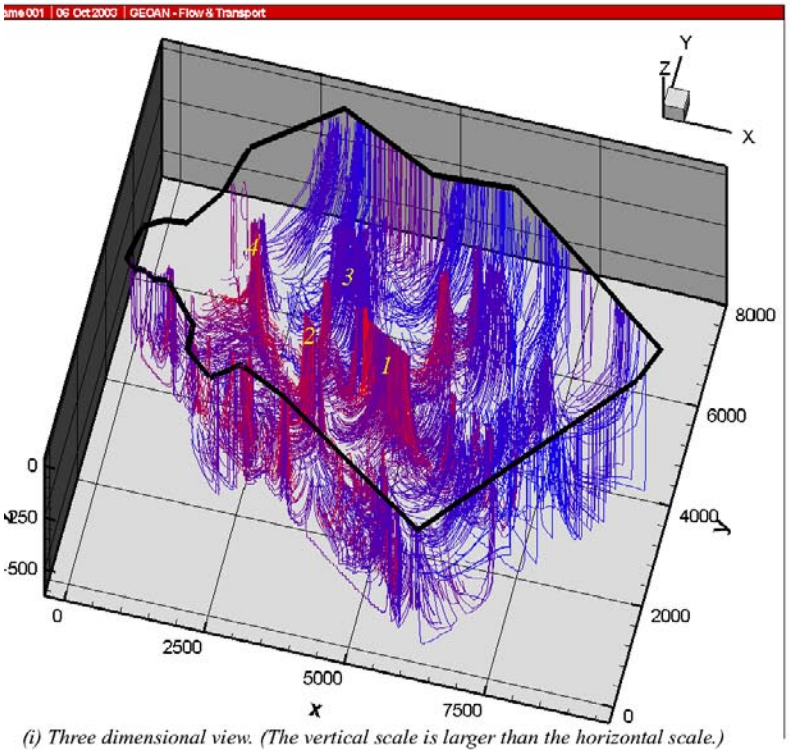

(i) Three dimensional view. (The vertical scale is larger than the horizontal scale.)

Figure 9-5. *Base case – Normal year – Steady State solution – Flow paths from a depth of 420 m (no release positions below the sea). Only 10% of the analysed paths are plotted in the figure. The colour scale corresponds to logarithm of the breakthrough time for complete paths. Red corresponds to shortest time and blue corresponds to the longest time. The yellow numbers denote the flow of deep groundwater to the four lakes: Fiskarfjärden (1) and Eckarfjärden (2) and Bolundsfjärden (3) and Gällsboträsket (4).*

9.2.3 Flow paths – distribution within different materials

Flow paths will be released at a depth of 420 m; these paths will develop within the model and will be distributed within the different materials of the model, dependent on start position and resistance to flow and gradients. The model demonstrates the following distribution for flow paths (from a depth of 420 m):

- 96% of all flow paths will flow through some part of the rock masses between the fracture zones.
- 82% of all flow paths will flow through some part of a fracture zones.
- 0.7% of all flow paths will pass through a surface clay layer. (No lakes).
- 20% of all flow paths will reach the quaternary deposits from rock masses between fracture zones.
- 80% of all flow paths will reach the quaternary deposits via fracture zones.

9.2.4 Flow paths – distribution and type of discharge areas

The distribution of discharge areas of the flow paths from great depth is not the same as the distribution of discharge areas for all flow paths, from all depths, as given in Figure 7-2. Flow paths from great depth will flow towards the strongest sinks of the flow system. The strongest sinks occur at areas with a small groundwater potential (groundwater head). Such areas are: (i) the sea floor, (ii) the lakes and (iii) other strong discharge areas (e.g. swamps, streams etc). The flow towards these strong sink will partly take place along fracture zones.

The spatial distribution of the discharge areas for flow paths from a depth of 420 m is given in Figure 9-2 and in Figure 9-5. The figure demonstrates that the discharge areas of the paths from a depth of 420 m are concentrated to a few different types of hydrogeological structures:

- 34% discharges below the sea, the discharge will take place along fracture zones, or if no fracture zones occur in the local area, along the deepest parts of the sea floor.
- 66% discharges above the sea. Nearly all of the flow paths (with very few exceptions) discharges into the lakes (including Bolundsfjärden as one of the lakes), and in the lakes the discharge areas are often concentrated to where a fracture zones intersect a lake.

We may conclude as follows: Flow paths released on-shore (no paths released below the sea) and at repository depth (i.e. 420 m) will either discharge into the sea (i.e. 34%) or above the sea (i.e. 66%). Considering the discharge areas above the sea, nearly all of the flow paths from repository depth will discharge into lakes, and especially where a fracture zones intersects a lake. This conclusion is well illustrated in Figure 9-3 and Figure 9-5.

Figure 9-5 also demonstrates that there is a tendency that large values of the breakthrough times take place for flow paths (simulated particles) that discharge below the sea. These flow paths tend to have start positions not far from the shoreline and at some distance from fracture zones. Flow paths having start positions close to fracture zones tend to produce the shortest breakthrough times, as these paths follow the fracture zones to the ground surface. Lakes located above fracture zones are discharge areas for flow paths with short breakthrough times.

9.2.5 Flow paths – Amount of discharge into lakes

There are some lakes within the studied area, e.g. Fiskarfjärden, Eckarfjärden, Bolundsfjärden, Gällsboträsket, and the location of these lakes are given in Figure 4-2, Figure 7-2 and in Figure 9-2, etc. Considering the Base case and all flow paths from repository depth (420 m):

- About 20% of the paths studied discharges in the Lake Fiskarfjärden.
- About 10–30% of the paths studied discharges in the Lake Bolundsfjärden. (Results for Bolundsfjärden depend on its definition as sea, lake or swamp).
- About 3% of the paths studied discharges in the Lake Eckarfjärden.
- About 6% of the paths studied discharges in the Lake Gällboträsket.
- About 5% of the paths studied discharges in the Lake Bruksdammen.

Considering all flow paths 34% discharges into the sea, more (ca 60%) if Bolundsfjärden is defined as part of the sea.

The lake Gällboträsket is a strong sink for groundwater from great depth, even though it is a very small lake. The lake is a strong sink because in the established models two fracture zones intersect below the lake, and much groundwater from great depth will follow the fracture zones to the small lake.

As previously stated, groundwater from great depth flows towards the strongest sinks, and the deeper the release points, the more the flow will be concentrated to a few strong discharge areas. This is demonstrated in Figure 9-6. Consider the amount of flow paths that will discharge into the sea and into the lake Fiskarfjärden (while keeping in mind that no paths are released below the sea), 35% of all paths, released at a depth of 420 m,

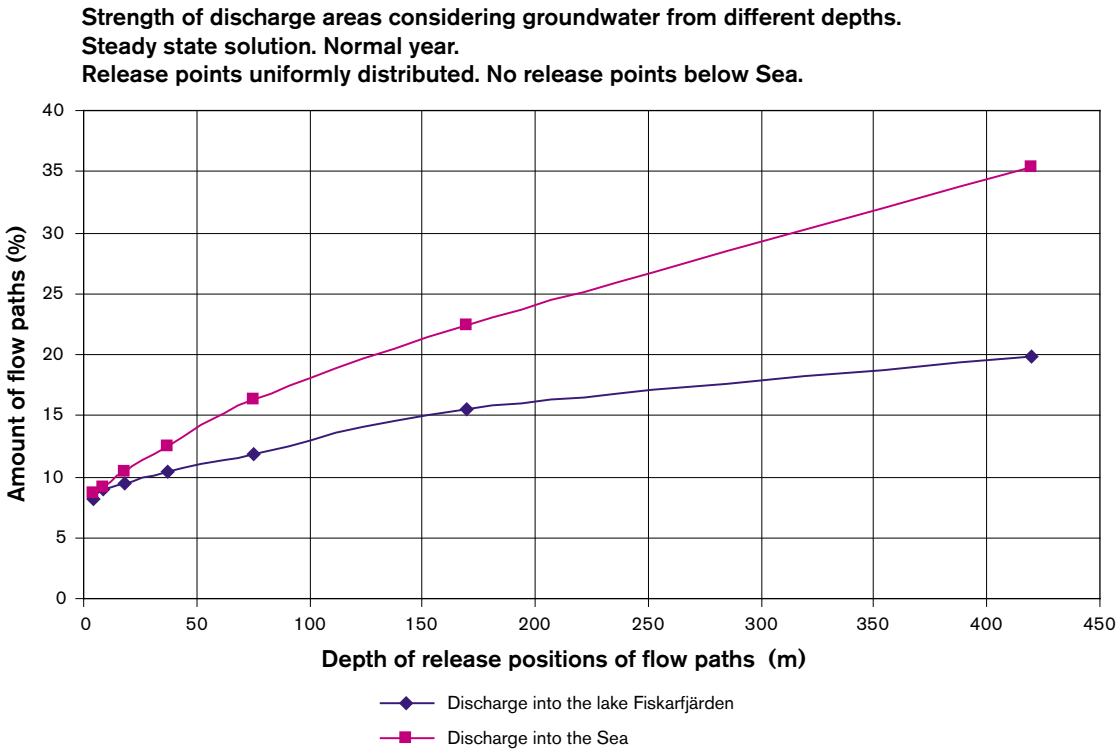

Figure 9-6. *Strength of discharge areas considering groundwater from different depths. Steady state solution. Normal year. Release points uniformly distributed. No release points below the sea.*

will discharge into the sea; but if the paths are released at a depth of 50 m, only 14% will discharge into the sea; 20% of all paths released at s depth of 420 m will discharge into the lake Fiskarfjärden; but if the paths are released at a depth of 50 m, only 11% will discharge into the lake.

9.2.6 Flow paths – Discharge via lake sediments or via lake perimeter

Considering discharge areas above the sea, the results of our modelling demonstrate that nearly all of the groundwater from repository depth that discharge above the sea will discharge into a lake.

The lakes of our models are defined according to Figure 6-1. The contact between the lake and the groundwater system is defined as follows.

Along the lake perimeter, the groundwater system is in direct contact with the lake via a highly permeable material (a wave eroded material). The lake perimeter is defined with the specified head boundary condition, and the specified head corresponds to the surface water level of the lake.

Along the base of the lake, the contact between the groundwater system and the lake takes place through a material having a low permeability; this material represents sediments at the base of the lake. The groundwater system below the lake (and inside of the lake perimeter) is partly confined by the lake sediments, but some groundwater flow may take place across the sediments and the magnitude of this flow depends primarily on the permeability of the lake sediments. Inside of the lake perimeter, the boundary condition is the specified head boundary condition (as along the perimeter), and the specified head corresponds to the surface water level of the lake.

In our model there are three different flow routes of water into a lake (i) as a surface flow directly into the lake, (ii) as a groundwater flow via the lake perimeter, or (iii) as a groundwater flow via sediments at the base of the lake (lake-floor sediments).

We have estimated the percentage of the groundwater flow paths (released at a depth of 420 m) that uses the two different groundwater flow routes. It is important to note the difference between the percentage of all released flow paths, and the percentage of all paths that reaches a lake studied. For example, study the lake Fiskarfjärden, for the Base case 20% of all the released flow paths will discharge in this lake. The balance of the number of groundwater flow paths at each flow rout is: 59% via lake bottom sediments and 41% via the lake perimeter.

If the lake sediments are impermeable 100% of the groundwater flow will discharge at the lake perimeter. For situations with more permeable sediments, more and more of the groundwater will use the flow route via the sediments. The amount of flow that will discharge via sediments at the base of the lake depends on the flow-resistance of the sediments. The flow-resistance is defined as: a resistance to groundwater flow, in analogy with the resistance to flow of electricity; the resistance is equal to length divided by conductivity: $R = t/K$. The resistance is denoted as R (dimension: time) the thickness of the studied sediments is denoted as t (dimension: length) and K is the conductivity (dimension: length/time). The resistance is calculated along the flow-direction, and as the lake sediments are low permeable, the flow-direction is vertical through the sediments. Hence, the concept of resistance includes both the thickness of the sediments and the permeability of the sediments.

The actual resistance of the sediments of the lakes studied are not known in detail. The thickness of the sediments may vary a lot, and it is not unlikely that a layer of sediments will demonstrate a thickness of several metres along the lake-floor. The conductivity of the sediment is probably very low – in line with that of clay or perhaps smaller. For the Base case, the resistance of the lake sediments are set to 1E+10 s, which for example corresponds to 1 m of a material with a conductivity equal to 1E–10 m/s; or 5 m of a material with a conductivity equal to 5E–10 m/s.

We have established a number of sensitivity cases for the purpose of investigating the importance of the flow-resistance of the sediments. The only difference between the sensitivity cases and the Base case is the value of resistance at the base of the lakes. In the sensitivity cases, the resistance were varied between 1E+8 s and 1E+13 s.

The results of the sensitivity analysis are given below in Figure 9-7 and in Figure 9-8.

Considering lake Fiskarfjärden and the Base case (Figure 9-7), the balance of the number of flow paths at each flow rout is: 59% of the flow paths discharges via lake bottom sediments and 41% via the lake perimeter. Reducing the sediments resistance (e.g. by increasing the permeability) by two orders of magnitude will produce the following balance: 80% of the flow paths discharges via lake bottom sediments and 20% via the lake perimeter. Increasing the sediments resistance (e.g. by reducing the permeability) by two orders of magnitude will

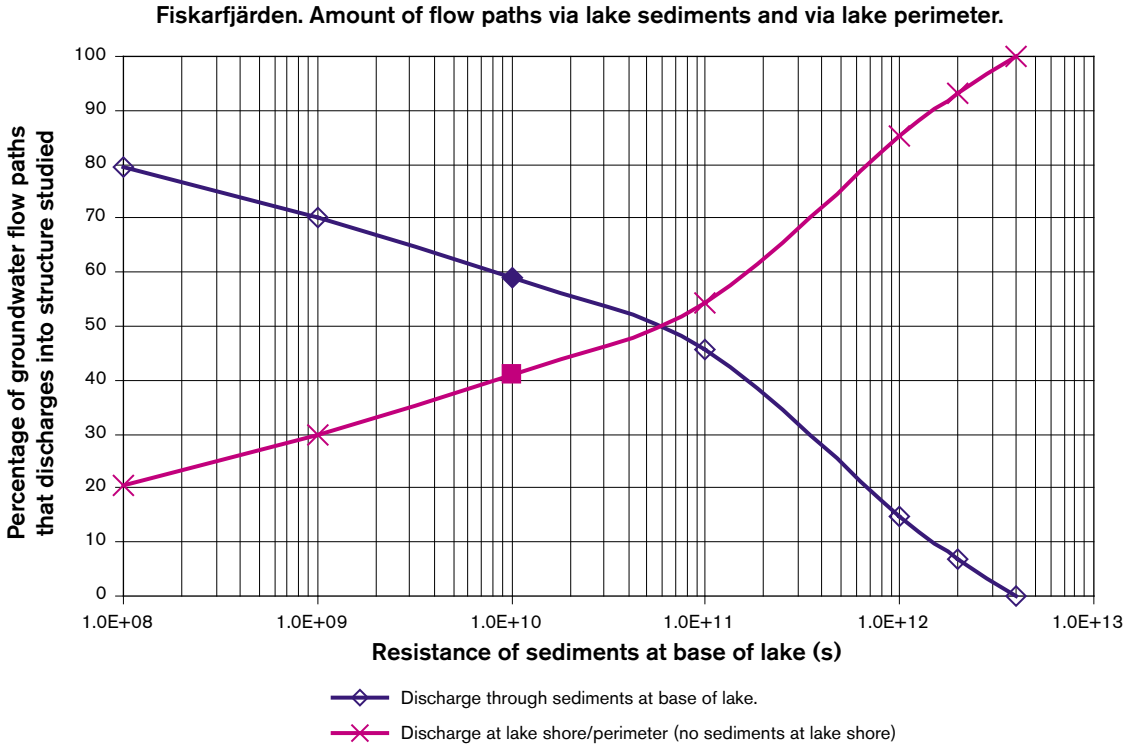

Figure 9-7. *Lake Fiskarfjärden, Balance of flow paths, considering amount of flow paths that discharges via lake sediments or via lake perimeter, for different values of flow-resistance of the sediments at the base of the lake. Start positions of flow paths are uniformly distributed at a depth of 420 m (flow varies between paths), no release positions below the sea. Steady state solution, normal year.*

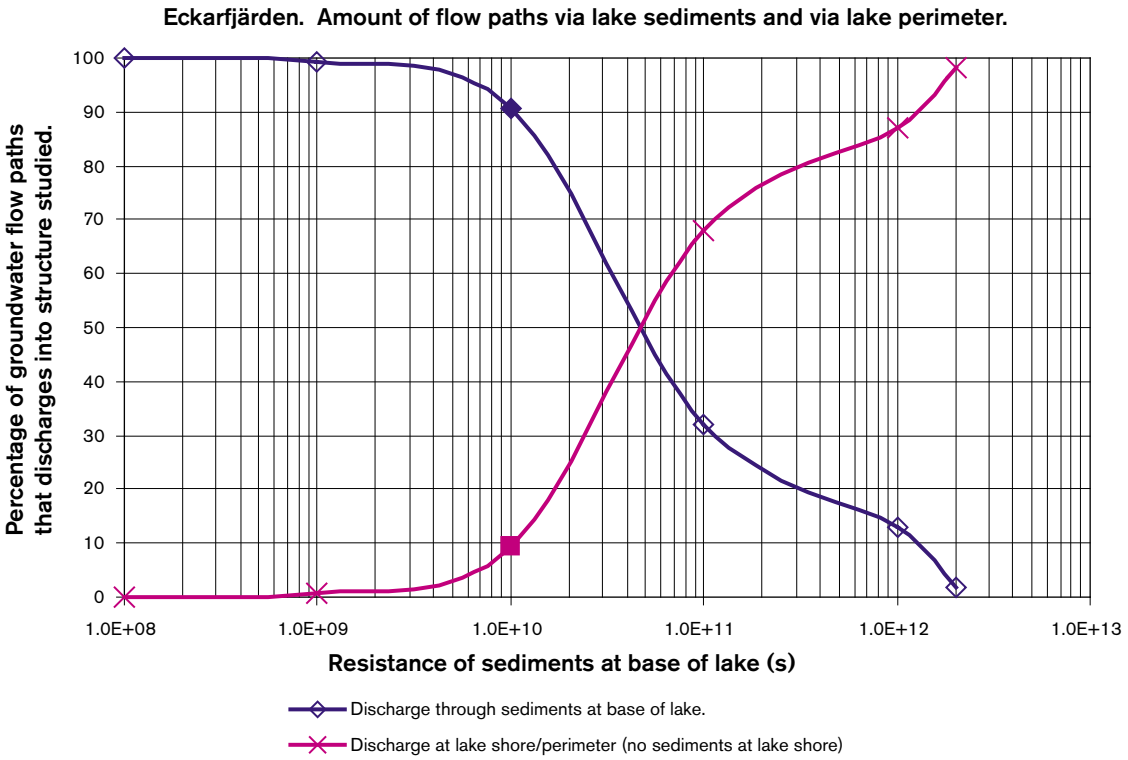

Figure 9-8. *Lake Eckarfjärden, Balance of flow paths, considering amount of flow paths that discharges via lake sediments or via lake perimeter, for different values of flow-resistance of the sediments at the base of the lake. Start positions of flow paths are uniformly distributed at a depth of 420 m (flow varies between paths), no release positions below the sea. Steady state solution, normal year.*

produce the following balance: 15% of the flow paths discharges via lake bottom sediments and 85% via the lake perimeter. Applying a sediment resistance equal to 4E+12 s will produce the following balance: < 1% of the flow paths discharges via lake bottom sediments and > 99% via the lake perimeter.

Considering lake Eckarfjärden and the Base case (Figure 9-8), the balance of the number of flow paths at each flow rout is: 90% of the flow paths discharges via lake bottom sediments and 10% via the lake perimeter. Reducing the sediments resistance (e.g. by increasing the permeability) by one order of magnitude will produce the following balance: > 99% of the flow paths discharges via lake bottom sediments and < 1% via the lake perimeter. Increasing the sediments resistance (e.g. by reducing the permeability) by two orders of magnitude will produce the following balance: 13% of the flow paths discharges via lake bottom sediments and 87% via the lake perimeter. Applying a sediment resistance equal to 2E+12 s will produce the following balance: < 1% of the flow paths discharges via lake bottom sediments and > 99% via the lake perimeter.

A comparison of the flow balance of Fiskarfjärden (Figure 9-7) and Eckarfjärden (Figure 9-8) demonstrates that the flow route via the lake perimeter/shoreline is more important in lake Fiskarfjärden than in lake Eckarfjärden. This may follow from the island that occurs in Fiskarfjärden. The island will provide lake Fiskarfjärden with some extra distance of lake perimeter and shoreline, which also happens to be above a fracture zone.

The results of these calculations demonstrate that the balance of the number of flow paths at each flow rout depends strongly on the resistance. Considering a lake with a thick layer of low permeable sediments at the base of the lake (a large resistance), for such a situation nearly all flow paths discharges at the lake perimeter. And for a situation with a lake having sediments of small resistance, most flow paths discharges at the base of the lake via the lake sediments.

It should be noted that the above-presented calculations did not include the process of diffusion; the only transport process studied was that of advection. For a dissolved pollutant, diffusion through the sediments may be an important process. One should also remember that the flow paths do not represent a given flow, the flow paths were released in a regular pattern, not dependent on flow. Hence, the balance of number of flow paths given above is not the same thing as a flow balance.

9.2.7 Flow paths – Length

The lengths of the flow paths (released at depth of 420 m) have been analysed. The lengths will of course vary; therefore the results are given as probability distributions. The results are summarised in Table 9-1 below.

Considering the complete paths (see Figure 9-9), there are flow paths that flows more or less straight upward from the start point to the discharge point, such paths are released in fracture zones, the lengths of these paths is close to the depth of the start point, it follows that 5% of the paths are shorter than 490 m. There are also paths that take a much more complicated route to the point of discharge, through rock mass, fracture zones and quaternary deposits; such a path may have a large length and 5% of the paths are longer than 2 km. The median length of the flow paths is 920 m.

Table 9-1. Distribution of lengths of flow paths. Start positions at a depth of 420 m, results for paths that terminate above sea. Normal year. Steady state solution. (Base case).

Steady state paths	Flow path lengths (metres) Percentiles						
Studied distribution [1]	1th	5th	10th	50th	90th	95th	99th
Complete paths	451	490	534	924	1,717	2,028	2,668
Paths in uppermost 1.5 m [2]	1.9	2.9	3.9	11.5	34.5	43.0	64.1
Paths in uppermost 3 m [3]	3.4	4.5	5.6	13.2	38.4	47.4	74.9
Paths in uppermost 3 m And below lakes [4]	3.5	4.8	6.2	18.4	45.1	54.2	83.2
Paths in uppermost 3 m And outside of lakes [5]	3.4	4.2	5.1	11.3	26.8	35.9	57.0

[1] Start positions at a depth of 420 m, results for paths that terminate above sea. Steady state solution. Normal year.
[2] Length of paths in the uppermost 1.5 m of quaternary deposits.
[3] Length of paths in the quaternary deposits, i.e. in the uppermost 3 m of model.
[4] Length of paths in the quaternary deposits, but only lengths below lakes.
[5] Length of paths in the quaternary deposits, but only lengths outside of the lakes.

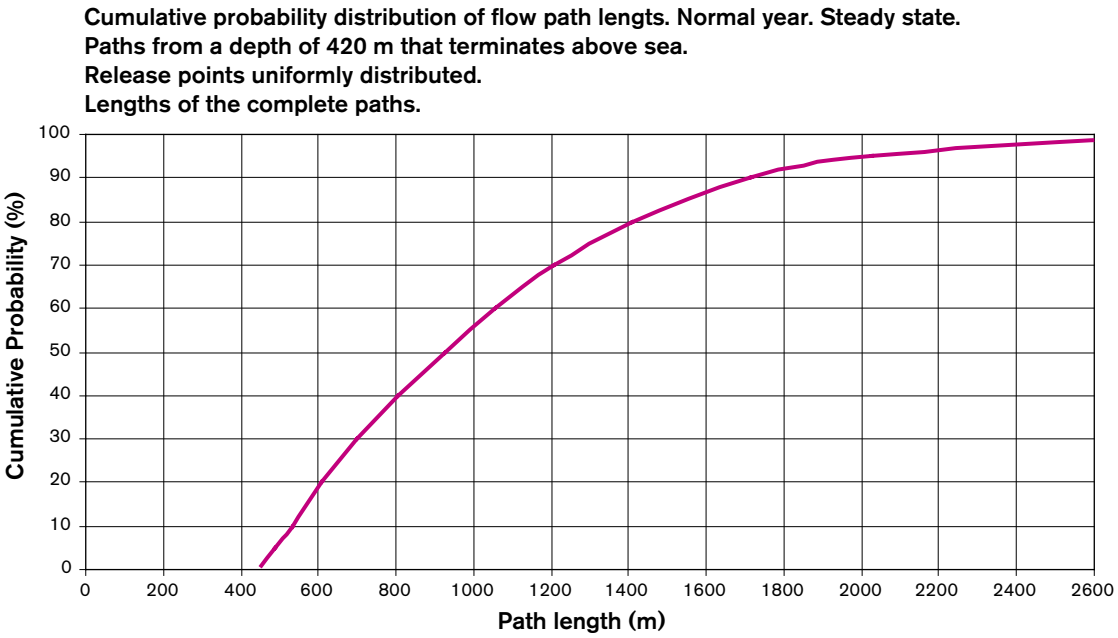

Figure 9-9. *Distribution of lengths of flow paths, length of complete paths. Start positions at a depth of 420 m, results for paths that terminate above sea. Normal year. Steady state solution.*

The uppermost 3 m of the model are defined as quaternary deposits. Lengths of flow paths in the quaternary deposits are calculated for the uppermost 1.5 m as well as for the whole thickness of quaternary deposits (uppermost 3 m of model) see Figure 9-10 below.

Considering the lengths of flow paths in the uppermost 1.5 m of the quaternary deposits, most simulated paths have a length between 2 m (1st percentile) to 64 m (99th percentile); the median is 11 m. Considering the total lengths of flow paths in the quaternary deposits (uppermost 3 m of model), most simulated paths have a length between 3.5 m (1st percentile) to 75 m (99th percentile); the median is 18 m. These results indicate that flow paths from great depth tend to flow through the quaternary deposits by use of rather short flow routs.

Only a small percentage (< 5%) of the flow paths demonstrate path lengths in the surface near material (in the uppermost 1.5 m of quaternary deposits) that is longer than 43 m. This is in line with the results presented in Figure 9-2 (the figure presents discharge areas for flow paths from great depth) as most flow paths from great depth flows towards lakes and other strong sinks, and reaches these areas from below, and hence the surface near part of the flow paths will be short. This is also well demonstrated in Figure 9-3 and in Figure 9-5.

We have calculated lengths of paths (released at great depth) in the quaternary deposits considering: (i) total lengths, (ii) lengths below lakes and (iii) lengths outside of lakes. For the Base case the results are given above in Figure 9-11. As can be seen in the figure the lengths below the lakes are larger than the lengths outside of the lakes, the lengths below the lakes are however very much dependent on the resistance of the lake sediments.

As most flow paths from great depth discharges at lakes, the distribution of flow path lengths in the quaternary deposits depend on the properties of the lakes. Everything else being equal, path lengths in quaternary deposits depend on resistance of lake sediments. A certain amount of long flow paths may take place below a lake, assuming that the lake carries a continuous layer of low permeable sediments along the base of the lake, because the simulated particles tend to flow towards the lake perimeter where no sediment occur.

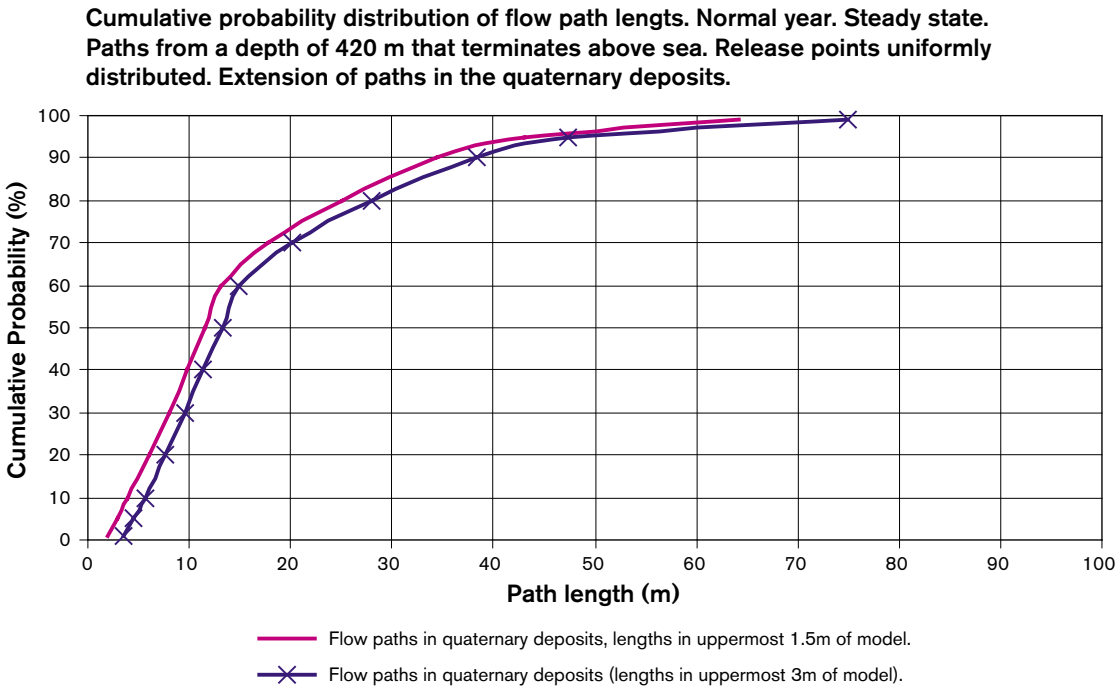

Figure 9-10. *Distribution of lengths of flow paths, length of paths in the uppermost 1.5 m of the quaternary deposits. Start positions at a depth of 420 m, results for paths that terminate above sea. Normal year. Steady state solution.*

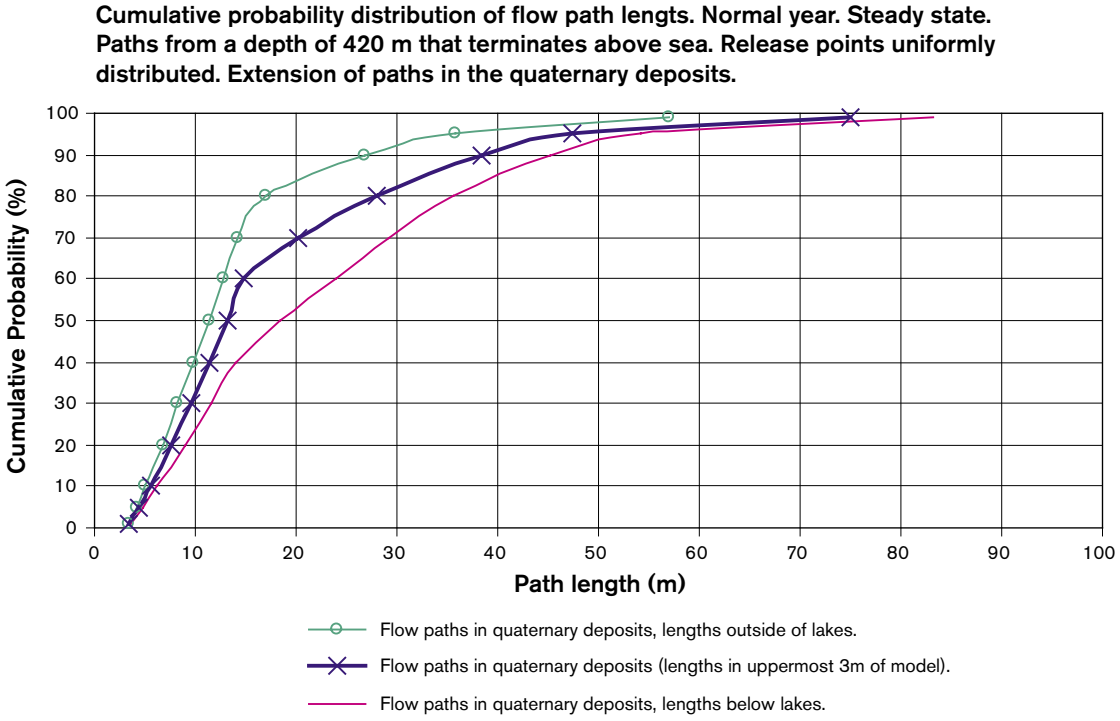

Figure 9-11. *Distribution of lengths of flow paths, length of paths in the quaternary deposit – lengths below lakes and lengths outside of lakes. Start positions at a depth of 420 m, results for paths that terminate above sea. Normal year. Steady state solution.*

If no lake sediments occur, no long flow paths will develop below a lake. This is well demonstrated in Figure 9-12, below. The figure presents lengths (percentiles) of flow paths in quaternary deposits, as a function of resistance of sediments at base of lakes (all lakes have been assigned the same resistance). For situations with resistances larger than ca 1.0E+10 s, the lengths of the longest paths increases dramatically, until a resistance of 1.0E+12 s is reached. At such a large resistance nearly all flow paths discharges along the lake perimeter (compare with Figure 9-7 and Figure 9-8) and the path length distribution will not change much, even if the resistance of lake sediments increases further.

In the quaternary deposits, long flow paths may take place below lakes, especially for a situation in which the resistance of the lake sediment is large; but the lengths of the flow paths (in the quaternary deposits) outside of the lakes are not much influenced by the resistance of the lake sediments. This is well demonstrated by Figure 9-13. For different values of resistance of lake sediments, the figure presents path length distributions considering: (i) the quaternary deposits outside of the lakes, as well as (ii) the quaternary deposits below the lakes. It is demonstrated by the figure that path length distribution, considering lengths outside of the lakes, is approximately the same for all the different studied values of sediment resistance; and that the increase in total path lengths, which comes with increasing values of sediment resistance, takes place below the lakes.

The complete lengths of the flow paths from great depth are not very dependent on the properties of the lake sediments, because in comparison to the total length of the flow paths from the release positions (at a depth of 420 m), the lengths inside the quaternary deposits is not significantly large. This is well demonstrated in Figure 9-14.

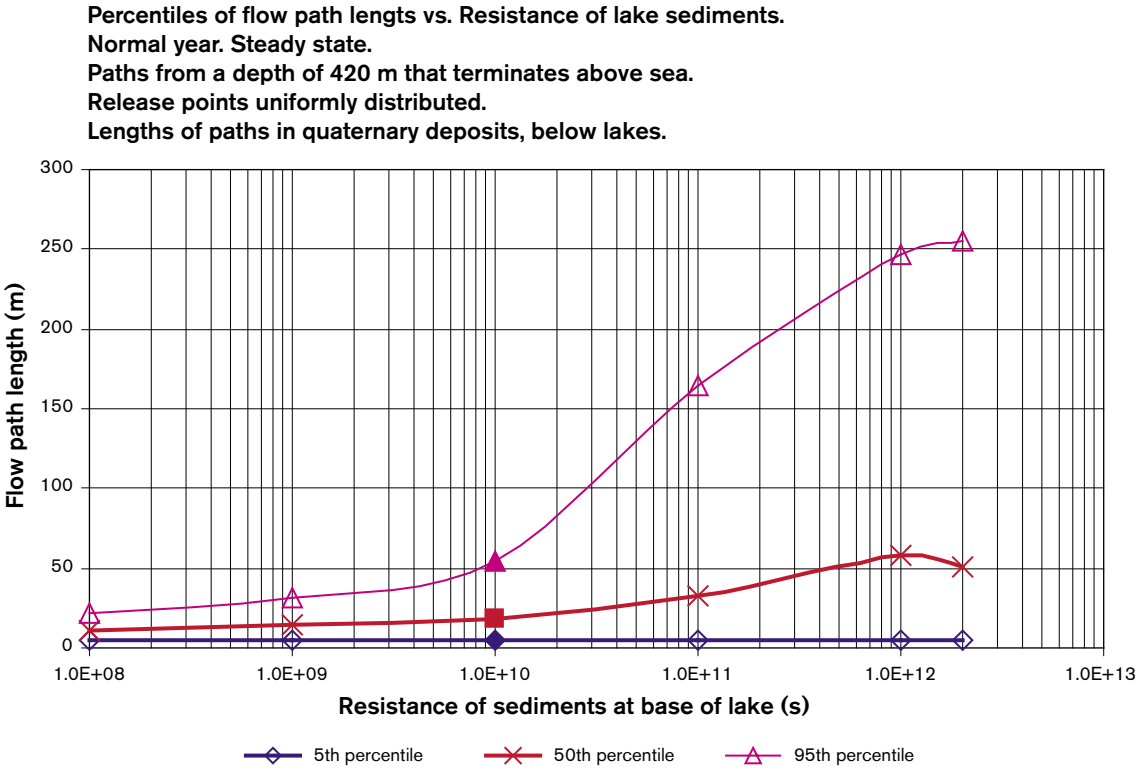

Figure 9-12. *Distribution of lengths of flow paths in quaternary deposits, as a function of resistance at base of lakes. Start positions at a depth of 420 m, results for paths that terminate above sea. Normal year. Steady state solution.*

(i)

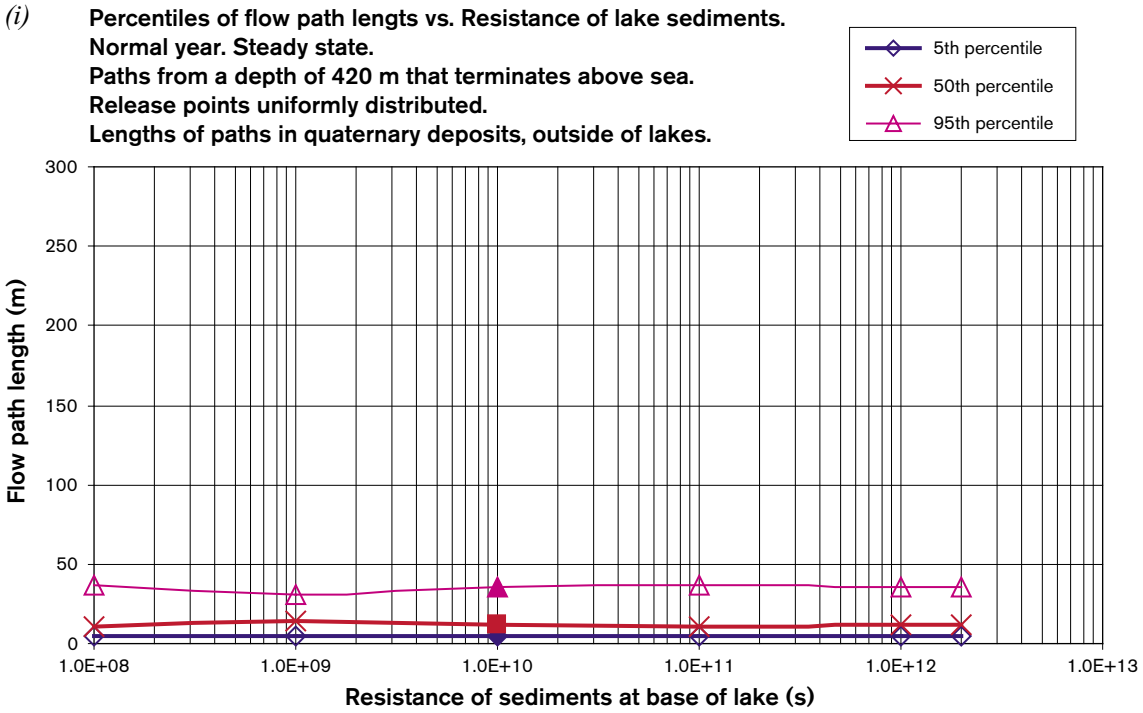

(ii)

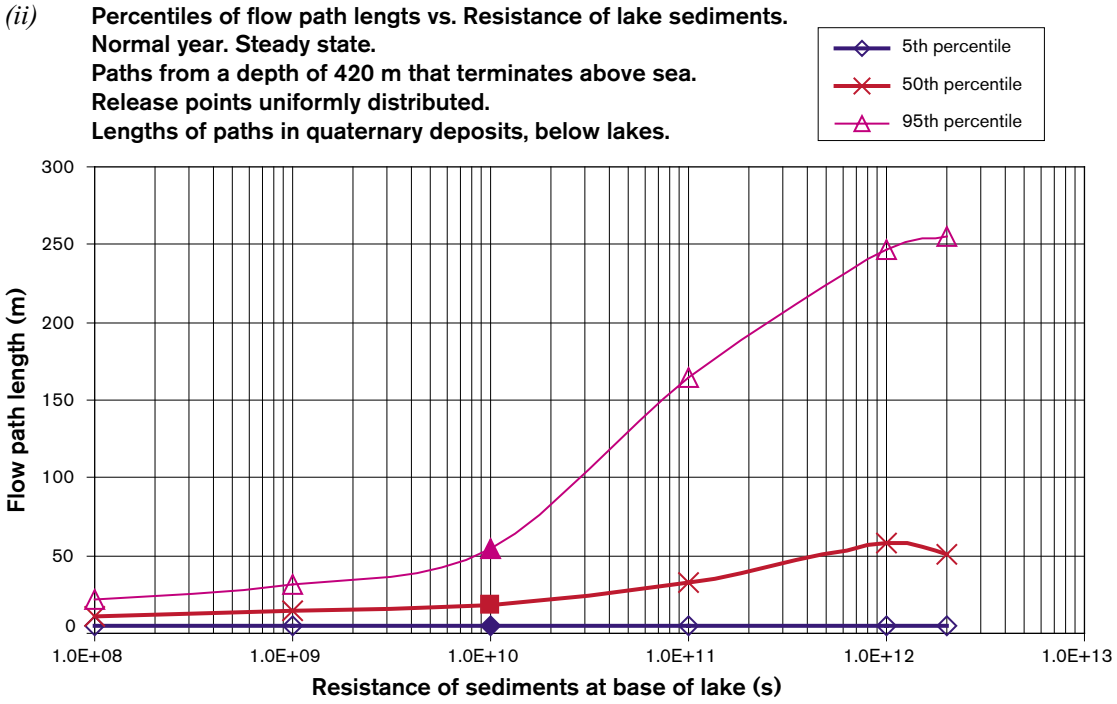

Figure 9-13. *Distribution of lengths of flow paths in quaternary deposits, as a function of resistance at base of lakes. Figure (i) presents lengths of paths in quaternary deposits, lengths outside of lakes. Figure (ii) presents lengths of paths in quaternary deposits, lengths below lakes. Start positions at a depth of 420 m, results for paths that terminate above sea. Normal year. Steady state solution.*

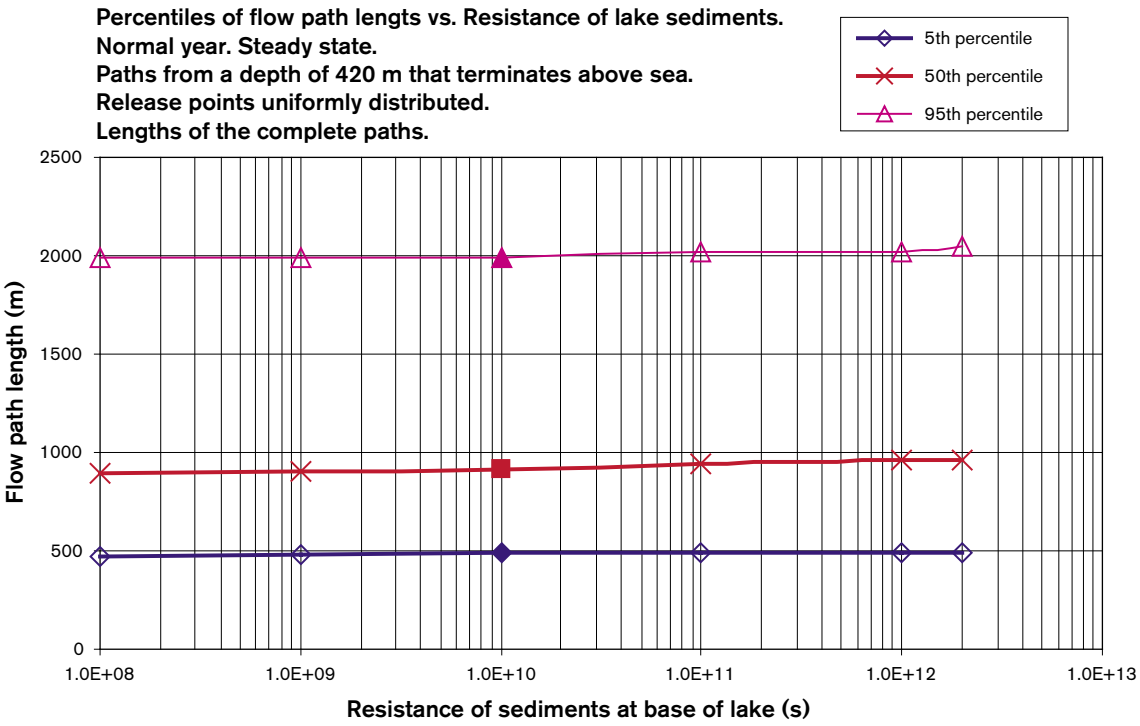

Figure 9-14. *Distribution of lengths of complete flow paths (from release position to discharge position), as a function of resistance at base of lakes. Start positions at a depth of 420 m, results for paths that terminate above sea. Normal year. Steady state solution.*

9.2.8 Flow paths – Breakthrough time

The breakthrough times of the flow paths (released at depth of 420 m) have also been analysed. The times vary; therefore the results are given as probability distributions. As for the previously presented results (path lengths), we have studied the results (time) for:

(i) The complete paths, with rock mass, fracture zones and quaternary deposits. These distributions represent the breakthrough time, from release positions to points of discharge.

(ii) Extension of flow paths in quaternary deposits. These distributions represent the same flow paths (released at a depth of 420 m) as in (i), but the results given are time spent within the uppermost 1.5 m, or uppermost 3 m of the quaternary deposits.

(iv) Extension of flow paths in the quaternary deposits below or outside of the lakes. The vertical extension of these domains corresponds to the vertical extension of the quaternary deposits (depth 3 m). The horizontal extension is given by the horizontal extension of the lakes. The derived results (distributions) represent the same flow paths (released at a depth of 420 m) as in (i), but the derived results are time spent in the quaternary deposits below or outside of the lakes.

Because of the uncertainty in the properties of the lake sediments, we have not included time spent in lake sediments in the calculation of breakthrough time. The results are summarized in Table 9-2, as well as in Figure 9-15 and in Figure 9-16 below.

Considering the complete paths, there are flow paths that flows more or less straight upward, in a fracture zone, from the start point to the discharge point; such paths will produce short breakthrough times – the 1st percentile is equal to 16 years. There are also

paths that spend a very long time in the flow media, often by use of a long flow route between fracture zones, and for such paths the breakthrough times are large – the 99th percentile is equal to 6,000 years. The median is 680 years.

Table 9-2. Distribution of breakthrough time of flow paths. Start positions at a depth of 420 m, results for paths that terminate above sea. Normal year. Steady state solution. (Base case).

Steady state paths	Flow path breakthrough time (years) Percentiles						
Studied distribution [1]	1st	5th	10th	50th	90th	95th	99th
Time spent in model, considering complete paths	15.7	52.9	107	680	2,750	3,680	6,040
Time spent in uppermost 1.5 [2]	0.1	0.4	0.9	4.5	161	245	376
Time spent in uppermost 3 m [3]	0.2	0.9	2.0	12.5	359	621	867
Time spent in uppermost 3 m And below lakes [4]	0.8	0.9	2.0	66.0	225	317	983
Time spent in uppermost 3 m And outside of lakes [5]	0.2	0.3	2.0	5.2	508	685	818

Note! Time spent in lake sediments is not included in the analyses.

[1] Start positions at a depth of 420 m, results for paths that terminate above sea. Steady state solution. Normal year.
[2] Time spent in the uppermost 1.5 m of quaternary deposits.
[3] Time spent in quaternary deposits, i.e. in the uppermost 3 m of model.
[4] Time spent in quaternary deposits, but considering only time below lakes.
[5] Time spent in quaternary deposits, but considering only time outside of the lakes.

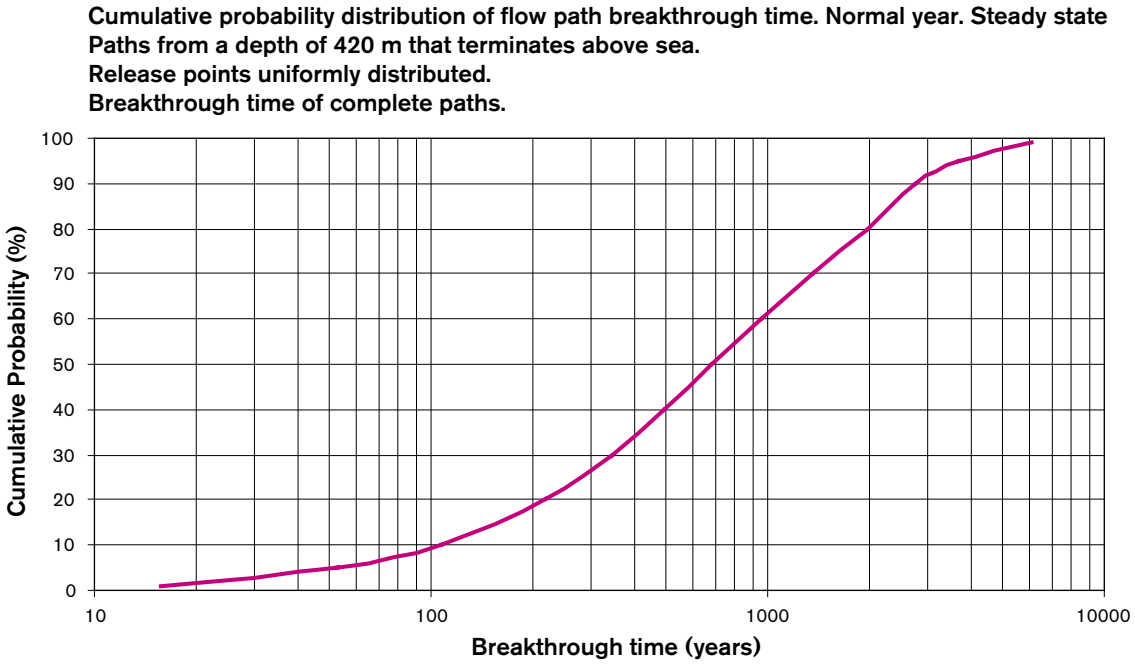

Figure 9-15. *Distribution of breakthrough times of complete flow paths. Start positions at a depth of 420 m, results for paths that terminate above sea. Normal year. Steady state solution.*

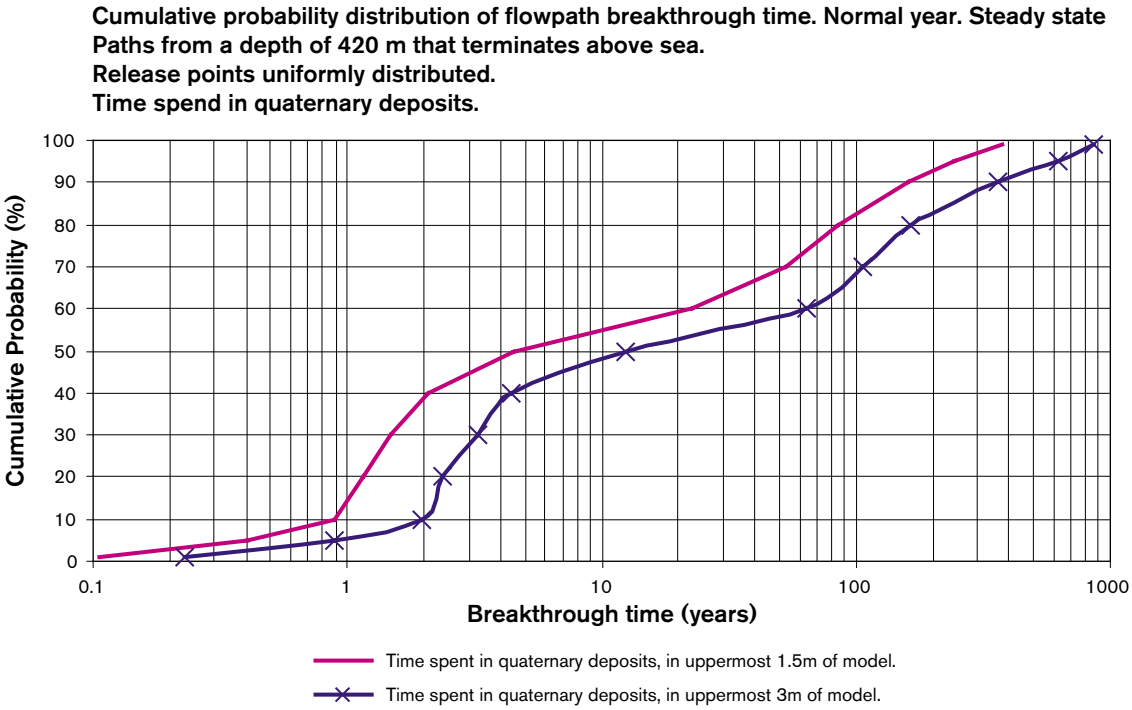

Figure 9-16. *Distribution of flow time of flow paths, time spent in the uppermost 1.5 m of the quaternary deposits. Start positions at a depth of 420 m, results for paths that terminate above sea. Normal year. Steady state solution.*

Considering the flow in the quaternary deposits (vertical extension 3 m), some flow paths spend only a few months in this zone – the 5th percentile is equal to 0.9 years, the median is however 12.5 years, and some flow paths stay in the quaternary deposits for hundreds of years, flowing slowly under the lakes – the 99th percentile is equal to 867 years. For the uppermost 1.5 of quaternary deposits we get the following results: the 10th percentile is equal to 0.9 years, the median is 4.5 years, and the 99th percentile is equal to 376 years.

Regarding the flow in the quaternary deposits, but only the flow below lakes, we note that the time spent below lakes can be considerable: the 10th percentile is equal to 2 years, the median is 66 years, and the 99th percentile is equal to 983 years. (Time spent in lake sediments is not included.)

Regarding the flow in the quaternary deposits, but only the flow outside of the lakes, we get the following results: the 10th percentile is equal to 0.2 years, the median is 5.2 years, and the 99th percentile is equal to 818 years. It is likely that large values of time, demonstrated by the 99th percentile, reflect a flow in quaternary deposits below clay layers (but outside of lakes).

When studying the results given above, the following should be kept in mind:

- The transport process of diffusion was not included in these simulations.
- The calculated breakthrough times are directly proportional to the effective porosity, and the value of the effective porosity is uncertain.
- Time spent in lake sediments is not included in these analyses.

9.2.9 Comparison of breakthrough time, advective velocity and path lengths, in different domains along the flow paths

By studying the advective movement of the virtual particles (flow paths) through the model, and by comparing length of paths, velocities and times spent in different domains along the flow paths, we are able to derive some general conclusions regarding the advective flow from great depth to the discharge areas at ground surface.

We have analysed the movement of the particles (development of flow paths) for three different domains of the model: (i) the rock mass between fracture zones, (ii) the fracture zones and (iii) the quaternary deposits. For the three different domains the following properties of the flow paths have been analysed: (i) the velocity, (ii) the length and (iii) the time spent in the different domains.

The lengths of the flow paths within the rock mass, the fracture zones and the quaternary deposits, are given in Figure 9-17. It is demonstrated by the figure that the longest flow path lengths are within the fracture zones. In the rock mass between fracture zones, the flow path lengths are shorter. The median flow path length, in the rock mass between the fracture zones, is 441 m; and the median flow path length in the fracture zones is 537 m. The path lengths are the shortest in the quaternary deposits; the median is only 13 m.

The advective velocities in the rock mass, the fracture zones and the quaternary deposits are very different, which is illustrated in Figure 9-18. The velocities in the fracture zones are between 40 and 50 times faster than in the rock mass between the zones. It should however be noted that the effective porosity assigned to the fracture zones is probably

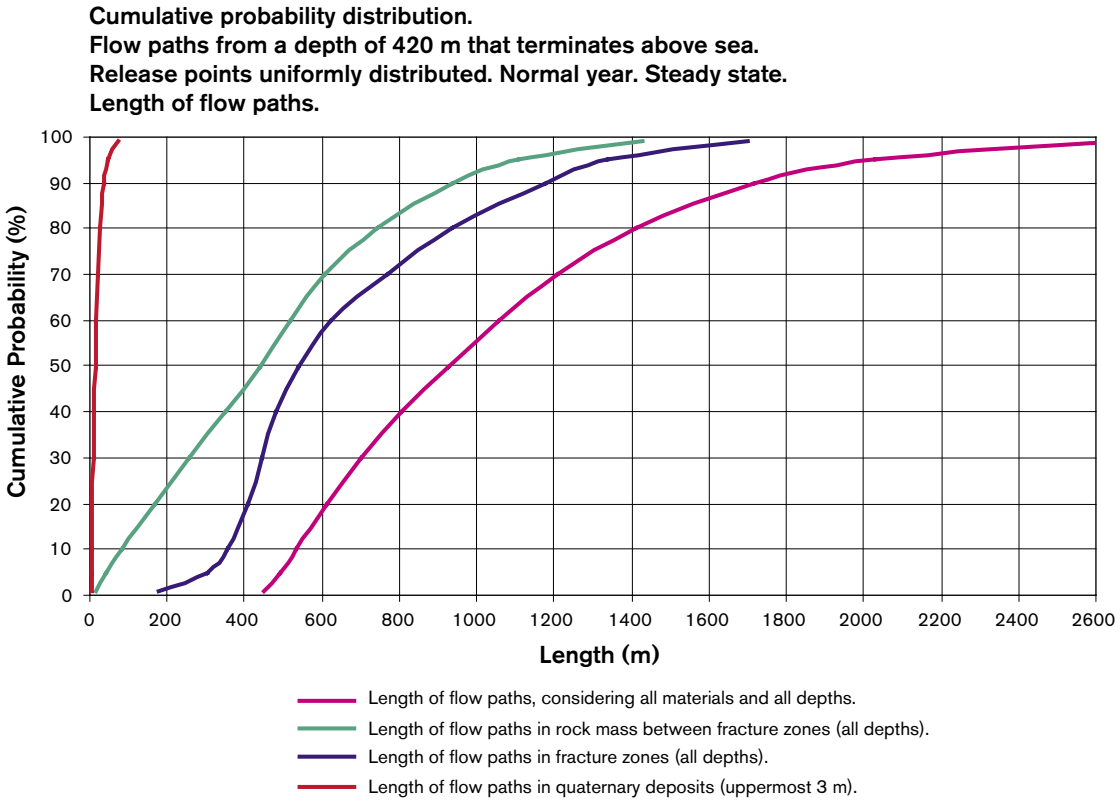

Figure 9-17. *Length of flow paths in different domains. Start positions at a depth of 420 m. Uniform distribution of release positions. Results for flow paths that terminate above sea. Normal year. Steady state solution.*

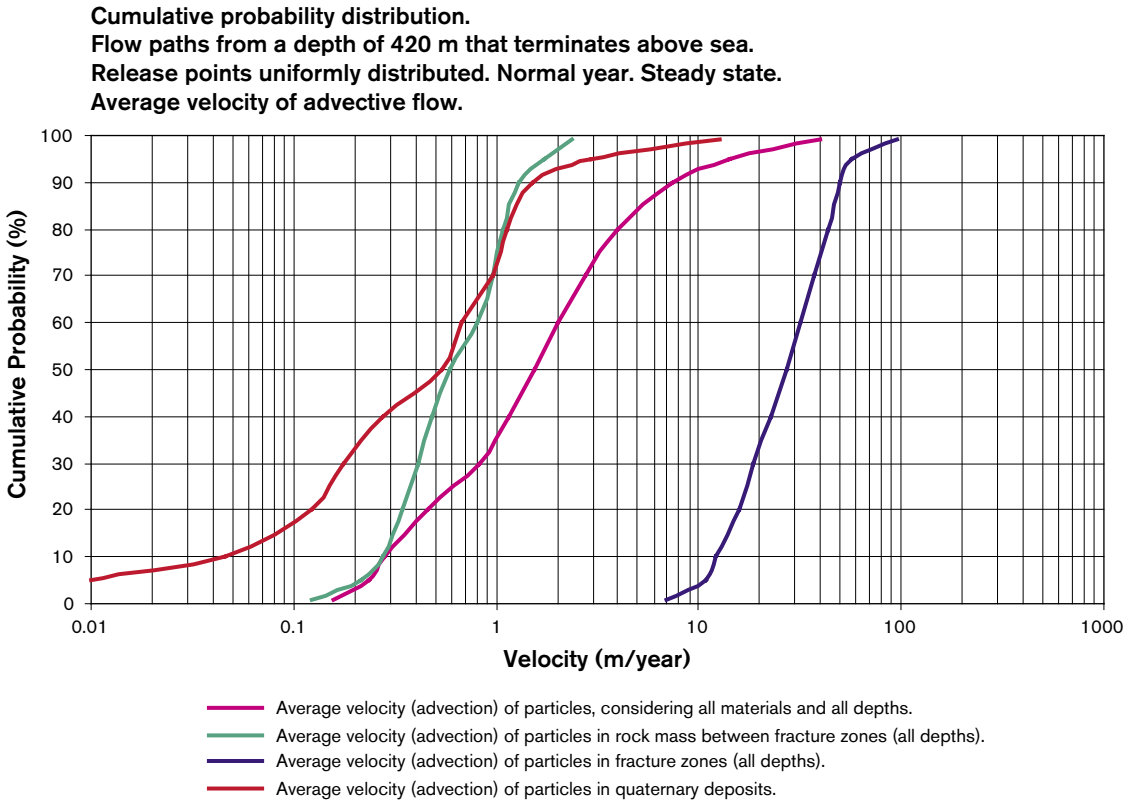

Figure 9-18. *Average advective velocity of virtual particles (flow paths) in different domains. Start positions at a depth of 420 m. Uniform distribution of release positions. Results for flow paths that terminate above sea. Normal year. Steady state solution.*

on the small side of a likely range of values, which will result in high velocities in the zones. The velocities in the quaternary deposits are in general low; this follows from either the relatively large porosity (moraine, gravel etc), or from the small conductivity (clay), or from a combination of these properties. The lowest velocities of all the different domains studied are within the clay (and perhaps within the lake sediments) of the quaternary deposits. There is however also flow paths within the quaternary deposits that are faster than those of the rock mass between fracture zones (about 8% of the flow paths of the quaternary deposits are faster than those of the rock mass). It should also be mentioned that the average velocity of the lower moraine of the quaternary deposits is much smaller than the velocity of the fracture zones. Hence the advective flow velocity of the groundwater is dramatically reduced when the groundwater leaves the fracture zones and enters the quaternary deposits.

The advective breakthrough time is the quota between length and velocity. It follows that even if the velocities are low in the quaternary deposits, the quaternary deposits are not very important for the total breakthrough times of the complete paths, as the flow length in the quaternary deposits are very short. In a similar way the fracture zones are not very important for the total breakthrough times of the complete paths, as the velocity in the fracture zones are so high.

These conclusions are well demonstrated by Figure 9-19, which presents the time spent in different domains, and the total breakthrough time of the complete flow paths. For most, the total break through times depends very strongly on the time spent in the rock mass between fracture zones; in comparison, the time spent in fracture zones and in the

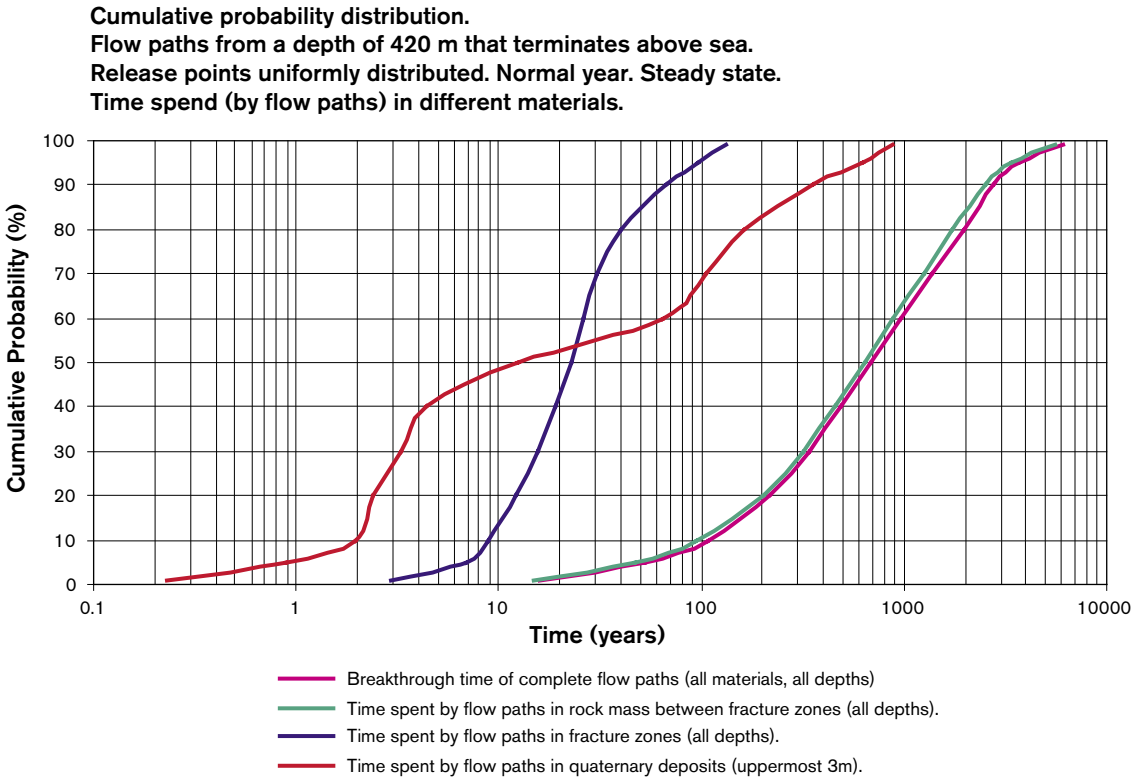

Figure 9-19. *Time spent by flow paths in different domains, and total breakthrough time. Start positions at a depth of 420 m. Uniform distribution of release positions. Results for flow paths that terminate above sea. Normal year. Steady state solution.*

quaternary deposits is not very important. (This conclusion is based on two of the curves in Figure 9-19: the curve representing: (i) time spent in rock mass between fracture zones, and the curve representing (ii) breakthrough time of complete paths; as these two curves are very similar it is demonstrated that it is the time spent in rock mass that is the most important contributor to the total breakthrough time.)

It should be noted that the conclusions corresponds to flow paths released at a depth of 420 m; and that the time spent in lake sediments are not included in these analyses. All calculations were carried out for a normal year and a steady state solution. Flow paths were released in a uniform pattern and only flow paths that discharged above the sea were included in the analyses.

9.2.10 Flow paths – Results for a model without quaternary deposits

We have established models without any quaternary deposits. The quaternary deposits were changed into rock mass and fracture zones, hence the rock mass and the zones were extended all the way up to the ground surface. These models have been established for the purpose of comparisons to the Base case, and they are identical to the Base case, except for the conductivity of the uppermost layers and the boundary conditions of the uppermost layers.

9.2.10.1 Flow paths – distribution within different materials

Considering flow paths from a depth of 420 m, the models studied without quaternary deposits produce about the same distribution of flow paths within different materials (except the quaternary deposits) as a model with quaternary deposits. The results given in Section 9.2.3 are also applicable to a model without quaternary deposits.

- With quaternary deposits:
  - 96% of all flow paths will flow through rock masses, between fracture zones.
  - 75% of all flow paths will flow through some part of the fracture zones.
- Without quaternary deposits:
  - 96% of all flow paths will flow through rock masses, between fracture zones.
  - 77% of all flow paths will flow through some part of the fracture zones.

9.2.10.2 Flow paths – distribution and type of discharge areas

The distribution of discharge areas of the flow paths from great depth is not the same as the distribution of discharge areas for all flow paths. Flow paths from great depth will flow towards the strongest sinks of the flow system. The spatial distribution of the discharge areas for flow paths from a depth of 420 m is nearly identical when comparing the models with and without quaternary deposits. The results given in Section 9.2.4 are also applicable to the model without quaternary deposits.

- With and without quaternary deposits, considering flow paths from a depth of 420 m:
  - 34% discharges below the sea, the discharge will take place along fracture zones, or if no fracture zones occur in the local area, along the deepest parts of the sea floor.
  - 66% discharges above the sea. Nearly all of the flow paths (with very few exceptions) discharges into the lakes (including Bolundsfjärden as one of the lakes), and in the lakes the discharge areas are often concentrated to where a fracture zones intersect a lake.

9.2.10.3 Flow paths – Length

The length-distribution of flow paths, from a depth of 420 m, produced by a model without quaternary deposits is very much the same as the length-distribution produced by a model with quaternary deposits (considering complete paths). The difference is that for the model without quaternary deposits, the short paths are somewhat shorter and the long paths are somewhat longer (compared to those of a model with quaternary deposits); the differences are however less than 6%. The median length without quaternary deposits is 4% longer than the median with quaternary deposits.

9.2.10.4 Flow paths – Breakthrough time

The breakthrough time-distribution of flow paths, from a depth of 420 m, produced by a model without quaternary deposits is rather similar to the breakthrough time-distribution produced by a model with quaternary deposits (considering complete paths). The difference is that for the model without quaternary deposits, the breakthrough times are shorter.

The largest differences, in percent, take place for the shortest breakthrough times. The main reason for the differences is that in a model without quaternary deposits, the fracture zones extends all the way up to the surface, and the zone will be fast routes to the discharge areas. In the model with quaternary deposits, the fracture zones will not extend up to the ground

surface, and in addition the quaternary deposits will contain a layer of "lower moraine" (see Table 6-1), and this layer will delay the flow in the zones and increase the breakthrough times. Considering the 5th percentile, the difference is 16%, for the median the difference is 7%, and for the 95th percentile the difference is 2%

9.2.11 Flow paths – Type of discharge areas considering a steady state situation, with a potential recharge according to a dry-year

The results presented below were derived by use of a steady state solution. The potential recharge in the model was set to that of a dry-year, equal to 61 mm/year. This is much smaller than the potential recharge of a normal year (i.e. 239 mm/year). The studied case is not a realistic case, because by modelling steady state conditions we model an average situation assuming that the average recharge is that of a dry-year (and not that of a normal year). Hence, the studied case will produce lower groundwater levels than the case representing a normal year, but also lower levels than a transient case representing a dry-year that follows after a normal year. The flow paths will develop inside a head field that will not change with time. The produced flow paths are time independent. The presented case, which combines a steady state solution and a the potential recharge of a dry-year, was introduced for the purpose of comparing the discharge areas produced by this case to the discharge areas produced by the normal year. We are especially interested in comparing the discharge areas for flow paths released at a depth of 420 m.

The calculated discharge areas are given in Figure 9-21 below. Considering a steady state solution and a dry-year, flow paths from a depth of 420 m will discharge at the same discharge areas as the steady state paths of the normal year. This is demonstrated by comparing Figure 9-21 (dry-year) and Figure 9-2 (normal-year). Hence, the discharge areas for flow paths from great depth are very stable and will not change much, even if the groundwater situation in the quaternary deposits changes a dramatically.

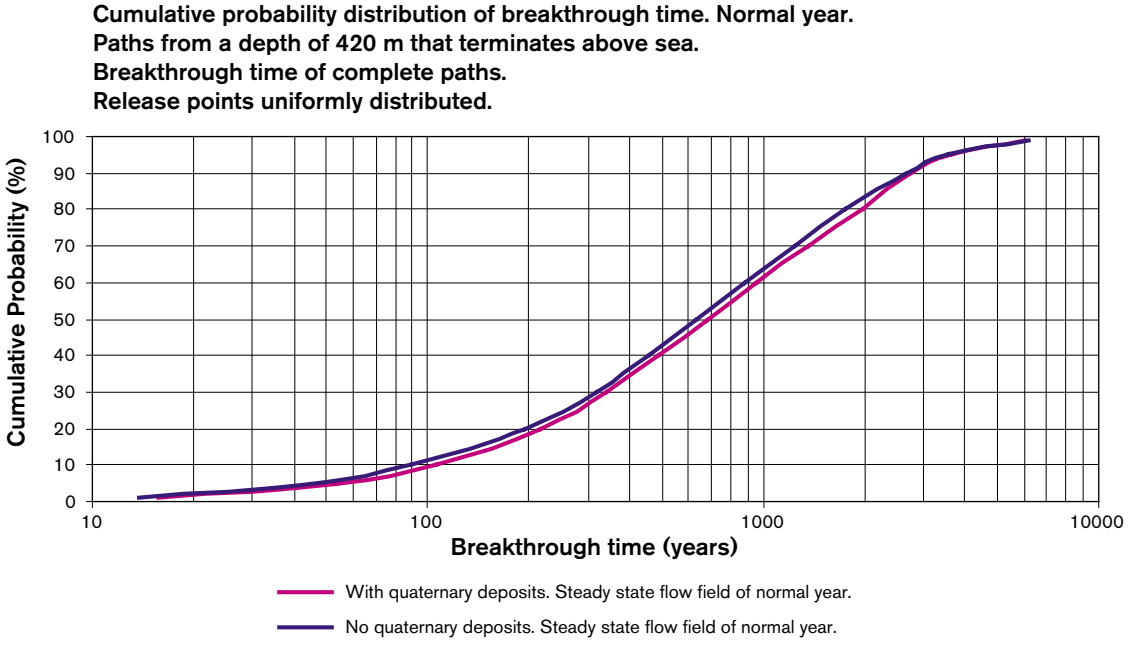

Figure 9-20. *Comparison of models with and without quaternary deposits. Distribution of breakthrough times of complete flow paths. Start positions at a depth of 420 m, results for paths that terminate above sea. Normal year. Steady state solution.*

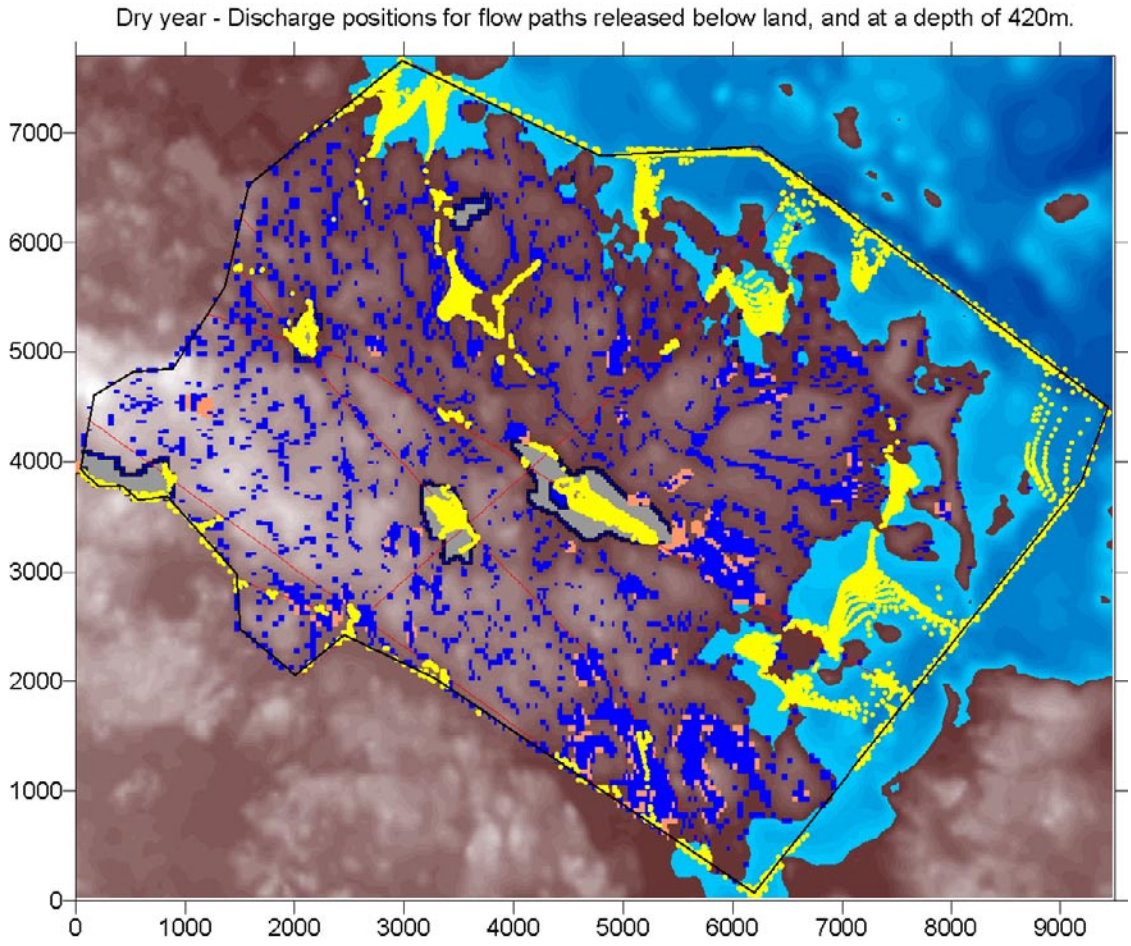

Figure 9-21. *Base case – Dry-year – Steady State solution – Discharge areas. Yellow dots denote discharge areas for paths from a depth of 420 m (no release points below the sea). Blue squares denote all discharge areas above the sea, areas that are not defined as lakes.*

9.3 Transient simulations with time dependent flow paths

9.3.1 Methodology

The results presented below were derived by use of transient simulations and time dependent flow paths. The simulated situation represents the changing flow conditions during a normal year.

Simulated virtual particles produce advective flow paths that will develop inside a changing flow field, and the particles may stay in the studied flow domain during a simulated period of many years; it follows that the simulated normal year is repeated many times as the studied flow path develops in the model.

From a numerical viewpoint the calculations are somewhat more complicated than for the steady state flow paths. For the transient paths the particles develop within 12 different flow fields, each flow field represents a single month of the normal year. Each particle is studied separately.

- At time equal to zero the particle is released at a depth of 420 m.
- The particle will start to move by use of the first flow field (January).

- The particle is allowed to move for one month in the first flow field.
- After one month of movement in the first flow field, the flow field is changed to that of the second month.
- After two months of movement, the flow field is changed to that of the third month. In this way the flow field changes with time, until 12 months is reached.
- After 12 months of movement, the flow field is again changed to the first month, and the procedure continuous until the particle discharges at ground surface.

Hence, the results of this section represents time dependent flow paths that develop inside a transient flow field, representing the different flow conditions during the different months of a series of normal years. We will call this type of flow paths for transient flow paths.

9.3.2 Transient flow paths – distribution within different materials

Transient flow paths will be released at a depth of 420 m; these paths will develop within the model and will be distributed within the different materials of the model, dependent on start position and resistance to flow and gradients. The results for the transient paths were the same as for the steady state paths, see Section 9.2.3.

9.3.3 Transient flow paths – distribution and type of discharge areas

Considering transient flow paths from a depth of 420 m, Figure 9-22 presents the discharge areas for the transient flow paths during the month of March (for which the unsaturated zone is the largest) and for April (for which the unsaturated zone is the smallest). Transient flow paths from great depth will discharge at the same discharge areas as the steady state paths. This is demonstrated by comparing Figure 9-22 (transient paths) and Figure 9-2 (steady state paths).

9.3.4 Transient flow paths – Length

The lengths of the transient flow paths (released at depth of 420 m) have been analysed. The length-distribution of the transient paths is very much the same as the length-distribution of the steady state paths. The results are given in Table 9-3.

Table 9-3. Distribution of lengths of flow paths. Start positions at a depth of 420 m, results for paths that terminate above sea. Normal year. Time dependent paths in a transient flow field.

Transient paths	Flow path lengths (metres) Percentiles						
Studied distribution [1]	1th	5th	10th	50th	90th	95th	99th
Complete paths	450	489	533	927	1,723	2,033	2,668
Paths in uppermost 1.5 [2]	1.9	2.9	3.9	11.5	34.8	43.8	68.2

[1] Start positions at a depth of 420 m, results for paths that terminate above sea.
[2] Length of paths in the uppermost 1.5 m of quaternary deposits.

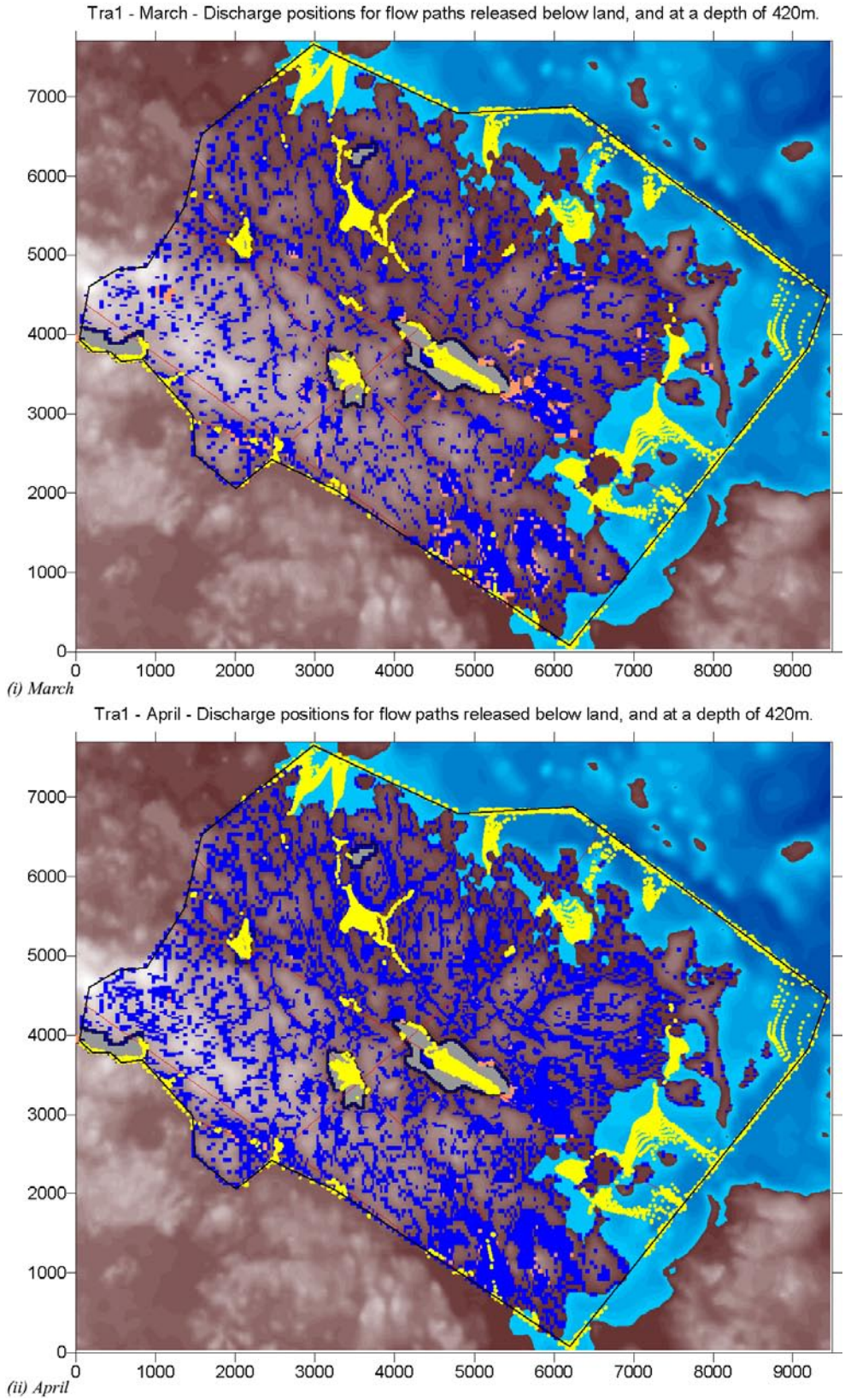

Figure 9-22. *Base case – Normal year – Transient paths – Discharge areas. Yellow dots denote discharge areas for transient paths from a depth of 420 m (no release points below the sea). Blue squares denote all discharge areas above the sea, areas that are not defined as lakes. Discharge areas are presented for March (i) and April (ii).*

Considering complete paths, the difference is that for the transient paths, the short paths are somewhat shorter and the long paths are somewhat longer, compared to steady paths; the differences are however less than 0.5%.

Considering the extension of the paths in the uppermost 1.5 m, the difference is that the transient paths are somewhat longer above the 50th percentile, compared to steady paths. The longer the paths, the larger the difference, for the 99th percentile the difference is 6%.

For the complete paths, a comparison between transient paths and steady state paths is given in Figure 9-23.

For the extension of the paths in the uppermost 1.5 m of quaternary deposits, a comparison between transient paths and steady state paths is given in Figure 9-24.

9.3.5 Transient flow paths – Breakthrough time

The breakthrough times of the transient paths (released at depth of 420 m) have also been analysed. As for the previously presented results (lengths), we have studied the results (time) for:

(iii) The complete paths, with rock mass, fracture zones and quaternary deposits. These distributions represent the breakthrough time, from release positions to points of discharge.

(iv) The uppermost 1.5 m of the quaternary deposits. These distributions represent the same flow paths (released at a depth of 420 m) as in (i), but the results given are time spent for flow within the uppermost 1.5 m of the quaternary deposits.

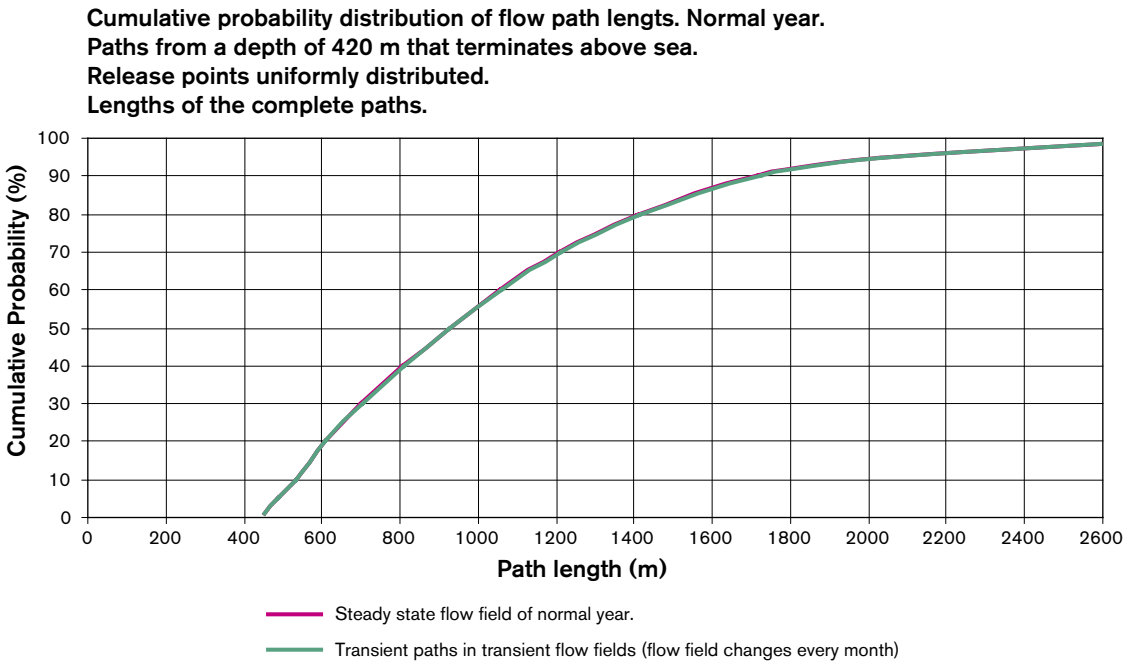

Figure 9-23. *Distribution of lengths of flow paths, length of complete paths. Start positions at a depth of 420 m, results for paths that terminate above sea. Normal year. Time dependent paths in a transient flow field.*

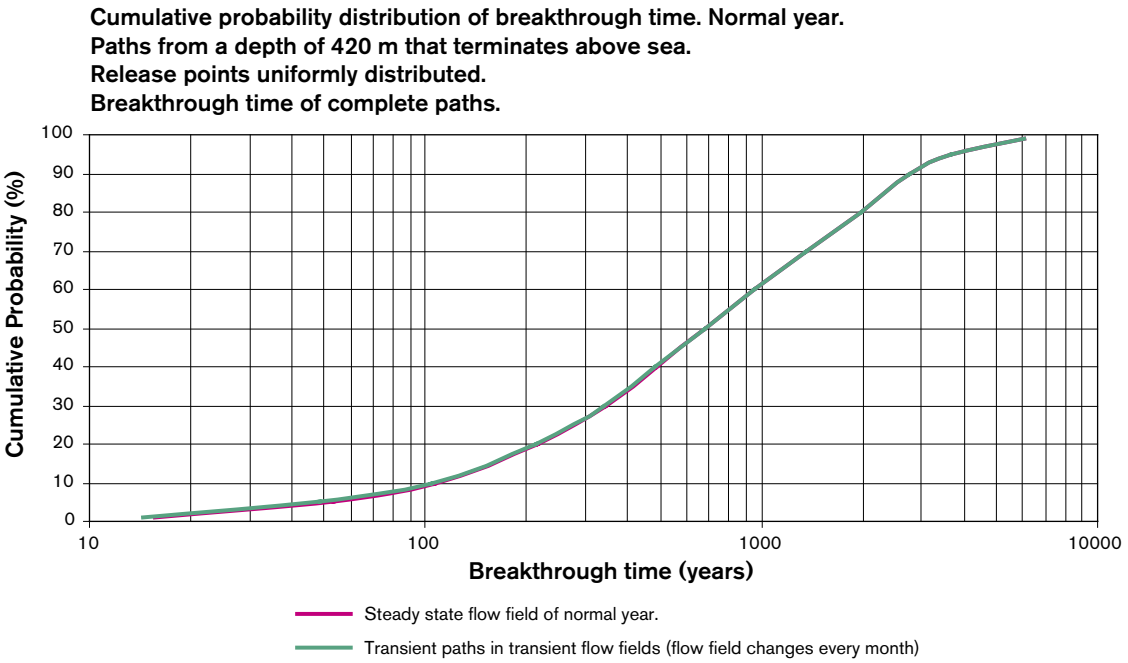

Figure 9-24. *Distribution of lengths of flow paths, length of paths in the uppermost 1.5 m of the quaternary deposits. Start positions at a depth of 420 m, results for paths that terminate above sea. Normal year. Time dependent paths in a transient flow field.*

Because of the uncertainty in the properties of the lake sediments, we have not included time spent in lake sediments in the calculation of total breakthrough time.

The break through time-distribution of the transient paths is very much the same as that of the steady state paths. The results are given in Table 9-4.

Considering complete paths, the difference is that the transient breakthrough times are shorter, compared to steady paths, except for the 99th percentile that is longer. The maximum difference, in percent, takes place for the shortest breakthrough times, and the maximum difference is less than 9%.

Considering the time spent in the uppermost 1.5 m, the difference is that the transient paths produce somewhat shorter times below the median of the distribution (compared to steady paths), the maximum difference is about 10%.

Table 9-4. Distribution of breakthrough time of flow paths. Start positions at a depth of 420 m, results for paths that terminate above sea. Normal year. Time dependent flow paths in a transient flow field.

Transient paths	Flow path breakthrough time (years) Percentiles						
Studied distribution [1]	1th	5th	10th	50th	90th	95th	99th
Complete paths	14.4	48.7	103	676	2,741	3,675	6,050
Paths in uppermost 1.5 [2]	0.1	0.4	0.8	4.1	161	243	376

[1] Start positions at a depth of 420 m, results for paths that terminate above sea. Steady state solution. Normal year.
[2] Time spent in the uppermost 1.5 m of quaternary deposits.

Considering the complete paths, a comparison between transient paths and steady state paths is given in Figure 9-25.

Considering the extension of the paths in the uppermost 1.5 m of quaternary deposits, a comparison between transient paths and steady state paths is given in Figure 9-26.

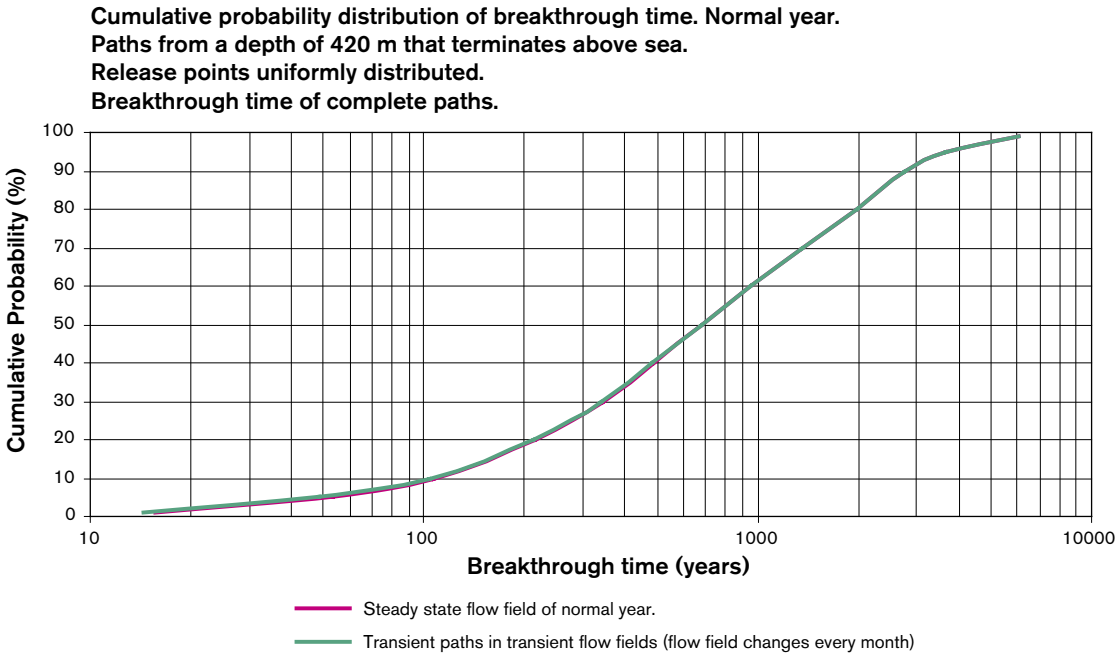

Figure 9-25. *Distribution of breakthrough times of complete flow paths. Start positions at a depth of 420 m, results for paths that terminate above sea. Normal year. Time dependent paths in a transient flow field.*

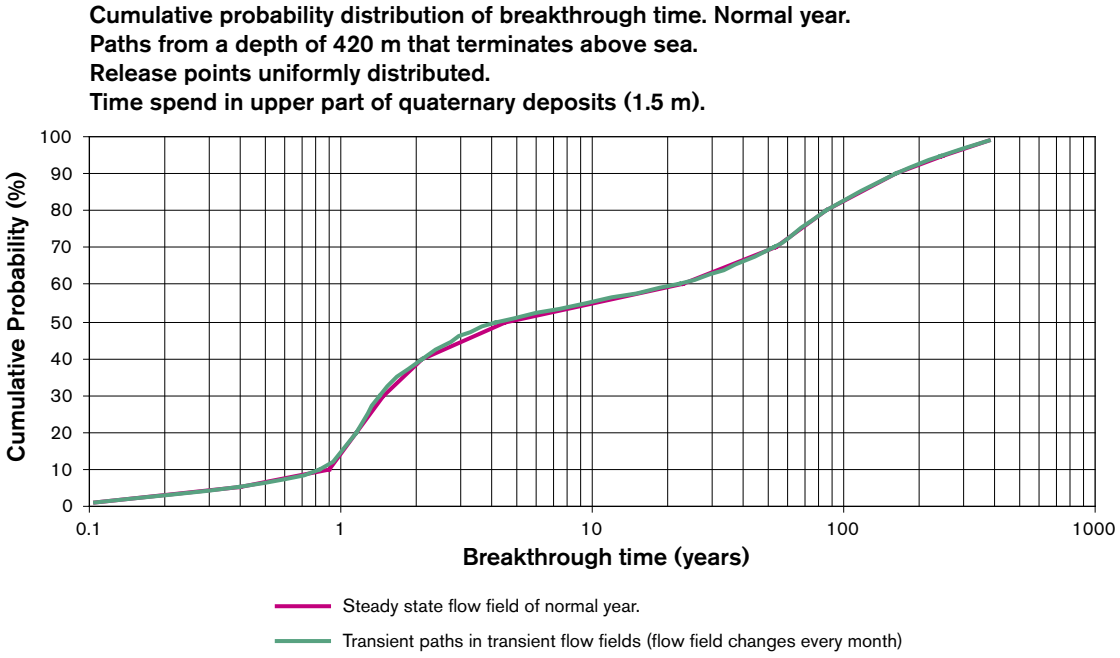

Figure 9-26. *Distribution of flow time of flow paths, time spent in the uppermost 1.5 m of the quaternary deposits. Start positions at a depth of 420 m, results for paths that terminate above sea. Normal year. Time dependent paths in a transient flow field.*

10 Conclusions

General conclusions

The purpose is to study the flow of groundwater from rock masses at great depths and into the surface near deposits by use of mathematical models; and to estimate the spatial and temporal distribution of groundwater from great depths in the surface near deposits (quaternary deposits). The study is about the hydraulic interaction between the geosphere and the biosphere.

The discharge areas for the flow paths from great depth are given by the topography and located along valleys and lakes; the spatial and temporal extension of these areas do not vary much for different values of the permeability of the uppermost part of the flow medium or for the applied different values of groundwater recharge.

In this study flow paths were released on-shore inside of the shore line (no paths were released below the sea) and at an approximate repository depth (i.e. 420 m), the flow paths will either discharge into the sea (i.e. 34%) or above the sea (i.e. 66%). Considering the discharge areas above the sea, nearly all of the flow paths from repository depth will discharge into lakes, and especially where a fracture zones intersects a lake. The flow routes (from great depth) to the discharge areas are influenced by the fracture zones, which tend to be directed along valleys and therefore lead the flow paths to the lakes, which are also located along valleys.

Considering a lake with a thick layer of low-permeable sediments at the base of the lake (a large flow-resistance), for such a situation nearly all flow paths discharges along the lake perimeter where no sediments occur. And for a situation in which a lake has sediments of small resistance along its base, for such a situation most flow paths discharge at the base of the lake through the lake sediments.

Most flow routes from repository depths demonstrate short path lengths in the quaternary deposits. Only a small percentage (< 5%) of the flow paths demonstrate path lengths in the surface near material (in the uppermost 1.5 m of quaternary deposits) that are longer than about 50 m. This is because most flow paths from great depth flow towards lakes and other strong sinks, and reaches these areas from deep below and hence the surface near part of the flow paths will be short.

Nevertheless, a small amount of flow paths (less than approximately 5% of all paths) demonstrate lengths between 50 m and 250 m in the quaternary deposits below lakes, that is however for a situation in which the resistances of the lake sediments are large. Outside of the lakes, the lengths of the studied flow paths in the quaternary deposits tend to be shorter and are not much influenced by the resistance of the lake sediments.

For most flow paths from great depth, the total break through times depend very strongly on the time spent in the rock mass between fracture zones. In comparison, the time spent in fracture zones and in the quaternary deposits is not very important. It should be noted that these conclusions corresponds to flow paths released at repository depth; and that the analyses do not include times spent in lake sediments.

The groundwater flow situation in the quaternary deposits varies significantly during a year, because the groundwater recharge varies during a year. This variation is however not very important for the flow paths from great depth. The simulations of transient flow paths from

a depth of 420 m produced results (length, breakthrough time and discharge areas) that were almost the same as the results produced by a steady state situation and a normal year. Even a steady state simulation of a dry-year produced the same discharge areas as a simulation of a normal year; also a model without quaternary deposits produced the same discharge areas.

11 References

Bear J, Verruit A, 1987. Modeling groundwater flow and pollution. D. Reidel publishing company, P.O.Box 17, 3300 AA Dorfrecht, Holland. ISBN 1-55608-014-X.

Bear J, Bachmat Y, 1990. Introduction to Modeling of Transport Phenomena in Porous Media. Kluwer Academic Publishers, Dordrecht, The Netherlands. ISBN 0-7923-0557-4

Brandt M, Jutman T, Alexanderson H, 1994. Sveriges vattenbalans, Årsmedelvärden 1961–1990 av nederbörd, avdunstning och avrinning. SMHI Hydrologi 49, Sveriges Meterologiska och Hydrologiska Institut, Norrköping. (In Swedish).

Carlsson L, Gustafsson G, 1984. Provpumpning som geohydrologisk undersöknings-metod. Rapport R41: 1984, Byggforskningsrådet. (In Swedish).

Carlsson L, Winberg A, Arnefors J, 1986. Hydraulic modelling of the final repository for reactor waste (SFR). Compilation and conceptualization of available geological and hydrological data. SKB PR SFR 86-03, Svensk Kärnbränslehantering AB.

Chow V T, Maidment D R, Mays L W, 1988. Applied hydrology McGraw-Hill, New York. USA.

Darcy H, 1856. Les Fontaines Publiques de la Ville de Dijon, Dalmont, Paris, France.

Freeze R A, Cherry J A, 1979. Groundwater, Prentice Hall Inc. ISBN 0-13-365312-9.

Grip H, Rhode A, 1985. Vattnets väg från regn till bäck, Hallgren & Fallgrens studieförlag AB. ISBN: 91-7382-762-2. (In Swedish)

Gustafson G, Stanfors R, Wikberg P, 1989. Swedish hard rock laboratory evaluation of 1988 year preinvestigations and description of the target area, the island of Äspö. SKB TR-89-16, June 1989. Svensk Kärnbränslehantering AB.

Holmén J G, 1992. A three-dimensional finite difference model for calculation of flow in the saturated zone. Department of quaternary geology, Uppsala University, Uppsala, Sweden, ISBN 91-7376-119-2, ISSN 0348-2979.

Holmén J G, 1997. On the flow of groundwater in closed tunnels. Generic hydrogeological modelling of a nuclear waste repository, SFL 3–5. SKB TR-97-10, Svensk Kärnbränslehantering AB.

Holmén J G, Stigsson M, 2001. Modelling of Future Hydrogeological Conditions at SFR, Forsmark. SKB R-01-02, Svensk Kärnbränslehantering AB.

Holmén J G, Stigsson M, Marsic N, Gylling B, 2003. Modelling of groundwater flow and flow paths for a large regional domain in northeast Uppland. SKB R-03-24, Svensk Kärnbränslehantering AB.

Lind B B, Lundin L, 1990. Saturated hydraulic conductivity of Scandinavian tills. Nordic Hydrology 21(2): 107–118.

Nace R L ed, 1971. Scientific framework of world water balance. UNESCO Tech.Papers Hydrol., 6, 27 pp.

Nordic Glossary of Hydrology, 1984. Editor Johansson I. Almqvist & Wiksell International. Stockholm Sweden. ISBN 91-22-00692-3.

Pollock D W, 1989. Documentation of computer program to compute and display path lines using results from the U.S. Geological survey modular three-dimensional finite difference groundwater flow model, (Modpath manual). US Geological survey, 411 National Centre Reston, VA 22092, USA.

Påsse T, 1996. A mathematical model of the shore level displacement in Fennoscandia. SKB TR-96-24, Svensk Kärnbränslehantering AB.

Rodhe A, 1987. The Origin of Streamwater Traced by Oxygen-18. Doctoral Thesis, Department of Physical Geography, Division of Hydrology, Uppsala University, Report Series A, No 41, ISSN 0281-8264.

SKB, 1993. Slutförvar för radioaktivt driftavfall – SFR2. Slutlig säkerhetsrapport. Reviderad utgåva – Maj 1993, (SKB Final repository for radioactive waste – SFR1. Final safety report. Revised edition – May 1993). SKB, Svensk Kärnbränslehantering AB.

SMHI, 1999. Swedish Meteorological and Hydrological Institute, Norrköping. (Sveriges meteorologiska och hydrologiska institut). Data provided by SMHI through the internet: http://www.smhi.se/sgn0102/n0205/index.htm, June 2, 1999. SMHI. Major surface water divides. SMHI: Svenskt Vattenarkiv.

Stigsson M, Follin S, Andersson J, 1998. On the simulation of variable density flow at SFR, Sweden. SKB R-98-08, Svensk Kärnbränslehantering AB.

Sigurdsson T, 1987. Bottenundersökning av ett område ovanför SFR, Forsmark. SFR 87-07, Svensk Kärnbränslehantering AB.

Voss C I, Andersson J, 1993. Regional flow in the Baltic Shield During Holocene Coastal Regression. Ground Water, Vol 31, No 6.

Walker D, Rhen I, Gurban I, 1997. Summary of the hydrogeological conditions at Aberg, Beberg and Ceberg. SKB TR-97-23, Svensk Kärnbränslehantering AB.

Wikberg P (ed), Gustafson G, Rhén I, Stanfors R, 1991. Äspö Hard Rock Laboratory. Evaluation and conceptual modelling based on the pre-investigations 1986–1990. SKB TR-91-22, June 1991. Svensk Kärnbränslehantering AB.